UNIVERSITY OF LIVERPOOL

Production, Characterisation and Application of Humanised Anti-Histone Antibodies in Critical Illness

Thesis submitted in accordance with the requirements of the University of Liverpool for the degree of Doctor in Philosophy

By

Dunhao Su

August, 2015

ABSTRACT

Histones are group of positively charged proteins that form nuclear cores for building chromatins with double stranded DNAs. During cell death, the nuclear breakdown products can be released extracellularly and rapidly cleared by leucocytes and macrophages. However, during extensive and rapid cell death, such as in severe trauma, sepsis, and necrotising pancreatitis, the nuclear breakdown products cannot be immediately cleared and can be degraded to release histones. Over recent years, the toxicity of extracellular histones has been discovered, including cytotoxicity through interrupting cell membranes, stimulation of cytokine release and inflammatory responses and activation of coagulation cascades. High levels of circulating histones can cause injury to many distant organs, such as the lungs, heart, liver and kidneys, and may contribute to multiple organ failure in critical illness. Therefore, it is important to detoxify histones in order to reduce distant organ damage and rescue these critically ill patients.

It is known that activated protein C is able to cleave histones to reduce their toxicity. However, due to its sideeffects, it has been withdrawn from clinical use. Heparin, a commonly used anticoagulant, is able to bind to histones and reduce their toxicity. However, heparin may also cause side effects, such as heparin-induced thrombocytopenia, preventing its clinical application because histones also cause severe thrombocytopenia. Anti-histone antibodies have been reported to reduce histone toxicity and rescue mice with sepsis. However, no clinically usable anti-histone antibodies are available. In this study, I focused on the development of anti-histone antibody fragments.

In this project, a murine anti-histone single chain variable fragment (scFv) was designed and produced. After confirming its roles in detoxifying histones, the anti-histone scFv was

humanised using the human IgG framework and mouse anti-histone complementarity-determining regions (CDRs) to generate a humanised anti-histone scFv (HahscFv). The specificity of the HahscFv was confirmed by Western blotting, and its role in detoxification of histones was also verified *in vitro*. In addition, I have developed a new approach to produce human anti-histone antibody fragments. This approach includes isolation of anti-histone antibodies from sera of patients with systemic lupus erythematosus (SLE) using affinity purification, determination of amino acid sequences of the isolated heavy and light chains, using tandem mass spectrometry (MS/MS) and reproduced these antibody fragments (scFv) using recombinant DNA technology. The specificity and binding affinity of this purified human anti-histone antibody were determined. The functional roles of the scFv with highest affinity to histones were verified both *in vitro* and *in vivo*.

Moreover, I have also screened for the presence of histone-binding proteins in human serum using a pull down assay with high stringency. I found that both prothrombin and anti-thrombin are strongly associated with histones. Furthermore, I have demonstrated the mechanism of histone-induced thrombin generation. This work improves the understanding of why histones are potent pro-coagulants. Importantly, the anti-histone scFv is able to block this process, suggesting a potential that anti-histone therapy, and in particular anti-histone antibodies, may reduce coagulation activation and the development of disseminated intracellular coagulation (DIC) in critical illness. Future work will be along these lines to realise the promise of saving lives and reducing the poor outcome in critical illness.

ACKNOWLEDGEMENTS

Firstly, I would like to thank my primary supervisor Prof. Cheng-Hock Toh for accepting me to study in his group, and supervising the entire project and giving me help, support and guidance throughout my PhD. Secondly, I would like to thank my secondary supervisor Dr. Guozheng Wang for kindly and closely supervising me through the whole PhD and ensuring appropriate conduction of various experiments in whole study.

I would like to take this opportunity to thank Dr. Simon Abrams for his great scientific and technical insights and suggestions for different parts of this project and for his ever willingness to help. I also would like to thank Dr Yasir Alhamdi, Miss Yasmina Sahraoui and Tingting Liu for their help.

Finally I would like to thank my dear family and friends for their kind support throughout my whole PhD studies.

CONTENT

LIST OF FIGURES

Chapter 1

Chapter 2

Chapter 3

Chapter 4

Chapter 5

LIST OF TABLES

Chapter 1

Chapter 4

PUBLICATIONS AND PRESENTATIONS

1. Alhamdi Y, Abrams ST, Cheng Z, Jing S, **Su D**, Liu Z, Lane S, Welters I, Wang G, and Toh CH. *Circulating histones are major mediators of cardiac injury in patients with sepsis.* **Crit. Care Med**. 2015. 43(10):2094-103 (Impact factor **6.147**).

2. Alhamdi Y, Zi M, Abrams ST, Liu T, **Su D**, Welters, I, Dutt T, Cartwright EJ, Wang G and Toh CH. *Circulating histone concentration differentially affect the predominance of left or right ventricular dysfunction in critical illness*. **Crit. Care Med**. 2015. In Press (Impact factor **6.147**).

3. Poster presentation in Institute of Infection and Global Health Day (2011): *Development of Humanised Anti-histone scFv to Neutralise Toxic Circulating Histones in Sepsis.* Liverpool, UK.

4. Poster presentation in Institute of Infection and Global Health Day (2012): *Development of humanised anti-histone single chain variable fragment to neutralise toxic circulating histones in sepsis.* Liverpool, UK. Won the best poster prize.

5. Poster presentation in Institute of Infection and Global Health Day (2014): *Human anti-histone antibodies isolation, sequence determination and functional analysis.* Liverpool, UK. Won the best poster prize.

6. Oral presentation in Department of Clinical Infection, Microbiology and Immunology Research Meeting (2015): *Production, Characterisation and Application of Humanised Anti-histone Antibodies in Critical Illness*. Liverpool, UK.

ABBREVIATIONS

Ab	Antibody
AHA	Anti-histone antibody
ahscFv	Anti-histone scFv
ALI	Acute lung injury
ANOVA	Analysis of variance
APC	Activated protein C
APP	Acute phase proteins
BALF	Bronchoalveolar lavage fluid
bp	Base-pair
BSA	Bovine serum albumin
CDR	Complementarity determining regions
CF	Cystic Fibrosis
CHO	Chinese hamster oveary
CitH3	Citrullinated histone H3
CRP	C-reactive protein
cscFv	Control scFv
ctH	Calf thymus histone
DIC	Disseminated intravascular coagulation
DMEM	Dulbecco's modified eagle medium
DNA	Deoxyribonucleic acid
E. coli	*Escherichia coli*
EBV	Epstein-Barr virus
EDTA	Ethylenediaminetetraacetic acid

ELISA	Enzyme-linked immunosorbent assay
ERK	Extracellular signal-regulated kinases
Fab	Fragment antigen-binding
FBS	Fetal bovine serum
Fc	Fragment crystallisable
Fc1	Flow cell 1
Fc2	Flow cell 2
FDR	False discovery rate
FVa	Factor Va
FXa	Factor Xa
GSH	Reduced glutathione
GSSG	Oxidised glutathione
H1	Histone H1
H2A	Histone H2A
H2B	Histone H2B
H3	Histone H3
H4	Histone H4
HahscFv	Human anti-histone single chain variable fragment
HCF	Human chromosome fragment
HEK	Human embryonic kidney
HRP	Horseradish peroxidase
IBs	Inclusion bodies
ICNARC	Intensive Care National Audit and Research Centre
ICU	Intensive care unit
IgA	Immunoglobulin A

IgG	Immunoglobulin G
IgM	Immunologbulin M
IL	Interleukin
IPTG	Isopropyl-β-D-thiogalactopyranoside
ISTH	International Society on Thrombosis and Haemostasis
kDa	kilodalton
LB	Luria-Bertani
LPS	Lipopolysaccharide
MahscFv	Mouse anti-histone single chain variable fragment
MODS	Multiple organ dysfunction syndrome
MOF	Multiple organ failure
MPO	Myeloperoxidase
MS/MS	Tandem mass spectrometry
NET	Neutrophil extracellular trap
NGS	Next generation sequencing
Ni-NTA	Nickel-Nitrilotriacetic acid
nr	Nonredundant
OD	Optimal density
PAD4	Peptidyl-arginine deiminase 4
PAF	Platelet activating factor
PBS	Phosphate Buffered Saline
PBS-T	Phosphate Buffered Saline Tween
PDB	Protein data bank
PGE1	Prostaglandin E1
PI	Propidium iodide

PMA	Phorbol myristate acetate
PMN	Polymorphonuclear
ProT	Prothrombin
PRP	Platelet rich plasma
PRRs	Pattern-recognition receptors
PT	Prothrombin time
PTM	Post-translational modification
PVDF	Polyvinylidene fluoride
RA	Rheumatoid arthritis
RC	Reagent C
ROS	Reactive oxygen species
RT	Room temperature
SA	Streptavidin
scFv	Single chain variable fragment
SD	Standard deviation
SDS-PAGE	Sodium dodecyl sulphate polyacrylamide gel electrophoresis
SIRS	Systemic inflammatory response syndrome
SLE	Systemic lupus erythematosus
SPR	Surface plasmon resonance
STBM	Syncytiotrophoblast microparticles
SVV	Small-vessel vasculitis
TAT	Thrombin-antithrombin
TBE	Tris borate EDTA
TBS	Tris buffer saline
TBS-T	Tris buffer saline Tween-20

TC	TransChromo
TLR	Toll-like receptor
TM	Thrombomodulin
TMB	3,3,5,5-Tetramethylbenzidine
TNF	Tumour necrosis factor
TNFα	Tumour necrosis factor alpha
vWF	von Willebrand factor
WST-8	Water-soluble tetrazolium salt

Chapter 1 General Introduction

1.1 Critical illness

In general, critically ill patients encompass those admitted to the intensive care unit (ICU) due to the requirement for intensive management and careful monitoring. The conditions for such a requirement include sepsis, trauma, surgery, pancreatitis, ischemia-reperfusion injury and many other conditions that result in systemic complications. These culminate in an increasing number of failing organs that typically begin with respiratory and cardiac failure, leading on to multiple organ failure (MOF). Such sequence of events invariably has catastrophic implications to patient outcome [1]. The number of patients treated in ICU is increasing with Intensive Care National Audit and Research Centre (ICNARC) data shown in figure 1.1. Conditions mentioned above have one thing in common – the result of inflammation.

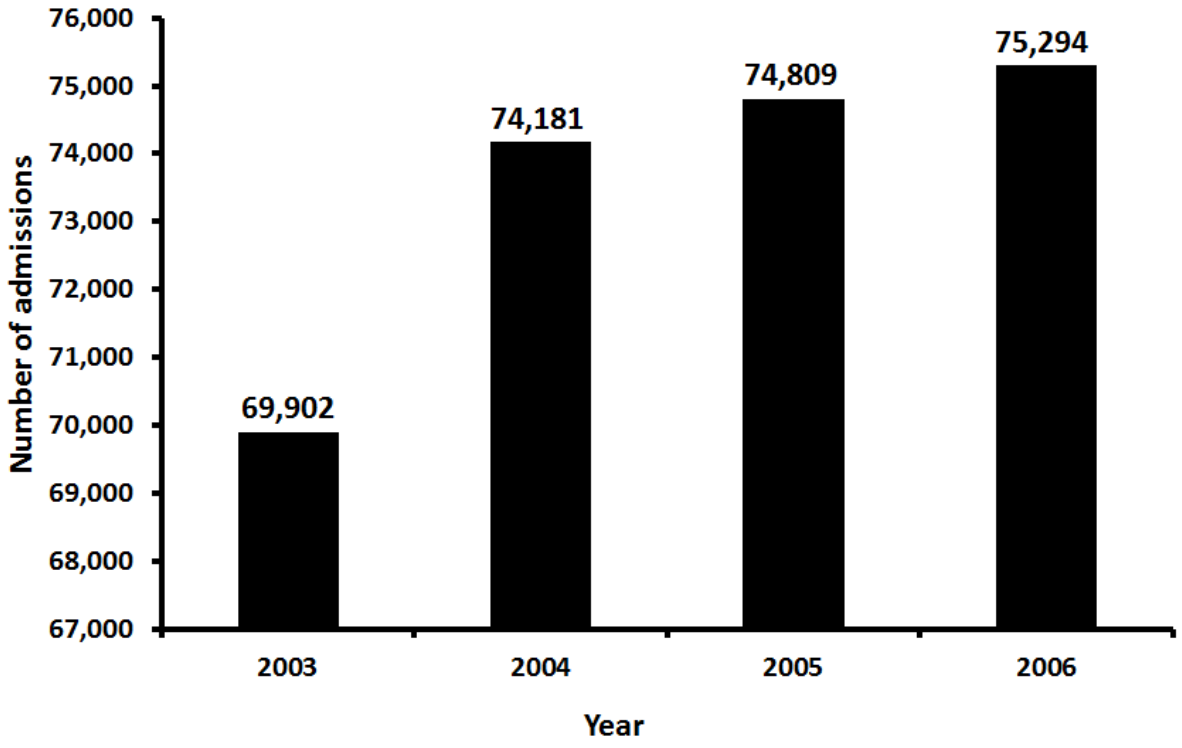

Figure 1.1 Number of Admissions in critical care units by year in the UK. This figure is adapted from reference [2].

1.1.1 Critical illness and inflammatory response

The inflammatory response is a complex biological process that aims to protect the host from harmful stimuli such as infection or damaged cells. The purpose of this response is to eliminate the source of cell injury, remove cellular debris, and to initiate tissue repair. As a generic host response to insult or injury, it is considered part of the innate immune response. Molecular components of the inflammatory response are divided into cytokines (e.g. Interleukin (IL)-1β, IL-6, IL-8 and Tumour necrosis factor alpha (TNFα)), plasma proteins, acute phase proteins (APP) and cellular components such as leukocytes and the endothelium.

As critical illness is usually triggered by a noxious stimulus, e.g. infection or non-microbial causes such as trauma or infarction, the systemic inflammatory response syndrome (SIRS)

almost always ensues [6]. Table 1.1 below illustrates the criteria used to assess the development of SIRS [7] with the presence of two or more of these criteria required to establish a diagnosis of SIRS. Invasive infection on the background of SIRS is defined as sepsis, which is a multi-factorial syndrome arising from the host response to infection and is associated with extensive systemic cell and tissue damage [8]. The American College of Chest Physicians and the Society of Critical Care Medicine [6, 9], defined as the development of organ failure in the course of sepsis as "severe sepsis", while the presence of persistent acute circulatory failure despite adequate volume resuscitation as "septic shock".

Table 1.1 Criteria for the diagnosis of SIRS.

Criterion	Value
Temperature (°C)	>38 or <36
Heart rate (beats per minute)	> 90
Respiratory rate	>20 or $PaCO_2$ <32 mmHg
White blood cell count	>12,000 or >10% neutrophils

Although the diagnosis of the systemic inflammatory response in critically ill patients currently relies mostly on clinical criteria, many researchers have identified promising biochemical and/or immunological parameters that are elevated in SIRS, such as interleukins [10], adrenomedullin [11], extracellular phospholipase A_2 [12], C-reactive protein (CRP) [13] and most recently nuclear break down products such as extracellular histones and nucleosomes [14]. Therefore, some authors have suggested that it might be possible, if supported by adequate clinical and epidemiologic studies, to better characterise and diagnose

systemic inflammation in critical illness through use of these biomarkers [6]. In general, intensivists feel that the current diagnosis of SIRS is not sufficiently specific and needs strengthening with inclusion of biological parameters.

1.1.2 Critical illness and coagulation

The activation of coagulation is a process by which fibrin clots are formed to stem blood loss. This is highly regulated to prevent excessive bleeding (haemorrhage) but not cause thrombosis. This process is also important in wound healing/repair and also prevents dissemination of microorganisms into the circulation. However, when coagulation activation is excessive due to continued presence of triggering factors and/or unchecked through depletion of regulatory factors, it can be detrimental to the host. Such an uncontrolled response could lead to haemorrhage through consumptive coagulopathy (through a significant decrease in the level of coagulation factors and platelet counts) and also microvascular thrombosis which can cause multiple organ failure (MOF). The condition is then referred to as disseminated intravascular coagulation (DIC), which the International Society on Thrombosis and Haemostasis (ISTH) has defined as "significant reduction in platelet counts and fibrinogen levels, significant prolongation in prothrombin time (PT) and substantial increment in fibrin-related markers" [15]. In essence, DIC reflects the increased generation of thrombin *in vivo* [16].

1.1.2.1 Thrombin generation

Thrombin plays a pivotal role in the control of coagulation and fibrinolytic processes. It can be immediately pro-coagulant in converting fibrinogen to fibrin, anticoagulant in terms of thrombomodulin-dependent protein C activation and pro-fibrinolytic through stimulating endothelial cells to release tissue plasminogen activator [17-19]. Disturbance or imbalance in these pathways can alter the clinical phenotype of increased bleeding and/or increased thrombosis in the microcirculation. Under physiological conditions, tissue factor exposure triggers coagulation activation that leads on to thrombin generation, which then back-activates the intrinsic pathway coagulation factors to amplify thrombin generation. Dysregulation of this process leads to propagation of thrombin generation and adverse consequences, if unchecked. More recently, histone H4 has been reported to promote prothrombin auto-activation into thrombin [20]. If Arg-320 is mutated, it could block prothrombin autoactivation [21]. H4 bound to prothrombin had been demonstrated by fluorescence titrations, and thus promoted prothrombin cleavage into various products e.g. prethrombin-1, prethrombin-2 and fragment 1.2. Moreover, H4 bound to prothrombin to induce a collapsed conformation, and further caused various conformations of inter-kringle linker domain that determined prothrombin's functions [20]. If this process is physiological, which is currently unproven, this would be a means by which thrombin can be generated without activation of the coagulation cascade.

1.1.2.2 Prothrombinase

A key step in thrombin generation is in the enzymatic assembly that enables conversion of the zymogen prothrombin into the enzyme thrombin. This complex formed by factor (F) Xa, co-factor FVa, prothrombin in the presence of calcium ions and phospholipid is referred to as the prothrombinase complex [22]. Prothrombin, also known as coagulation factor II normally

circulates in the blood at a concentration of approximately 0.1 mg/mL [23]. It is a single chain protein composed of fragment 1 (F1) (residues 1 – 155), F2 (residues 156 – 271) and the protease domain (α-thrombin) (residues 272 – 579). In F1, there is a Gla and a kringle-1 domain with F2 containing kringle-2 and the A and B chains of thrombin in α-thrombin. Prothrombin is linked by three flexible linkers which individually ligate between Gla domain, kringle-1, kringle-2 and A chain [24] (Fig. 1.2). In the prothrombinase complex, there are two cleavage pathways [25]. Prothrombin is initially cleaved at Arg-271 to split into two parts: the F1 and F2 complex, and prothrombin-2. Prothrombin can also be cleaved at Arg-320 to form meizothrombin (Fig. 1.2) because A and B chains are connected by a disulphide bond (Cys-293 and Cys-439) [25].

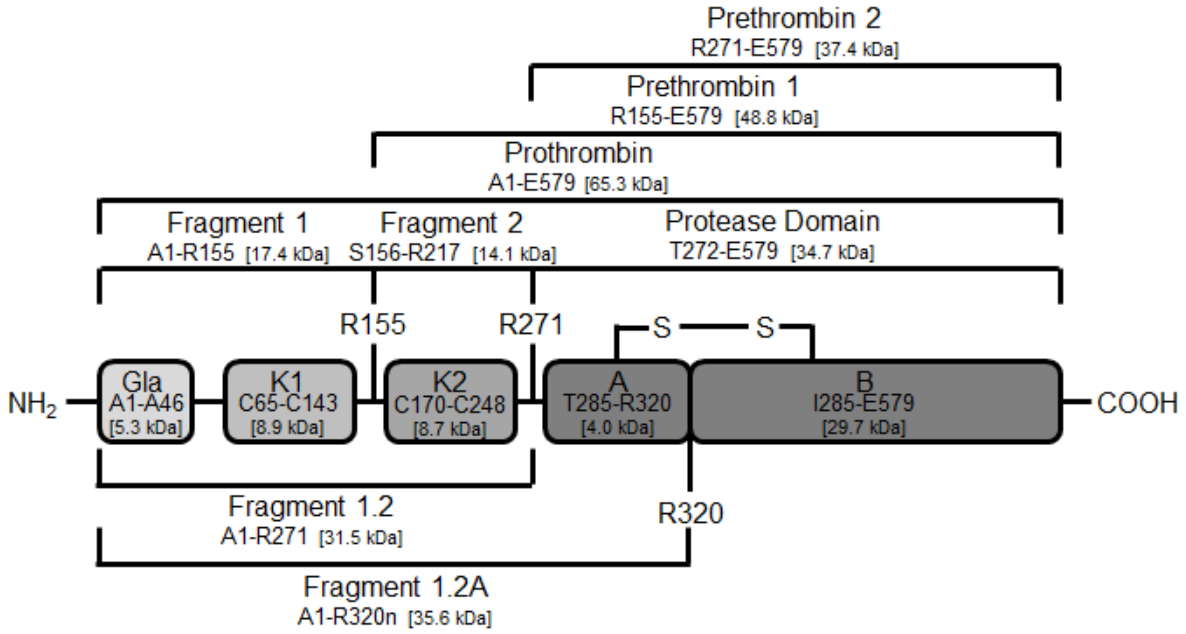

Figure 1.2 Schematic diagram for prothrombin structure. This figure is adapted from reference [24, 25].

1.1.3 Critical illness and cell death

Extensive and uncontrolled cell death plays a key role in the development of MOF during critical illness [26, 27]. After extensive cell death, cellular contents including the intra-nuclear nucleosomes (DNA-histones complexes) are released into the circulation and has been reported in various diseases such as cancers, sepsis and trauma [28]. During tissue damage and cell death, chromatin is cleaved into oligo- and mono-nucleosomes, which are then released extracellularly [29] and further degraded into individual histones (H1, H2A, H2B, H3 and H4), heterodimers (H2A/H2B and H3/H4) [30] as well as free DNA [31]. However, these are rarely detected in blood unless there is extensive cell death [28] as they are rapidly cleared by the liver [32].

1.2 Extracellular histones and toxicity

Histones are basic proteins usually found within the nucleus of eukaryotic cells. There are 5 members of the histone (H) family: H2A, H2B, H3, H4 (core histones) and H1 (linker histone) [33]. The core histones share common structural characteristics, consisting of a central helix flanked by two helix-strand-helix motifs. Nucleosomes are formed by an octomeric protein core consisting of heterodimers H2A/H2B and H3/H4 with 146-base pairs (bp) of DNA wrapped around them [34]. The linker histone (H1) binds to non-nucleosomal DNA and links individual nucleosomes together, allowing for higher order chromatin structures to be formed [35]. Whilst histones are essential building blocks within cells in forming the basis of chromatin, their effects outside the cell can be extremely toxic [14]. Work from our group has shown that extracellular histones bind phospholipids on membranes to cause profound calcium influx [36, 37] and subsequent cell damage. This indiscriminate toxic effect of histones is critical to increasing coagulation activation [38], platelet aggregation [39], pro-inflammatory cytokine release [40, 41] and endothelial damage [14].

The release of extracellular DNA and histones from neutrophils during neutrophil extracellular trap (NET) formation also facilitates thrombus formation and has shown relevance in animal models of deep vein thrombosis, transfusion-related acute lung injury, cancer, trauma and sepsis [14, 36, 42-44].

1.2.1 Extracellular histones in coagulation and thrombosis

The role of extracellular histones in the promotion of coagulation and thrombosis is becoming increasingly characterised as outlined in Figure 1.3. The general pro-coagulant properties of histones include endothelial damage with released von Willebrand factor (vWF) mediating leucocyte/platelet recruitment and loss of thrombomodulin (TM)-dependent protein C anticoagulant effects [14, 45, 46]. *In vivo,* histone infusion in mice results in rapid thrombocytopenia (significant reduction in platelet count) with histone and platelet staining in the lungs [39, 47]. Further evidence to support the role of histones in the activation of coagulation was demonstrated by our group. In mouse models, plasma thrombin–anti-thrombin (TAT) complexes, i.e. a marker of thrombin generation and therefore, of coagulation activation, were significantly elevated following either trauma (endogenous histone model) or histone infusion (exogenous histone model) [48]. Pathologically, the lungs were the predominantly affected organ with neutrophil infiltration, pulmonary oedema, haemorrhage, and microvascular thrombosis [48]. The formation of thrombi in lungs strongly supports the hypothesis that histone-triggered coagulation activation is involved in lung injury and possibly MOF [48].

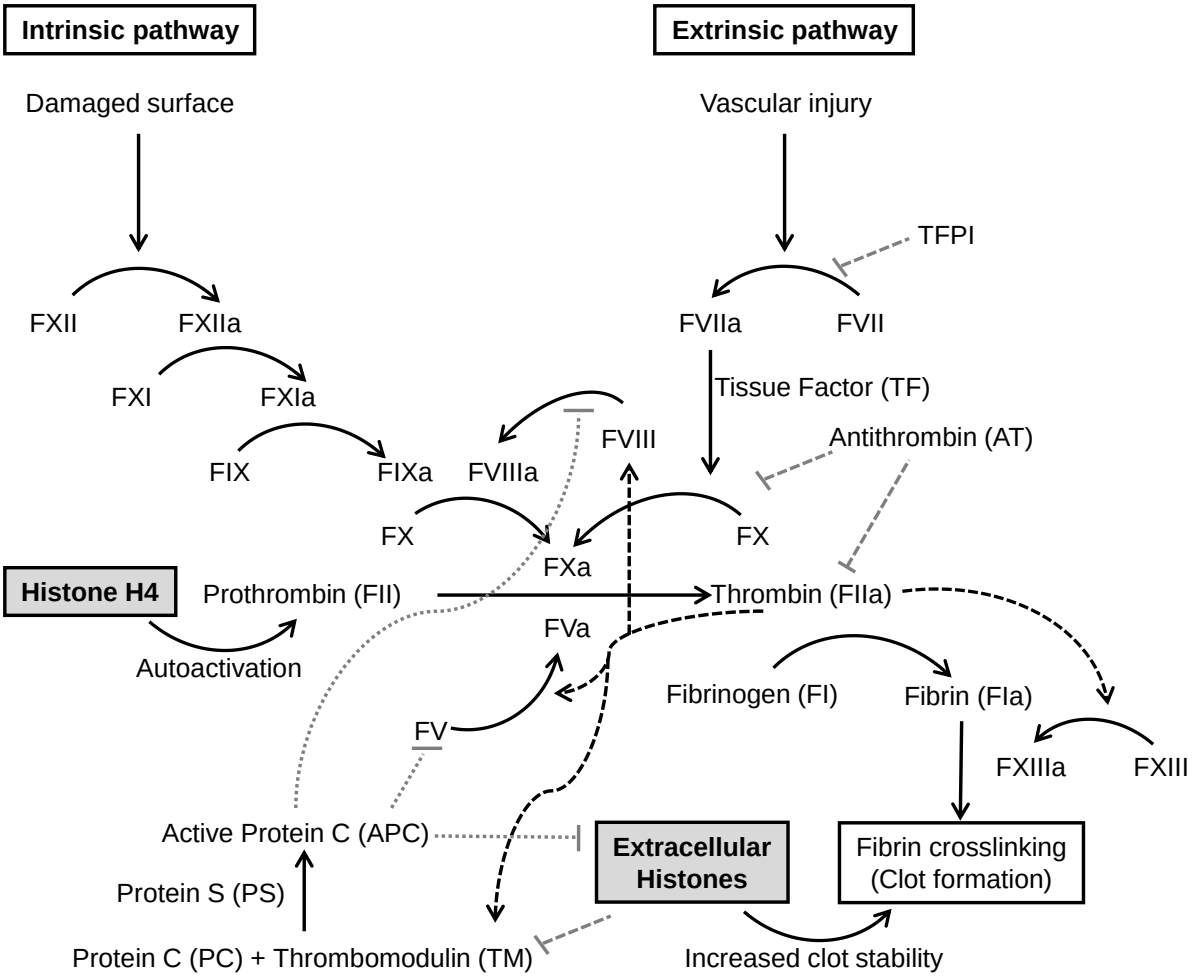

Figure 1.3 Role of histones in coagulation. This figure is adapted from references [20, 38, 49, 50].

Histones induce platelet aggregation *in vitro* with H4 invoking the strongest response [39]. Mechanistically, histones bind to platelets, induce calcium influx, and recruit coagulation factors such as fibrinogen [39]. Fibrinogen then cross-links platelet integrin αIIbβ3 which in turn results in large platelet aggregates [39]. Furthermore, Semeraro F *et al* demonstrate that histones dose dependently enhance thrombin generation in platelet rich plasma (PRP) in a Toll-like receptor (TLR) 2 and 4-dependent mechanism. Activation of these receptors induces intra-platelet signalling through extracellular stimuli-responsive (ERK), Akt, p38, and NFκB

[51]. More recently, polyphosphates have been found in human platelet dense granules to act as activator of factor XII and regulate coagulation and fibrinolysis. The purified polyphosphate with histones and FXII have been demonstrated to induce thrombin generation [52]. Moreover, blocking TLR2 and TLR4 using specific antibodies reduced platelets activation and thrombin generation in the presence of histones. Therefore, histones could induce a procoagulant phenotype via TLR2 and TLR4 [52].

1.2.2 Extracellular histones in innate immunity

As a feature of the innate immune response, neutrophils can eliminate microbes through either phagocytosis, generation of reactive oxygen species (ROS) and through degranulation of anti-microbial molecules. Neutrophils are the most abundant form of leucocytes and act as the first line of defence against invading pathogens [53]. Along with basophils and eosinophils, they form the polymorphonuclear (PMN) cell family. They are derived from stem cells in the bone marrow and have a short half-life when in circulation [54]. As a hallmark of acute inflammation, neutrophils are recruited and infiltrate a site of infection through chemotaxis [55].

Recently, it has been demonstrated that activated neutrophils can immobilise and kill invading microorganisms through the release of extracellular traps (NETs). During NETosis, a distinct form of active cell death, neutrophils unravel chromatin and extrude DNA and histones along with myeloperoxidase (MPO), cathepsin G and neutrophil elastase (NE) into the extracellular space. Studies have demonstrated that lysine-rich histones (H1, H2A, and H2B) and histone fragments, from shrimp [26], fish [20, 27–30], frog [31], chicken [32, 33], and mammals [34–38] share antimicrobial activity.

Pathways to NETosis include histone deimination by peptidyl-arginine deiminase 4 (PAD4) [56] and the involvement of NE and NADPH oxidase [57, 58]. PAD4 converts certain arginine residues on the core histones to citrulline [59]. Eliminating the positive charge at this residue, theoretically results in unravelling of the compact structure of the chromatin and causing chromosomal decondensation, followed by plasma membrane rupture.

A large variety of bacteria stimulate NETs including (Table 1.2), *Staphylococcus aureus* [60], *Streptococcus dysgalactiae* [61], *Klebsiella pneumonia* [58], *Listeria monocytogenes* [62], *Mycobacterium tuberculosis* [63], *Haemophilus influenza* [64], and *Shigella flexneri* [65]. Surface components of both Gram-positive and negative bacteria such as lipoteichoic acid and Lipopolysaccharides (LPS) have also been shown to trigger NETosis [66]. This observation has characterised NETs as part of the innate immune response [66]. The release of extracellular DNA and histones from NETs facilitates thrombus formation through platelet recruitment thereby limiting the dissemination of the invading microorganism into the systemic circulation [67].

Certain pathogens such as *Staphylococci* and *Streptococci* have evolved to evade this mechanism through the release of virulence factors that degrade NETs [68]. Another evolutionary mechanism developed by pathogens to suppress NETs can be observed in Cystic Fibrosis (CF). Clinical isolates from the lung of CF patients show a mucoid phenotype that makes *Pseudomonas aeruginosa* less sensitive to NET inhibition of growth [69]. Bacterial growth thrives despite the accumulation of NETs in these infected organs, with NETs contributing to the chronic lung obstruction observed in these patients [69].

Table 1.2 Inducers of NETs formation.

NETosis inducer	Reference
HOST FACTORS	
Extracellular histones	Ambras *et al*., 2013 [48]
GM-CSF + C5a	Yousefi *et al*., 2009 [70]
IL-8 (CXCL8)	Gupta *et al*., 2005 [71]
MIP-2(CXCL2)	Marcos *et al*., 2010 [72]
Singlet oxygen	Nishinaka *et al*., 2011 [73]
Platelet activating factor (PAF)	Yost *et al*., 2009 [74]
Syncytiotrophoblast microparticles (STBM)	Gupta *et al*., 2005 [75]
OTHERS	
Glucose oxidase	Yost *et al*.,2009 [74]
Calcium ionophore (ionomycin)	Parker *et al*., 2012 [76]
Phorbol myristate acetate (PMA)	Brinkmann *et al*.,2004 [65]; Remijsen *et al*., 2011 [77]
LPS (Bacterial component)	Brinkmann *et al*.,2004 [65]

In spite of the beneficial role that NETs play in innate immunity, pathological properties have been ascribed due to their ineffective degradation and clearance. One such effect is the development of autoimmunity, which has been shown in patients with atherosclerosis [78], Felty's syndrome [79], rheumatoid arthritis (RA) [80], small-vessel vasculitis (SVV) [81], and systemic lupus erythematosus (SLE) [82].

SLE is an autoimmune disorder characterised by the development of autoantibodies to neutrophil proteins, DNA and histones in particular [83], which are highly immunogenic [84]. These antigens and antibodies (Ab) form immune complexes that are either formed *in situ* or can be deposited in the kidneys contributing to organ failure in this disease [85]. Infections can result in a flare up of the disease due to the induction of the innate immune response and the production of NETs and therefore self-antigens. The presence of histones on NETs may be responsible for the ineffective clearance of NETs by degrading enzymes such as DNase1 and therefore resulting in a vicious circle of disease progression [82].

1.2.3 Extracellular histones and neutrophil recruitment, and activation

Neutrophil congestion inside lung capillaries in mice infused with histones was first reported by Xu and colleagues [14] and further characterized by our group [48]. Pulmonary alveolar capillaries become obstructed with neutrophils following significant neutrophil infiltration in the lungs of histone-infusion, septic, and trauma mouse models. In mice infused with histones, Myeloperoxidase (MPO) staining is found inside alveoli, indicating MPO release from neutrophils following histone infusion [48]. Similarly, *in vitro* histone-stimulated neutrophils, released significant MPO. MPO enhances the production of hypochlorous acid, which acts as an antimicrobial agent but can also damage host cells [86].

Furthermore, our group has demonstrated that histones directly induce NETs formation both *in vitro* and *in vivo*. Histone-treated neutrophils induced NETs within 3 hours to comparable levels to those induced by PMA stimulation (known inducer of NETs). Examination of the lungs of histone-infused mice demonstrated Citrullinated histone H3 (CitH3) positivity (a marker of NETs) [48]. Specifically, co-infusion with murine anti-histone single chain variable fragment (MahscFv) significantly abrogated this effect [48]. Taken together, histone-

induced NETs formation may serve as a mechanism for neutrophil congestion and thrombosis in lungs, which would exacerbate tissue injury [87], increase coagulation activation and pro-inflammatory cytokine release. This process has relevance in animal models of deep vein thrombosis, transfusion-related acute lung injury, cancer, trauma and sepsis [6, 9-12].

1.2.4 Extracellular histones and acute lung injury (ALI)

Following histone-infusion, mice die rapidly (within 4 hours) after developing cyanosis and dyspnoea, an indicator of pulmonary and cardiac failure. Pathological examination shows the lungs to be the predominantly affected organ with severe oedema, multifocal alveolar haemorrhage and congestion. Pathological changes in other organs (kidney and liver) were less obvious, except for occasional thrombus and vacuole formation. Specifically, histone-induced lung injury can be significantly reduced by co-infusion of MahscFv (10 mg/kg) [48]. Similar pathological changes are observed in a Gierer mouse model of severe trauma, demonstrating that endogenous histones are involved in lung injury, which could also be abrogated by infusion of the MahscFv (10 mg/kg) [48]. Moreover, the full development of ALI was induced by LPS, IgG immune complexes, or C5a in mice models requiring complement receptor C5aR and C5L2. H3 and H4 had been identified in bronchoalveolar lavage fluid (BALF) after C5a–induced ALI [88]. Taken together, these data indicate that the lungs are the most susceptible organ to the toxicity of circulating histones probably because of the dense nature of the capillary network in the pulmonary microcirculation [48].

1.2.5 Mechanisms of cytotoxicity of extracellular histones

Histone increased the permeability of cellular membranes [89]. This is most likely due to the positively charged histones binding to negatively charged phospholipids [34], which are the main structural components of plasma membranes [90]. Our group demonstrated that the membrane-binding property of extracellular histones is the major mechanism of toxicity. *In vitro,* fluorescein isothiocyanate (FITC)–labelled histones bind to endothelial cell membranes and *in vivo* histone-infusion generates histone staining on endothelial cell membrane surfaces. Immediately following histone treatment, histones binding to endothelial cells changes the membrane potential due to elevations in intracellular Ca^{2+}. Furthermore, histone-induced cell damage can be inhibited when extracellular Ca^{2+} is removed [48]. TLR4- and TLR2-neutralizing antibodies did not block the Ca^{2+} influx and showed no protective effect on cultured endothelial cells treated with histones. This demonstrates that extracellular histones bind phospholipids on cell membranes to cause calcium influx [48] and subsequent cell damage, and that activation of TLRs is not the major pathway for histone toxicity, at least to endothelial cells.

1.3 Neutralisation of histone toxicity

Following the discovery of extracellular histones toxicity, neutralising histone-induced toxicity has been demonstrated using antibodies to histones or activated protein C (APC) [14]. APC was found to cleave extracellular histones thereby reducing their toxicity. Co-infusing APC and histones resulted in significant improvement in mice survival [14]. Since this discovery, a series of substrates have been reported to reduce histone-induced toxicity, such as C-reactive protein (CRP) [91], heparin [92] and 10% Fetal calf serum (FCS) [93], which will be explained in the following sections.

1.3.1 Detoxification of extracellular histones

Recently, our group has found that the immune response plays a key role in detoxifying circulating histones. High levels of acute phase proteins (APP) are produced in response to infection, inflammation, injury and malignancy [14], which are regulated by cytokines such as interleukin (IL)-1, IL-6, IL-8 and TNFα [15-17]. We have shown that extracellular histones trigger leucocytes to release pre-synthesized IL-6, which in turn induces CRP release. CRP can then complex with histones to prevent histone-membrane binding. Histological examination showed that CRP-infusion reduced lung oedema, haemorrhage and thrombosis in mice challenged by a lethal dose of histones to rescue these mice. Clinically, CRP takes 4-6 hours to reach levels that neutralize the toxicity of circulating histones. This has important clinical implications in defining a time-critical window for histone-targeted therapy.

1.3.2 Histone toxicity is buffered by plasma

Pemberton *et al* [93] demonstrated that exogenous histones are toxic to cultured mouse intestinal epithelial cells in serum-free medium, but toxicity was reduced in 10% FCS. Furthermore, they showed that the addition of histones to plasma induces protein precipitation characterised by increased turbidity [93] and protein depletion following centrifugation of histone-treated plasma. Pemberton *et al* identified a total of 36 histone-associated plasma proteins by shotgun proteomic analysis. These included complement related proteins, coagulation factors, protease inhibitors and lipoprotein-associated proteins [93].

To clarify this in a clinical context, our group used serum from trauma, sepsis and acute pancreatitis patients and found that it was toxic to cultured endothelial cells once histone levels exceeded 50 µg/mL. Using normal serum supplemented with calf thymus histones, a similar dose response was seen. This therefore suggests that both serum and plasma is able to buffer up to 50 µg/ml histones when in the circulation but when this dose is exceeded, histone-induced toxicity can be observed. Indeed, investigating a cohort of patients with non-thoracic blunt trauma and examining the development of respiratory failure showed that this cutoff level for circulating histones was clinically relevant. Specifically, 76.5% of patients with circulating histones equal to or greater than 50 µg/mL, developed respiratory failure compared with 18.8% of patients below this threshold [48].

1.3.3 Heparin

The nonspecific binding of heparin to histones by Western blot analysis was reported in 1999 [94]. This study has further confirmed that heparin binds to histones and ribosomal proteins with high affinity after cell necrosis, whereas heparin did not bind to live cells [95]. Recently, non-anticoagulant heparin has been shown to prevent histone-induced toxicity both *in vitro* and *in vivo* at a low-dose [92].

1.3.4 Anti-histone antibodies

Autoantibodies to histones have been found in autoimmune diseases especially in SLE[96, 97]. Murine monoclonal antibodies (mAbs) to histones (LG2-1, LG2-2 and BWA3) have been developed and produced by Monestier *et al.* in 1993 in order to investigate chromatin proteins in the expansion of auto-reactive B cells [98]. LG2-1 binds H3 at residues 30-45, whereas LG-2 targeted H2B at residues 1-13. More interestingly, BWA3 was found to bind

both H2A and H4 at residues 1-20 and 1-29, respectively. These three antibodies bind to histones; because their complementarily determining regions (CDRs) are negatively charged and could interact with the positively charged histones [98]. The BWA3 mAb had been firstly used in 2009 to reduce histone-induced toxicity *in vivo* [14]. Since then, several researchers have used the BWA3 mAb to protect against histone-induced toxicity and lethality in various diseases models [43, 48, 88, 99, 100]. Anti-histone antibody protected mice against transfusion-related acute lung injury, and also attenuated acute lung injury in a murine model of trauma and in a histone-infusion mouse model [43, 48, 88]. Moreover, antibodies to histones neutralized the immunostimulatory effects of histones, inhibited intra-renal inflammation and neutrophil infiltration [99], and reduced neutrophil recruitment by necrotic cells [100].

1.4 Antibody structure and function

Immunoglobulins or antibodies are secreted by B Cells, in order to specifically bind and neutralise pathogens (such as bacteria and viruses) beyond innate immune responses [101]. There are several classes of antibodies, IgG (146 kDa) comprises 70-75% of circulating immunoglobulins, IgM (194 kDa) comprises about 10%, IgA (192 kDa) comprises about 15-20% and IgD comprises only less than 1% [102], as well as IgE [103]. Moreover, IgM and IgD make up the primary response, and IgA, IgG, and IgE are related to secondary response. An antibody (e.g. IgG) normally consists of 2 copies of heavy and light chains (Fig 1.2) [104] to form a "Y" shape protein held by disulphide bounds [101]. Each heavy (~55 kDa) and light (~25 kDa) chain has a constant and variable region, respectively [103]. Each variable domain has three hypervariable loops to determine antigen specificity known as complementarity determining regions (CDRs) [101]. The CDRs in heavy and light chains can be specific to determine the binding sites of antigen, especially heavy chain CDR3 (Fig. 1.4)

[105, 106]. The light chain has only one constant domain whereas the heavy chain has three domains: CH1 is the first domain link with variable region and following is CH2 and CH3, form the Fc fragment of the antibody. The Fc fragments have their own functions, for example, C1q also can bind to CH2 domain on IgG [107] and interacts with Fc receptors [104]. The heavy chain constant domains can be altered, yet the antigen specificity is still remained [104].

Neutralization, opsonization and complement activation are the major function of antibodies in the adaptive immune system. (a) Neutralization is the best known function. Antibodies bind to invading pathogens or their toxic products in order to block their interaction with the host cells [101]. (b) Opsonization is a process by which an antibody-antigen (e.g. bacteria, viruses, as well as fungi [108]) complex is eliminated by a phagocyte [101]. (c) Once antibodies bind to antigens, complement classical pathways are activated by C1q that bind to antibody-antigen complexes. Moreover, complement components are either deposited on a bacterial surface to kill bacteria directly or indirectly by phagocytosis [101, 109].

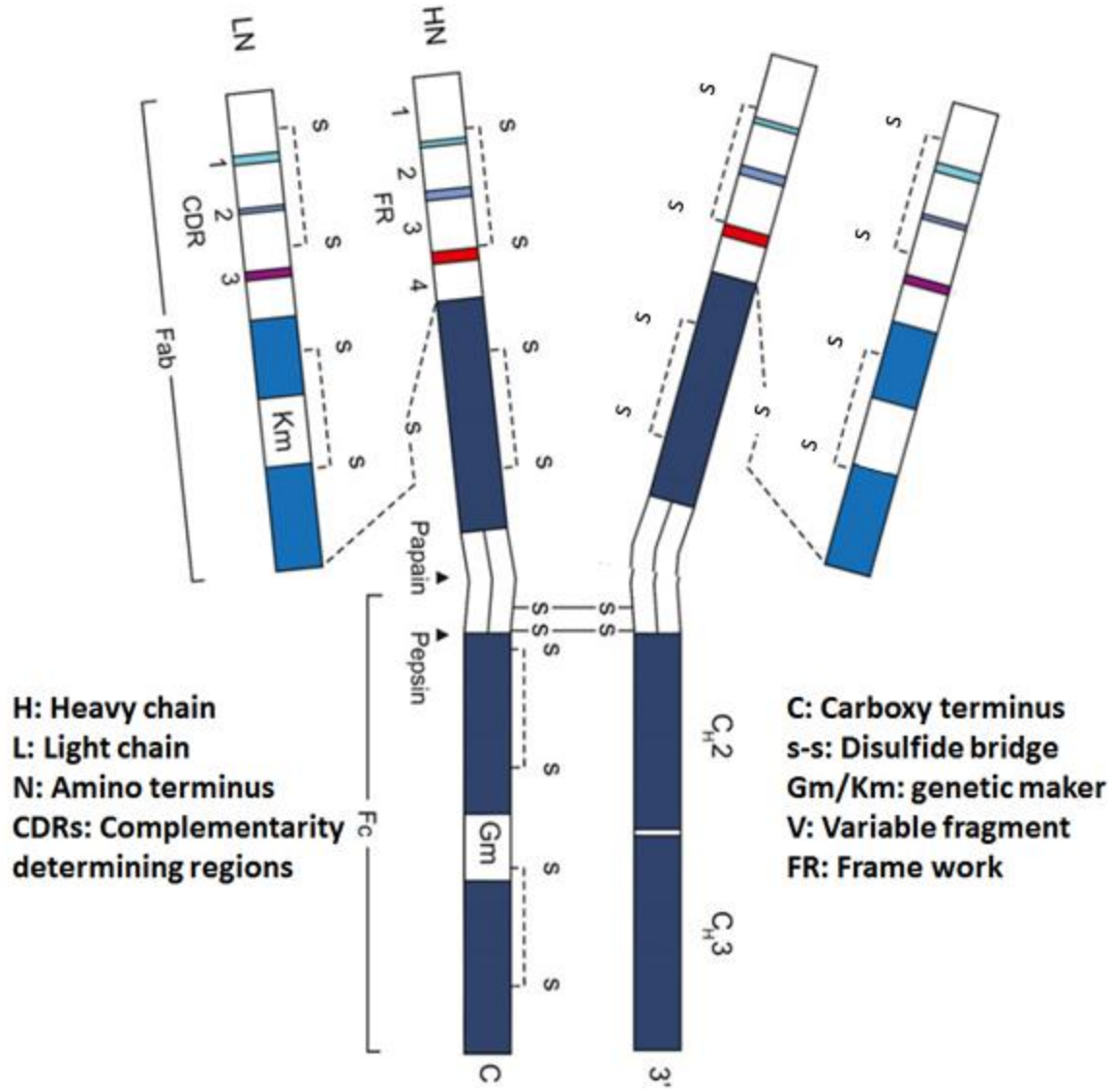

Figure 1.4 Typical antibody structure (known as IgG). This figure is adapted from reference [104]. Light and heavy chains are linked by disulphide bounds. Each chain contains variable regions including CDRs.

1.5 Antibody production

Antibodies are normally secreted from B lymphocytes of the adaptive immunity, to eliminate invading pathogens (e.g. bacteria, viruses and fungi) by specifically binding the antigens. Despite their intended protective nature, antibodies can be harmful. Serum containing polyclonal antibodies obtained from human placentas could prevent measles in the late 1930s [110]. However, it was noticed that mixed immunoglobulins from serum could induce systemic harmful reactions when they were intravenously injected into immunodeficient patients [111] thus purified IgG polyclonal antibodies were preferred [112]. A breakthrough was made by Kohler and Milstein [113] who first developed monoclonal antibody specficity to an eptitope in late 1970s. This opened a new gate for antibody therapy, as well as for molecular biology research [113]. With the development of recombinant DNA technology [114], antibody fragments could also be produced in *E. coli* [115] after screening the phages with high affinity to specific epitopes using phage display [116], RNA-display [117] and even DNA-display [118]. However, most antibody fragments expressed in *E.coli* are not soluble [119], spurring efforts to investigate refolding methods [119, 120] to produce soluble antibody fragments that could be used for futher applications [121].

1.5.1 Polyclonal antibodies

Polyclonal antibodies, as the name suggests, recognize at least one or more epitopes to the antigen. In 1890, the immunized rabbit serum with tetanus toxin rescued tetanus-challenged animals [122], suggesting that potential molecules in the serum can specificially target the tetanus toxin to reduce its toxicity. This was later called ‘serum therapy’ [123]. Injected serum however, could cause hypersensitivity reactions [123], therefore purified antibody-

based therapies [124] are more appropriate. Efficiency may be further enhanced by intravenously injecting purified polyclonal antibodies into the host [125].

Polyclonal antibodies are normally isolated from hyper-immunised rodents or rabbits [126, 127]. Subsequently, large-scale polyclonal antibodies could also be obtained from hyperimmunised cattle using transgenic procedures [128]. However, the binding efficiency of polyclonal antibodies to antigen is low, as the functionality and specificity suffers from batch-to-batch variation [126].

Table 1.3 Polyclonal antibody comparison with monoclonal antibody [126].

Polyclonal antibody	Monoclonal antibody
Animal (e.g. mouse) needs to be immunised with specific antigen	
Purified from serum	B cells from immunised animal are fused with myeloma cell to form hybridoma
Technology and skills required are low	Technology and skills required are intensive
Time period is relatively short	Time period is long due to hybridoma work
Recognise multiple epitopes of specific antigen	Only binds to one epitope on antigen
Each lot differs	Hybridoma secreting the same antibody, and each batch is the same

1.5.2 Monoclonal antibodies

In 1975, Kohler and Milstein developed mouse monoclonal antibodies [113]. They used B cell to hybridise with immortalized myeloma to form a new cell, called a hybridoma. A hybridoma retains the ability of the B cells by secreting specific monoclonal antibody, but has an infinite lifespan owing to the myeloma cell [113]. It is a milestone for antibody production (Fig 1.5). Monoclonal antibodies are good tools for scientific research [129] and more importantly, they can be used in immunotherapy, such as murine monoclonal antibody to CD3 had been approved by the US Food and Drug Administration in order to treat acute transplant rejection [130]. Since then, this technology has been widely used, and antibodies are being developed to serve as new therapies for the treatment of cancer, autoimmunity and inflammatory diseases [131] are ongoing. Monoclonal antibodies have many advantages over polyclonal antibodies. Table 1.3 summarises the differences between polyclonal and monoclonal antibodies.

A downside to injected murine monoclonal antibodies is that it could induce self-antibody production (autoantibodies) in a bid to neutralize or eliminate the therapeutic antibodies [132, 133]. Subsequently, human monoclonal antibody to Epstein-Barr virus (EBV) was then developed, but the production quality is low [134, 135]. Human antibody production in animals using TransChromo (TC) technology was developed, where a human chromosome fragment (HCF) as a vector containing human DNA was integrated into the genome of TC mouse™ [136]. In this way, the chance for self-antibody production against therapeutic antibody is greatly reduced. Such mice then rearrange human immunoglobulin genes and generate human antibodies.

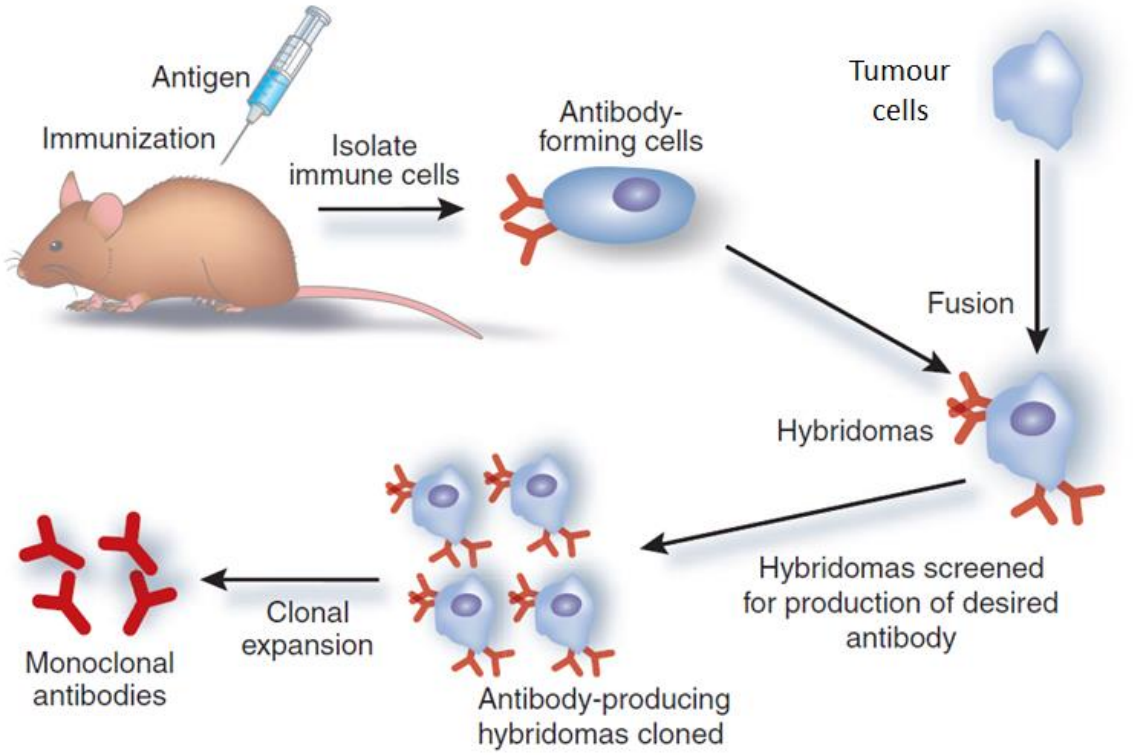

Figure 1.5 A typical monoclonal antibody production flow. This figure is adapted from [137]. Polyclonal antibodies can be harvested from immunized host (such as mouse), alternatively, antibody-forming cells can be fused with tumour cells to form hybridomas in order to secrete monoclonal antibody [137].

1.5.3 Recombinant antibodies

In 1973-1974, recombinant DNA technology has been developed [138]. The first licensed drug generated by this technology was insulin [139]. Antibody fragments were also developed using recombinant DNA technology, particularly the recombinant fragment antigen binding regions (Fab) [115] and single chain variable fragment (scFv) [140] are expressed in *E. Coli* and those fragments became popular antibody fragments generated with this technology. Both antibody fragments have been successfully produced and assayed. Due

to antigen binding regions of an antibody in heavy and light chain variable regions, and the complementarity determining regions (CDRs) from both chains determine the specificity of the antibody. The murine CDRs could be inserted into human antibody framework to replace its CDRs and form a humanised antibody to recognise the desired antigens [141]. In addition, antibodies could also be expressed intracellularly using mammalian cells [142]. More recently, a novel tool for rapid cloning and expression of recombinant antibodies has been investigated and developed [143]. The antibody heavy and light chains are assembled in a one-step process by cloning them into a single mammalian expression vector. The antibody was then expressed via DNA encoding the specific variable and constant regions rapidly. It increased confidence of *in vitro* antibody production [143].

To further improve the process, knowing the peptide sequence of the specific antibody is crucial. Moreover, researchers could use the same condition and peptide sequence to produce the heterogeneous binding antibodies [129]. Therefore, a novel proteomic approach to produce a recombinant monoclonal antibody has recently been developed in 2012 [144]. Briefly, polyclonal antibodies from an immunized rabbit were purified by chromatography, digested with multiple enzymes and mapped using tandem mass spectrometry (MS/MS). The determined CDRs especially CDR3 have been screened and assumed to be a high affinity and specificity antibody. This antibody was then expressed and secreted *in vitro* [144]. This technology has been lauded for furthering recombinant monoclonal antibody production.

1.5.4 Phage display

The process of antibody variable fragments successfully displayed on the phage surface by inserting antibody coding DNA sequence into phage genomes [116], is called phage display [145]. In general, phage display uses recombinant DNA technology to replicate DNAs

encoding desired polypeptides [145]. In the same way, cDNA coding human antibody heavy and light chain variable regions are from the V gene repertoires of lymphocytes and expressed on the surface of filamentous bacteriophage [146]. The displayed antibodies are specific for a particular antigen, which can be isolated with biopanning [147].

1.5.5 mRNA and DNA display

RNA display is a type of technique that creates a library of fusion products of coding RNAs or DNAs and their corresponding polypeptides generated by nucleotide synthesis and *in vitro* translation systems [148, 149]. Using target antigen, the polypeptides that have strong binding affinity to the antigen can be pulled down and the fused RNA or DNA coding sequence for the polypeptides will be recovered and used for expressing the polypeptide in a large scale using designated expression system [150].

The simple diagram of this new technique is as follows:

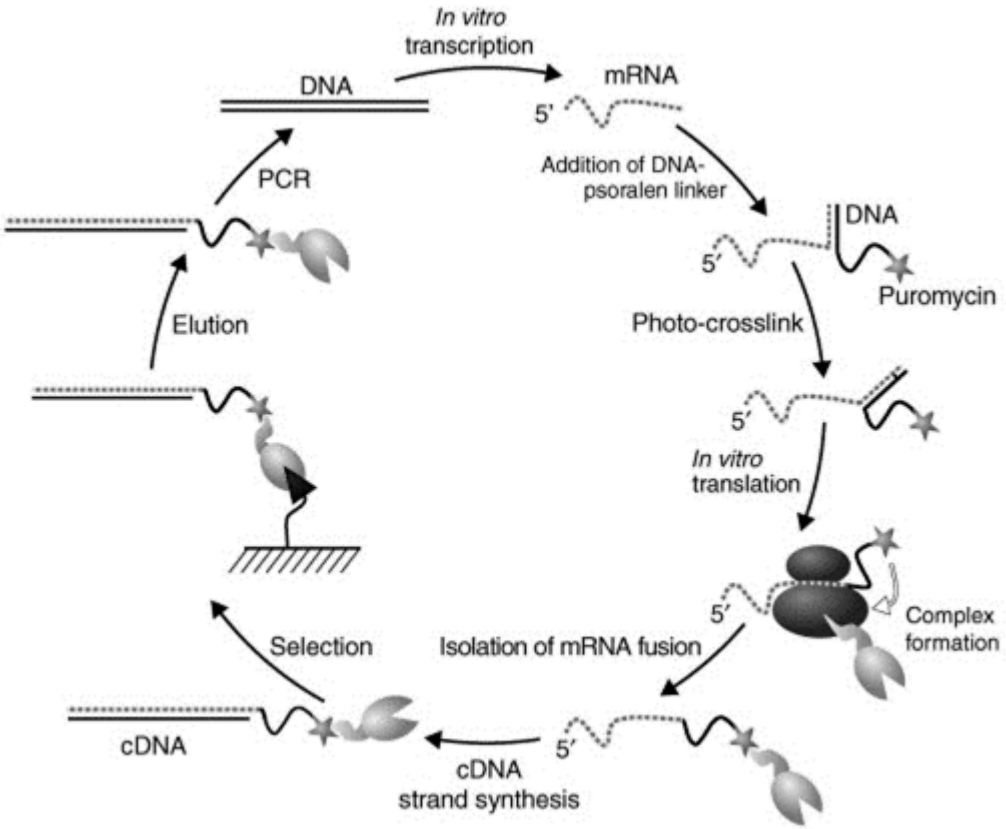

Figure 1.6 Overview of RNA display. This figure is adapted from reference [149] and advance developed in reference [151].

This technique has advanced the phage display and is more effective and straight forward in screening polypeptides that bind to specific antigens [152]. However, this is not suitable for antibody screening because antibody is a large and complicated molecule composed of two heavy and two light chains.

1.6 Mass spectrometry approaches

The principle of mass spectrometry (MS) is used for measuring the mass or the mass-to-charge ratio (*m/z*), including the ionization source, the mass analyser and the detector. Performing single and tandem mass spectrometry are two classes of proteomics [153]. Mass

spectrometry is a powerful tool for proteomic applications including sample approaches and bioinformatics tools (e.g. PEAKS) for data analysis [154]. On the other hand, mass spectrometry can also study human diseases and translate to the clinical setting and as such identity potential biomarkers [155].

Tandem mass spectrometry (MS/MS) has become an increasingly reliable tool to identify proteins, because the mass of the fragmented peptides could be measured [156]. MS is widely used to characterize proteins in order to investigate the process of cell biology, especially for protein identification [157]. The purified proteins are normal separated using sodium dodecyl sulphate polyacrylamide gel electrophoresis (SDS-PAGE), as well as two dimensional gel electrophoresis, which can separate proteins according to their molecular weight or isoelectric point (PI). The bands or spots are cut into slices and digested with specific enzyme (e.g. Trypsin), known as in gel digestion [158]. The digested proteins are normally paired with liquid chromatography MS/MS (LC-MS/MS) [158] (Fig. 1.7). For MS spectra data analysis after MS/MS, there are several approaches to search databases using genomes with the uninterpreted experimental MS/MS data, such as Mascot [159] and Sequest [160]. However, these software could give a false or incorrect identification [161]. Effective software for spectra analysis has been designed, known as PEAKS. This novel approach has multiple functions including *de novo* sequence, post-translational modification and SPIDER, which can easily align the peptide sequence [161, 162].

This method is ideal for isolating human antibodies and reproducing them by recombinant DNA technology. In chapter 3 and 4, MS/MS was used to identify the antibodies peptide sequence, as well as investigate the histone binding proteins from serum.

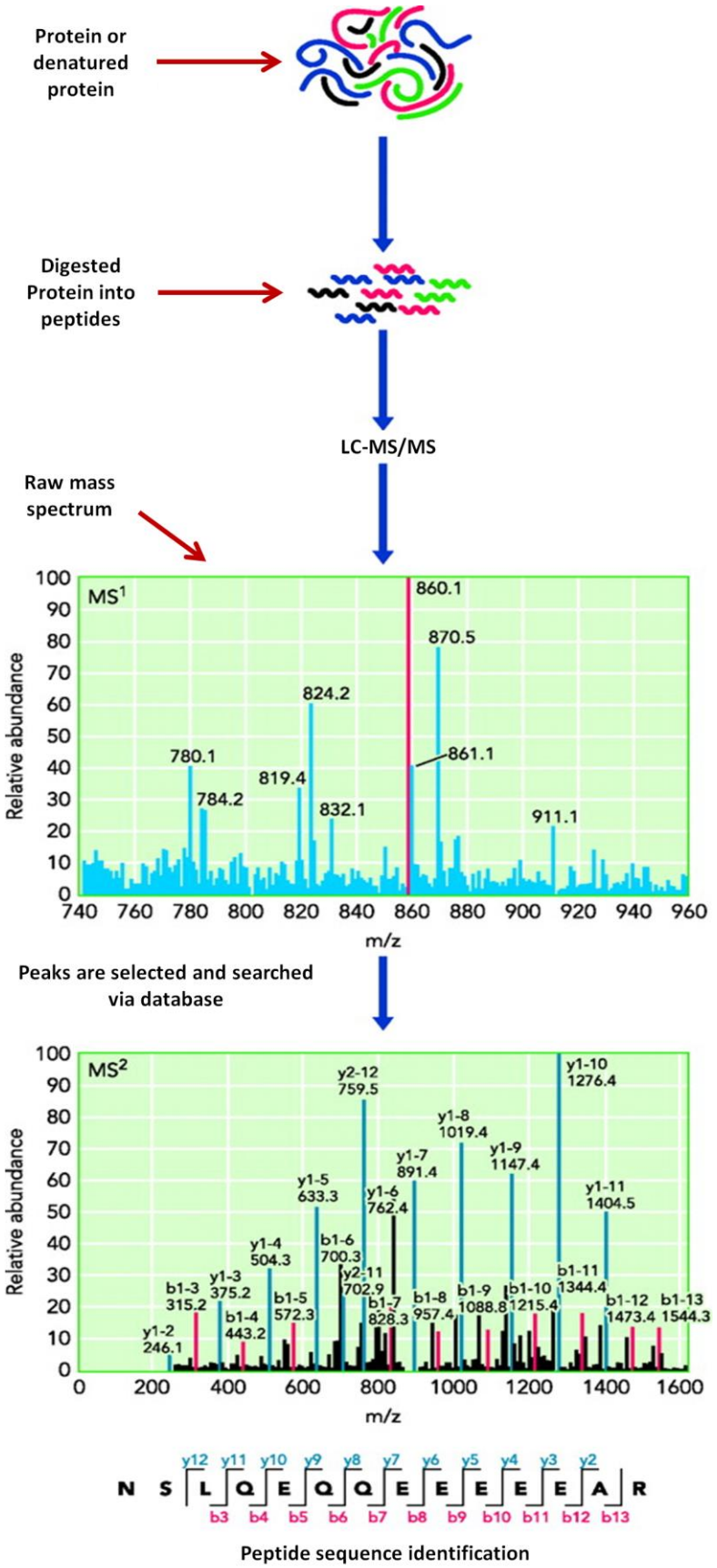
Protein or denatured protein
Digested Protein into peptides
LC-MS/MS
Raw mass spectrum
MS1
Relative abundance
m/z
860.1
870.5
824.2
780.1
861.1
819.4
784.2
832.1
911.1
Peaks are selected and searched via database
MS2
y2-12 759.5
y1-10 1276.4
y1-8 1019.4
y1-9 1147.4
y1-7 891.4
y1-5 633.3
y1-6 762.4
y1-11 1404.5
b1-6 700.3
y1-4 504.3
y2-11 702.9
b1-11 1344.4
b1-3 315.2
y1-3 375.2
b1-5 572.3
b1-7 828.3
b1-8 957.4
b1-9 1088.8
b1-10 1215.4
b1-12 1473.4
b1-13 1544.3
b1-4 443.2
y1-2 246.1
N S L Q E Q Q E E E E E A R
Peptide sequence identification

Figure 1.7 Overview of LC-MS/MS. This figure is adapted from reference [163]. Proteins can be digested by enzymes such as trypsin to form peptides. Peptides are further investigated in LC-MS/MS in order to acquire the raw mass spectrum. Each single peak is selected and searched via database.

Chapter 2 Production of Mouse Anti-Histone and Humanized Anti-Histone Antibody Fragments to Block Histone Toxicity

2.1 Introduction

Currently, there are no commercial anti-histone antibodies available for *in vivo* interventions. Much of our research work requires *in vivo* experiments with a large quantity of anti-histone antibodies [14, 48]. Moreover, circulating histones play important pathological roles in many critical illnesses, such as severe trauma, sepsis and necrotizing pancreatitis and as such anti-histone therapy is needed [48]. Clinically, a humanised anti-histone antibody has great potential to be used as a major anti-histone reagent. In this chapter, I first produced a MahscFv and tested its function in reducing histone toxicity. Then, I generated a humanised anti-histone scFv (HahscFv) by transferring the CDRs from the MahscFv to a human scFv. In addition, the MahscFv was conjugated with Fc fragments in order to enhance the clearance of antigen-antibody complexes by macrophages *in vivo* and the effectiveness tested in mice. For negative controls, control scFv (cscFv) and S100P protein were produced for certain experiments.

2.2 Methods

2.2.1 Competent bacteria preparation with Rubidium Chloride

Rubidium Chloride was used in the production of competent *E. coli*. Bacteria were cultured in 100 mL Luria-Bertani (LB) broth (Sigma, USA) to reach an optical density (OD) of 0.5 at absorbance 600 nm. Incubated broth was chilled on ice for 15 min, before centrifugation at 4,000 × g, 4 °C for 10 min. The resultant pellet was resuspended in 35 mL of ice cold RF1 (100 mM RbCl, 50 mM $MnCl_2$, 30 mM KAc, 10 mM $CaCl_2$, 15% (v/v) Glycerol, pH 5.8) and incubated for 15 min on ice. The resuspended pellet was then centrifuged again as mentioned above. The pellet was next resuspended in 8 mL ice cold RF2 (10 mM MOPS, 10 mM RbCl, 75 mM $CaCl_2$, 15% (v/v) Glycerol, pH6.8) and incubated for 15 min. 100 µL aliquots of the bacterial suspension were retained and stored at – 80 °C.

2.2.2 Bacterial transformation with plasmids

Bacterial heat-shock transformation was employed as previously describe [164]. Plasmid amplification was performed using Subcloning Efficiency™ DH5α™ Chemically Competent Cells *E. coli* (Invitrogen, USA). 2 µL of plasmid (the plasmid construction will be mentioned in section 2.2.7) was added to 50 µL of DH5α *E. coli* and incubated on ice for 20 min, followed by 45 s at 42 °C in water bath for the heat-shock step. DH5α were immediately transferred on ice. Next, 250 µL of LB broth was added and the mixture incubated at 37 °C for 45 – 60 min. After incubation, transformed DH5α *E. coli* were harvested at 6,000 × g for 5 min. The resultant pellet was then spread on an agar plate containing 100 µg/mL ampicillin (Sigma, USA) and incubated at 37 °C for 16 h.

2.2.3 Plasmid amplification

Following the manufacturer's protocol, a single colony of DH5α *E. coli* containing plasmid was selected and incubated in 6 mL LB broth containing 100 µg/mL ampicillin for 16 h at 37 °C and 180 rpm. After incubation, the DH5α *E. coli* suspension was centrifuged at 3,000 × g for 20 min. The harvested pellet was dried at room temperature for 20 min and resuspended with 250 µL buffer P1 (QIAprep Spin Miniprep Kit, QIAGEN) and transferred to a 1.5 mL Eppendorf. 250 µL of buffer P2 was then added to the cell lysis for no more than 5 min. 350 µL of buffer P3 was then added to neutralise the solution and centrifuged at 16,000 × g for 15 min. The supernatant containing the plasmid was then applied to a QIAprep spin column for 1 min and centrifuged for 1 min. 500 µL of buffer PB was added and incubated for 1 min and centrifuged. The column was then washed with 750 µL of buffer PE for 1 min and centrifuged. DNA was finally eluted with 50 µL of H_2O.

2.2.4 Restriction enzyme digestion and agarose gel electrophoresis

After plasmid elution using QIAprep Spin Miniprep Kit, 10 µL of plasmid was digested by restriction enzymes NdeI (NEB, USA) and BamHI (NEB, USA) at 37°C for 1 h. The digested DNA and 1 µL 2-log DNA Ladder (0.1-10.0 kb) (NEB, USA) were analysed by gel electrophoresis on a 1% (w/v) agarose gel. Images were taken under a UV light.

2.2.5 Large-scale plasmid amplification

Large-scale plasmid amplification was performed using a Midiprep Kit (Qiagen, Netherlands), as in the manufacturer's instruction. A single colony of DH5α *E. coli* was selected and grown in 5 mL of LB broth containing 100 µg/mL ampicillin at 37 °C for 8 h. This was then transferred to 100 mL of LB and grown for 16 h under the same conditions.

The DH5α *E. coli* were then harvested at 6,000 × g for 15 min at 4 °C, and the pellet resuspended with 4 mL of buffer P1. Cells were lysed with 4 mL of buffer P2 for 5 min, followed by neutralisation with 4 mL of buffer P4, before incubating the mixture on ice for 15 min. The resulting mixture was centrifuged at 20,000 × g for 30 min at 4 °C and the supernatant applied to a pre-equilibrated (with 4 mL of buffer QBT) QIAGEN-tip 100 column. Next, the column was washed with 10 mL of buffer QC twice. The DNA was eluted with 5 mL of buffer QF, precipitated by 3.5 mL isopropanol and centrifuged at 26,891 × g for 30 min at 4 °C. The DNA pellet was then washed with 2 mL of room-temperature 70% (v/v) ethanol and centrifuged for 10 min. The DNA pellet was then air-dried before resuspension with 200 µL H_2O.

2.2.6 DNA extraction using QIAquick Gel Extraction Kit (QIAGEN, Netherlands)

30 µL of purified Plasmid from the Midiprep above was digested with restriction enzymes NdeI (NEB, USA) and BamHI (NEB, USA) for 1 h at 37 °C. After digestion, DNA fragments were then separated by gel electrophoresis using 1% (w/v) Tris borate EDTA (TBE) agarose. After electrophoresis, the DNA band was isolated under UV light and placed in a universal tube. The gel was then extracted using a QIAquick Gel Extraction Kit. Briefly, three times the gel weight of buffer QG was added and heated at 50 °C for 10 min until no agarose gel pieces were left. An equal volume of isopropanol to gel weight was added and subsequently mixed. 750 µL of the mixture was then loaded onto a QIAquick column to bind DNA and centrifuged until all the solution was applied. 500 µL of buffer QG was added to column in order to remove all trace of agarose gel. The column was then washed with 750 µL of buffer QE and the DNA finally eluted with 50 µL of H_2O.

2.2.7 Ligation

To express the above proteins in *E. coli*, the pET-16b vector (Novagen, Germany) was used to ligate the coding DNAs including MahscFv, HahscFv, HahscFv-Fc and control scFv (CscFv). The pET-16b vector containing T7 expression system was digested with NdeI and BamHI and extracted using a QIAquick Gel Extraction Kit. Coding sequences for MahscFv were synthesized by GENEWIZ (USA), HahscFv and CscFv were synthesised by Life techonologies (Waltham, USA) with NdeI and BamhI restriction sites on 5' and 3' ends, respectively. The plasmids containing these coding sequences from the company were also digested with NdeI and BamHI restriction enzymes and the DNA fragments containing these coding sequences were separated from its vector using agarose gel electrophoresis and extracted using QIAquick Gel Extraction Kit. 4 µL of pET-16b vector and 12 µL of an insert (coding DNA) were mixed with 2 µL of T4 ligase buffer and 2 µL T4 ligase (NEB, USA) each, and incubated at room temperature for 1 h. After ligation, 5 µL ligation mixture was then transformed to DH5α competent cells *E. coli* and incubated on an LB agar plate containing 100 µg/mL ampicillin at 37 °C overnight.

2.2.8 DNA sequencing

To confirm that the DNA sequences were correct, the purified plasmids were sequenced by Beckman Coulter Genomics (Takeley, UK).

2.2.9 Protein induction

2 µL of plasmid was transformed into C41 (DE3) *E. coli*. The following day, single colonies were selected and each incubated in 3 mL LB broth containing 100 µg/mL (w/v) ampicillin for 1 h at 37°C. Bacteria were then induced at 37°C for 4 h with 1 mM IPTG (Melford, UK),

with a non-induced colony acting as negative control. After incubation, 1 mL of bacteria was centrifuged at 16,000 × g for 30 s. The pellet was re-suspended with 100 µL H_2O, then 20 µL of the cell lysate was analysed by 15% SDS-PAGE. Once the small scales induction was successful, a large scale induction was conducted. Bacteria were continually incubated in 500 mL LB broth containing 100 µg/mL ampicillin at 37°C and the bacteria optical density (OD_{600}) measured at 600 nm until reaching an OD reading of between 0.5 and 0.6. The bacteria were subsequently induced at 37°C for 4 h. The non-induced and induced bacteria were then run on a 15% SDS-PAGE.

2.2.10 Protein purification using a Nickel-Nitrilotriacetic acid (Ni-NTA) resin (QIAGEN, USA) column

After large scale induction, bacteria were harvested at 6,000 × g for 10 min at 4 °C. The pellet was resuspended in lysis buffer (50 mM Tris-HCl, pH7.4, 500 mM NaCl), and sonicated for 3 min with a rest period of 3 min on ice and repeated twice. The supernatant was then acquired through centrifugation at 26,981 × g for 30 min at 4 °C. The remaining pellet was resuspeneded with denaturation buffer (8 M urea, 50 mM Tris-HCl, pH7.4, 500 mM NaCl) and the sonication repeated. In order to identify the MahscFv, each supernatant was run on a 15% SDS-PAGE. For the native purification step, the MahscFv supernatant was applied to a Ni-NTA resin (QIAGEN, USA) column and washed with wash buffer (50 mM Tris-HCl, pH7.4, 500 mM NaCl, 50 mM Imidazole). MahscFv was eluted with native elution buffer (50 mM Tris-HCl, pH7.4, 500 mM NaCl, 250 mM Imidazole), and dialysed against PBS, exchanging the buffer twice in cold room. For MahscFv denaturation purification, the denatured inclusion bodies are also applied to a Ni-NTA resin (QIAGEN, USA) column, washed with denaturation wash buffer (8 M urea, 50 mM Tris-HCl, pH7.4, 500 mM NaCl, 50 mM Imidazole) and eluted with denaturation elution buffer (8 M urea, 50 mM Tris-HCl,

pH7.4, 500 mM NaCl, 250 mM Imidazole). The denatured MahscFv is refolded against a gradient urea concentration (4, 2, 1, and 0.5 M urea) using dialysis, and the buffer finally exchanged with PBS.

2.2.11 SDS-PAGE and Coomassie brilliant blue staining

Proteins were loaded into 10 – 15% SDS-PAGE and subjected to electrophoresis at 30 mAMP/gel for 1 h. Following electrophoresis, the gels were stained using Coomassie brilliant blue staining buffer containing 0.25% (w/v) Coomassie brilliant blue, 10 % (v/v) acetic acid and 30% (v/v) methanol for 30 min at room temperature, as described in [165]. After staining, the gel was destained with 10% (v/v) acetic acid and 30% (v/v) methanol for 6 hours, changing the destaining buffer four times.

2.2.12 Antibody conjugation to peroxidase

100 µL of ultra-pure H_2O and ~1 mg of purified antibody was added into EZ-Link™ Plus Activated Peroxidase (Thermo Fisher, USA), 10 µL of Sodium cyanoborohydride solution (Sigma, USA) was also mixed with the solution and incubated at room temperature for 1 h. After incubation, 20 µL Ethanolamine was added and incubated for 15 min at room temperature. Following conjugation of MahscFv-HRP, the solution was stored at 4°C for up to two weeks to preserve the activity.

2.2.13 Western blotting

2 µg of recombinant histone H1, H2A, H2B, H3 and H4, 10 µg of calf thymus histone and 5 µg of S100P (negative control) were loaded onto a 15% SDS-PAGE and run at 30 mAMP/gel

for 1 h, then transferred onto a 0.45 µm Immobilon®-P PVDF Membrane (Millipore, USA) at 400 mAmp for 1 h. The membrane was then blocked with 25 mL of blocking reagent 5% (w/v) Instant dried skimmed milk (Tesco, UK) and 2% (w/v) Bovine Serum Albumin (BSA) (Sigma, USA) suspending in Tris buffer saline Tween-20 (TBS-T) for 1 h at room temperature. The membrane was then incubated with MahscFv-HRP (1:500) (v/v) in block reagent for 1 h at room temperature, the membrane was also incubated with 5 µg/mL of HRP only as a control. After incubation, the membrane was washed 3 × with TBS-T and the MahscFv-HRP signals evaluated by Immobilon™ Western Chemiluminescent HRP Substrate (Millipore, USA) for 3 min at room temperature. Images were acquired using G:Box gel imaging system (Syngene, India) and software GeneSnap (Syngene, India). Alternatively, after membrane blocking, mouse primary antibody IgG was incubated using the same reagents for 16 h at 4°C, and subsequently anti-mouse IgG-HRP secondary antibody (1:10,000) was incubated with membrane for 1 h at room temperature (RT). The image was acquired using chemiluminiscent detection with G box gel imaging system (Syngene) and software GeneSnap (Syngene).

2.2.14 Protein concentration determination using Bradford assay and NanoDrop

Bradford assay, the concentration of purified proteins was tested using a *DC*™ Protein Assay (Bio-Rad, USA) and the Quick Start™ BSA standard set (Bio-Rad, USA) referring to the instruction manual. Briefly, 5 µL of standards and samples were loaded into a 96-well-plate and 25 µL of a mixture of reagents S and A (20 µL reagent S and 1 mL reagent A) were added into each well. 200 µL reagent B was finally added to each well, and incubated at room temperature for 15 min. The absorbance of the samples was read at 750 nm absorbance and the protein concentrations calculated using BSA standard curve.

Nanodrop, Protein concentration calculation have been described in details using nanodrop [166]. Here, the Nanodrop ND-1000 Spectrophotometer (USA) was used for calculation of antibody concentrations using OD readings at 280 nm. 2 µL of H_2O was initially applied to the nanodrop, and the 2 µL of PBS was used as a blank. The protein concentrations were calculated using the mass extinction coefficient number (each protein has a unique coefficient number).

2.2.15 Functional assay

Cell death was investigated by staining damaged nuclei with propidium iodide (PI) [167]. Briefly, EA.hy926 cells (endothelial cells) were cultured at 37 °C and 5% CO_2 in T75 Flask to reach 90-100% confluence. Cells were washed twice with 10 mL of PBS and detached with 2 mL of versene solution (Life technologies, USA) for 10 min at 37 °C and 5% CO_2, and neutralised with 10 mL of advanced Dulbecco's modified eagle medium (DMEM) (Life technologies, USA) containing 20% (v/v) Fetal bovine serum (FBS) (Sigma, USA), 1% (v/v) penicillin-streptomycin (Pen Strep) (Invitrogen, USA), 1% (v/v) L-Glutamine 200 mM (Invitrogen, USA). The cell suspension was then centrifuged at 500 × g for 5 min. The cell pellet was resuspended with 24 mL media and 1 mL aliquoted in each well of 24-well-plate, and incubated at 37 °C under 5% CO_2 overnight. Cell confluence was examined the following day by microscopy. The cells were then washed twice with PBS and 200 µL of treatment was then added into each well and incubated at 37 °C under 5% CO_2 for 1 h. 10 µg/mL of PI solution (Sigma, USA) was added into each well and incubated for 10 min under same conditions. After incubation, cells were detached with 40 µL of versene and washed with PBS twice by centrifugation at 500 × g for 5 min. Cells were finally resuspended into 200 µL of PBS and analysed using the BD FACSCalibur (USA) with the untreated controls designated as 100% viable and cell survival rates normalized thereafter.

The viability of EA.hy926 cells were also assessed by water-soluble tetrazolium salt (WST-8) cell proliferation assay kit (Enzo Life Sciences). 1.5×10^4 cells were cultured in a 96-well-plate using the same condition as above, until reaching 100% confluence. Firstly, cells were treated with a series of concentration of calf thymus histones (20, 30, 50, 100, 200 and 300 μg/mL) within 100 μL fresh media for 1 h, and washed by PBS twice. 10 μL of WST-8 dye was mixed with 100 μL fresh medium and incubated for 1 h. The absorbance (at a wavelength of 150 nm and a reference wavelength of 650 nm) of each well was finally measured using a plate reader (Multiskan Spectrum, Thermo Fisher Scientific). Cells were secondly treated with various concentrations of antibody (20, 50, 100, 200 and 300 μg/mL) for 5 min and subsequently treated with 250 μg/mL of calf thymus histones for 1 h. The measurement method was the same as above.

The assay for cardiomyocyte viability has been described in Dr Y. Alhamdi's publication [37]. Briefly, murine HL-1 cells (adult cardiomyocytes) [168, 169] were from Professor William Claycomb (Louisiana State University, USA) and cultured in Claycomb medium including 10% (v/v) FBS, 2 mM L-Glutamine, 100 U/mL Penicillin/Streptomycin and 100 μM Norepinephrin [169]. Cells were treated with 50 μL fully supplemented Claycomb media and 50 μL Septic patient's Sera to a 100 μL mixture into each well of 96-well-plate. Alternatively, 50 μg/mL of antibody was pre-treated with the HL-1 cells and septic sera were subsequently added. Cell viability was measured by WST-8 described as above.

2.2.16 MahscFv-Fc production

In order to eliminate any MahscFv-histone complexes in the circulating system during *in vivo* experiments and to demonstrate the solubility, MahscFv was ligated to a mouse Fc fragment from IgG1 [170]. This involved the design of a restriction site at each mouse Fc terminus

(NcoI and NdeI, respectively). The synthesised mouse Fc DNA was then digested with NcoI (NEB, USA) and NdeI, as well as the MahscFv plasmid (within pET-16b vector). The digested mouse Fc and MashcFv were ligated using T4 ligase buffer and T4 ligase (NEB, USA) to form a new plasmid MahscFv-Fc. The MahscFv-Fc was finally expressed in competent *E. Coli* BL21 (DE3) and purified using on-column refolding.

2.2.17 Binding assay using enzyme-linked immunosorbent assay (ELISA)

In order to investigate the binding between MahscFv and histones, two ELISA methods were developed. Method one involved 100 µL of ELISA coating buffer (50 mM Na_2CO_3, 50 mM $NaHCO_3$, pH9.6) containing 10 µg/mL of recombinant histones (H1, H2A, H2B, H3 and H4) which were individually coated onto a 96-well-plate overnight at 4°C. The next day, the plate was washed twice with PBS-T (PBS + 0.05% (v/v) Tween20), blocked with 5% (w/v) skimmed milk, 2% (w/v) BSA for 1 h and washed four times with PBS-T. The plate was then incubated with MahscFv-HRP (1:500) (v/v) containing PBS-T for 1 h at room temperature and then washed four times again. The MahscFv-HRP signal was assessed by 3,3,5,5-Tetramethylbenzidine (TMB) Substrate Reagent Set (BD,USA), and measured the absorbance at 450 nm. Method two utilized the fact that histones binding to streptavidin [171], whereby, 100 µL of 10 µg/mL MahscFv suspended within ELISA coating buffer was coated onto a 96-well-plate overnight at 4 °C. After washing and blocking the plate, various concentration of recombinant Histones were incubated for 1 h, and the washed plate then incubated with streptavidin-HRP for 30 min. The optimal density (OD) 450nm reading was acquired using the same procedure as in method one.

2.2.18 Animal experiments

Animal experiments were performed in China by Southeast University who holds the appropriate ethical approval. The full details of in mice experiments are described in Dr Yasir Alhamdi's paper [37].

2.3 Results

2.3.1 Diagrams of MahscFv, CscFv, MahscFv-Fc and HahscFv

Figure 2.1 shows schematic diagrams of mouse anti-histone scFv (MahscFv), control scFv (cscFv), MahscFv-Fc and humanised anti-histone scFv (HahscFv).

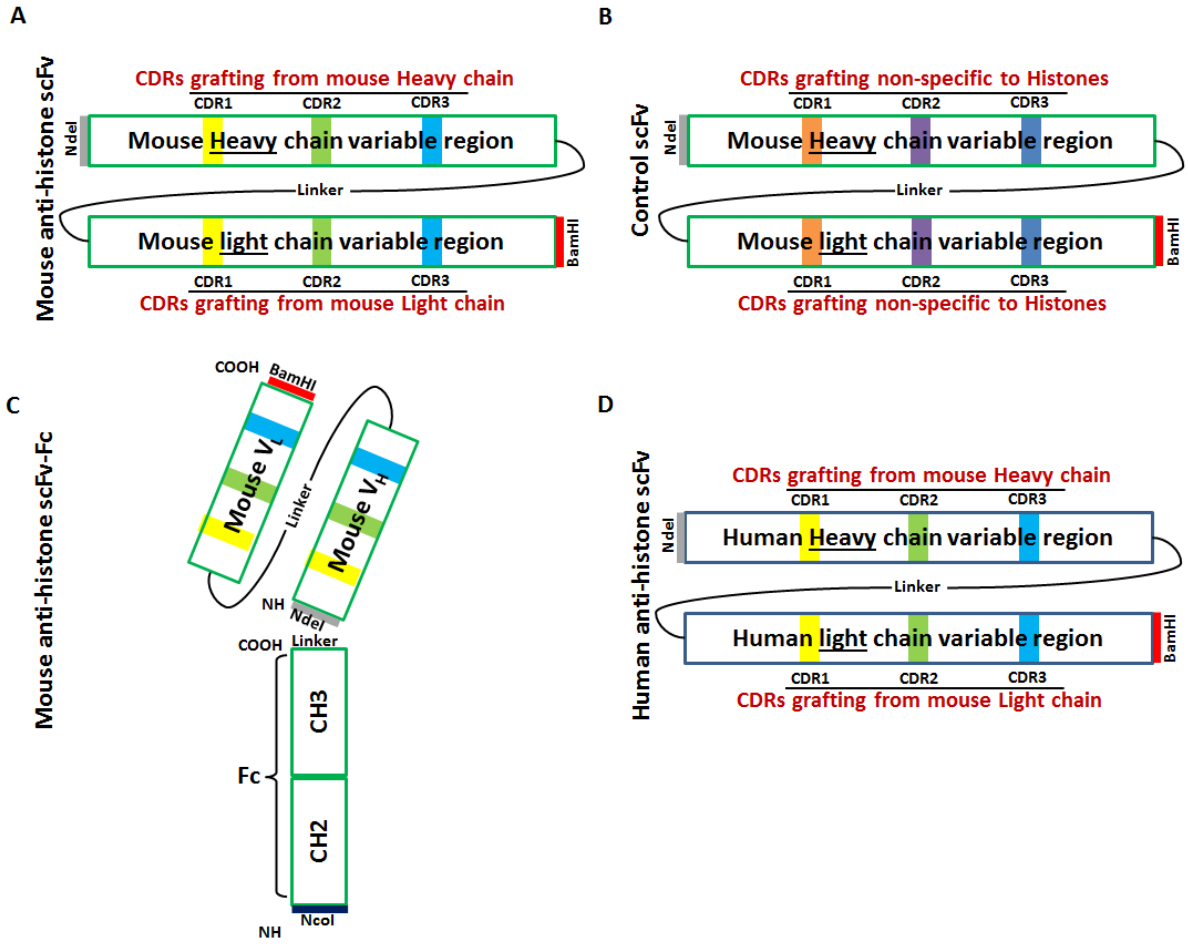

Figure 2.1 Schematic diagrams of MahscFv, CscFv, MahscFv-Fc and HahscFv. (**A**) Mouse anti-histone variable heavy and light chains were linked by a flexible linker (**B**) control scFv. (**C**) The MahcFv was linked to mouse IgG1-Fc fragment to form MahcFv-Fc. (**D**) CDRs of the MahscFv were used to replace CDRs of a human heavy and light chains to form a humanised anti-histone scFv (HahscFv).

2.3.2 Plasmids construction and proliferation

For plasmid construction and proliferation, a pET expression system was used [172]. scFvs were subcloned into pET-16b vector in an expression system that contains a T7 promoter and ampicillin resistant marker, as well as a His_{10}-tag. To ensure that the MahscFv DNA was successfully ligated to the pET-16b vector, the scFvs and pET-16b DNA were sequenced by SnapGene® and the plasmid maps are illustrated in Figure 2.2.

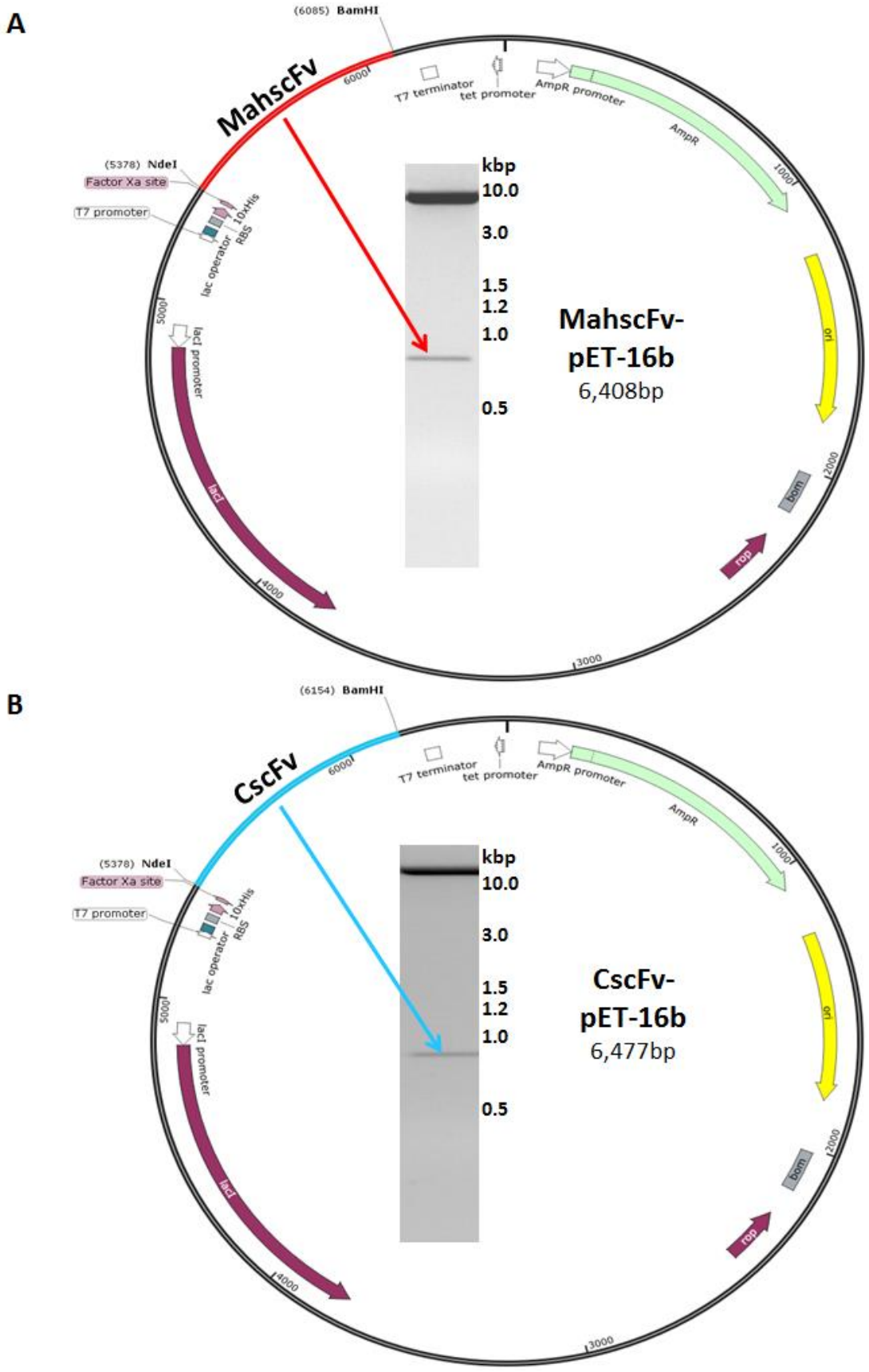
A
(6085) BamHI
MahscFv
6000
T7 terminator
tet promoter
AmpR promoter
AmpR
1000
(5378) NdeI
Factor Xa site
T7 promoter
10xHis
RBS
lac operator
5000
lacI promoter
lacI
4000
3000
ori
2000
bom
rop
kbp
10.0
3.0
1.5
1.2
1.0
0.5
MahscFv-
pET-16b
6,408bp
B
(6154) BamHI
CscFv
6000
T7 terminator
tet promoter
AmpR promoter
AmpR
1000
(5378) NdeI
Factor Xa site
T7 promoter
10xHis
RBS
lac operator
5000
lacI promoter
lacI
4000
3000
ori
2000
bom
rop
kbp
10.0
3.0
1.5
1.2
1.0
0.5
CscFv-
pET-16b
6,477bp

C

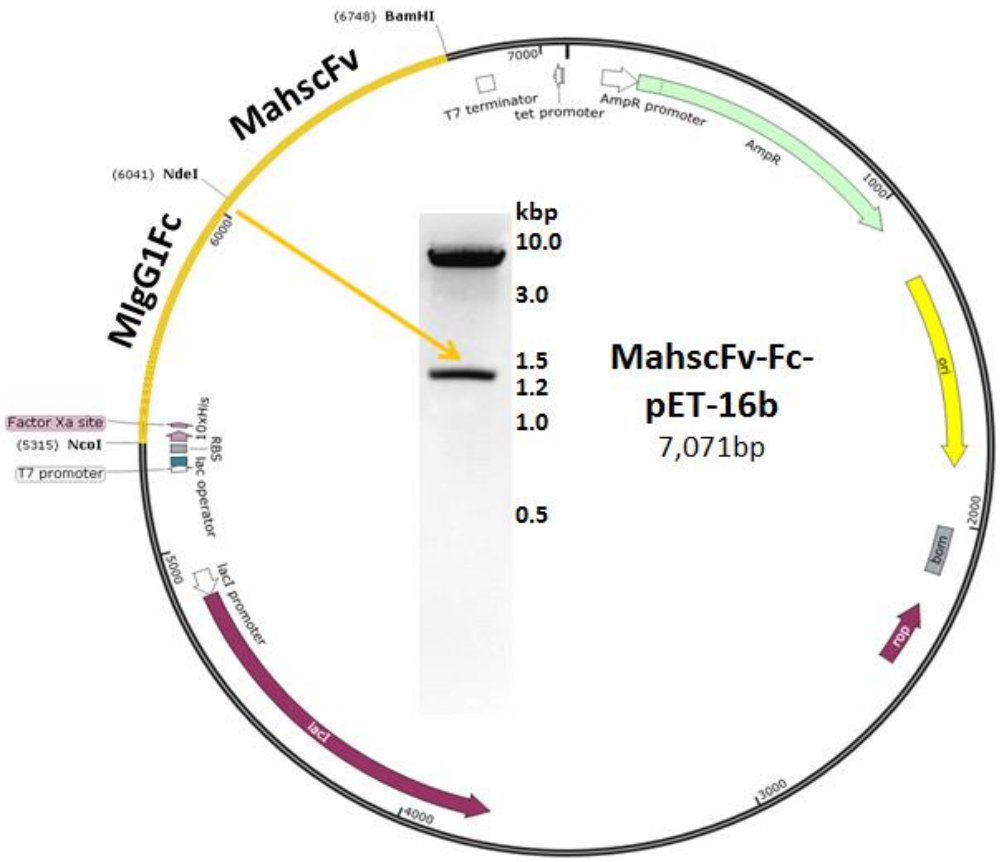
(6748) BamHI
MahscFv
MIgG1Fc
(6041) NdeI
T7 terminator
tet promoter
AmpR promoter
AmpR
ori
bom
rop
lacI promoter
lacI
Factor Xa site
(5315) NcoI
T7 promoter
10xHis
RBS
lac operator
kbp
10.0
3.0
1.5
1.2
1.0
0.5
MahscFv-Fc-
pET-16b
7,071bp

D

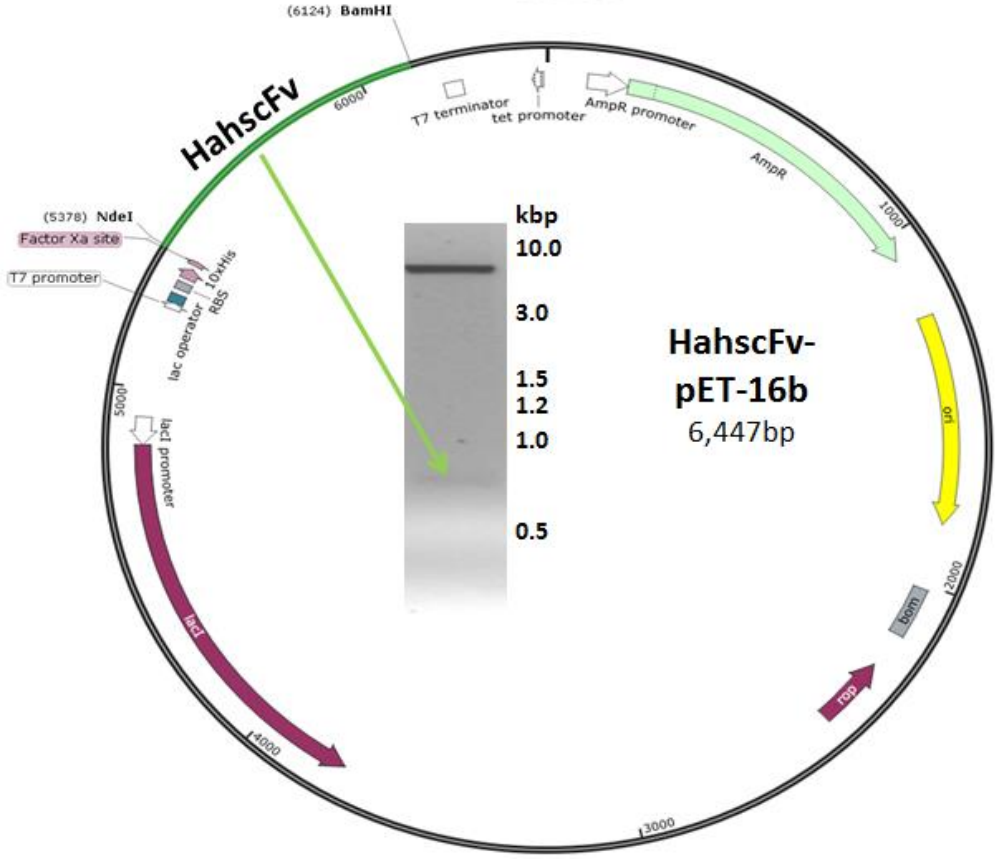
(6124) BamHI
HahscFv
(5378) NdeI
Factor Xa site
T7 promoter
10xHis
RBS
lac operator
T7 terminator
tet promoter
AmpR promoter
AmpR
ori
bom
rop
lacI promoter
lacI
kbp
10.0
3.0
1.5
1.2
1.0
0.5
HahscFv-
pET-16b
6,447bp

Figure 2.2 Plasmids for scFv expression. (**A**) MahscFv DNA was digested with BamHI and NdeI and ligated to pET-16b vector to form a novel plasmid of MahscFv-pET-16b (6,408 bp). Plasmid of the MahscFv was digested by BamHI and NdeI, and subjected on 1 % (w/v) agarose gel and showed a correct 702 bp band. (**B**) The designed CscFv DNA fragment was ligated into pET-16b vector using NdeI and BamHI restriction sites to form CscFv-pET-16b plasmid (6,477 bp) which was verified on a 1% (w/v) agarose gel using NdeI and BamHI digestion to achieve a correct 771 bp band. (**C**) Mouse IgG1 Fc DNA fragment (711 bp) including CH2 and CH3 was ligated to the plasmid of MahcFv-pET-16b using NcoI and NdeI restriction sites to form a new plasmid of MahscFv-Fc-pET-16b (7,071 bp) which was examined in a 1% (w/v) agarose gel using NcoI and BamHI digestion and showed the correct 1,425 bp band. (**D**) The same procedure was used to ligate the HahscFv to pET-16b to form HahscFv-pET-16b (6,447 bp) which was digested with NdeI and BamHI enzymes to achieved a correct 741 bp band on agarose gel. All plasmids were sequenced and no point mutations were found.

2.3.3 Protein induction and purification

The expression plasmids were transformed into BL21 (DE3) *E. coli* for protein expression. The correct molecular weight band could be observed in induced *E.coli* which was not apparent in the non-induced *E. coli* (Fig 2.3A left). The MahscFv was then purified by Ni-NTA resin, refolded with decreasing concentration of urea and separated by 15% SDS-PAGE and stained with Coomassie brilliant blue (Fig. 2.3A right). Using the same method, CscFv (29.7 kDa) was also induced in BL21 (DE3) *E. coli* (Fig. 2.3B left), and purified and examined on a 15% SDS-PAGE (Fig 2.3B right). Accordingly, the MahscFv-Fc (52.2 kDa) (Fig. 2.3C) and HahscFv (28.5 kDa) (Fig. 2.3D) were successfully produced in the DE strain. Following purification, all scFv proteins had a purity of greater than 90%.

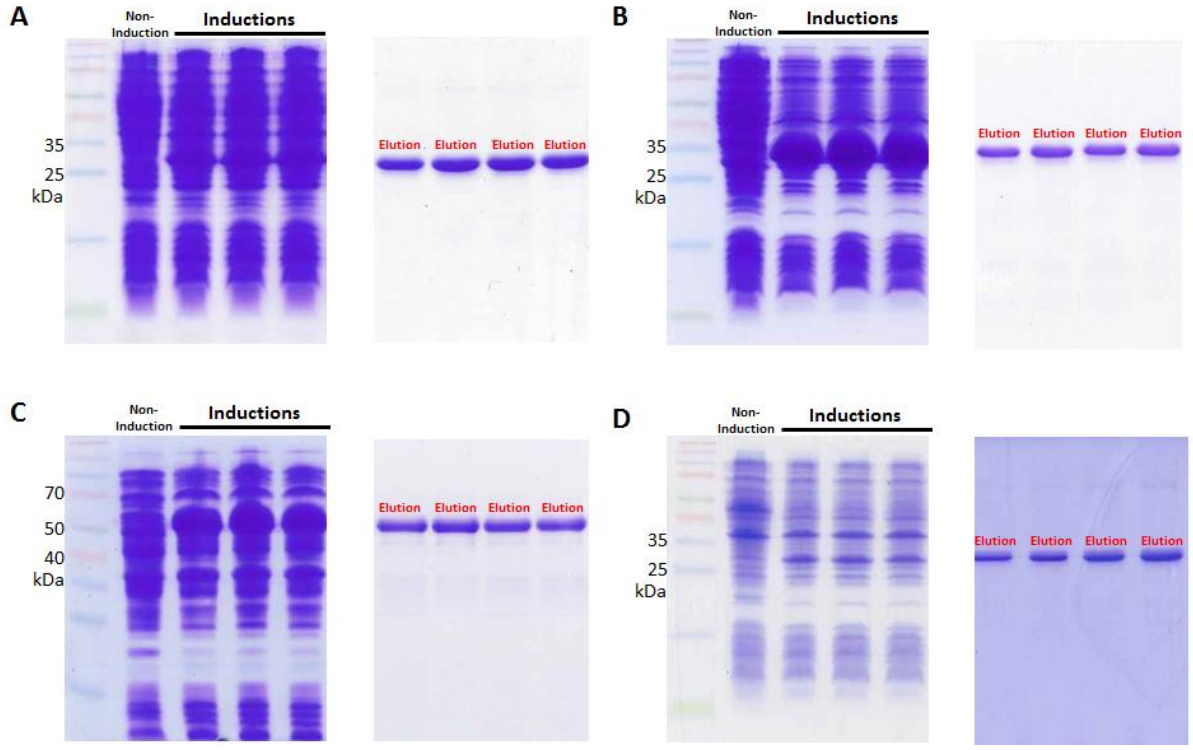

Figure 2.3 Antibody induction and purification. (A) MahscFv expression plasmid was transformed using BL21 *E. coli* and then induced at 30°C with 1 mM IPTG. The non-induced

E. coli was used as negative control. The induced band was 27 kDa which is matched with the calculated molecular weight. The MahscFv was insoluble and the inclusion bodies were denatured in Urea and refolded on Ni-NTA resin column. The purity of MahscFv was determined using SDS-PAGE and Coomassie brilliant blue staining and found to be greater than 90%. (B) CscFv, (C) MahscFv and (D) HahscFv were produced using the same procedure as above.

2.3.4 Binding analysis

To investigate whether these scFvs are specific to histones, recombinant histone H1, H2A, H2B, H3, H4, calf thymus histones and S100P (negative control) were run on a 15% SDS-PAGE and stained with Coomassie brilliant blue, in order to confirm the presence of each protein (Fig. 2.4A). The same amount of each protein was then loaded into a new gel and transferred to PVDF membrane and probed with MahscFv-HRP. Under reducing conditions the MahscFv bound to each recombinant histone, including calf thymus histones, but not S100P (Fig. 2.4B), whereas no band was found using the same proteins but probed with HRP alone (data not show). The same method was used to demonstrate the specificity of MahscFv-Fc. (Fig. 2.4C) and HahscFv (Fig. 2.4D). In contrast, CscFv-HRP did not bind to either histones or S100P (Fig. 2.4E).

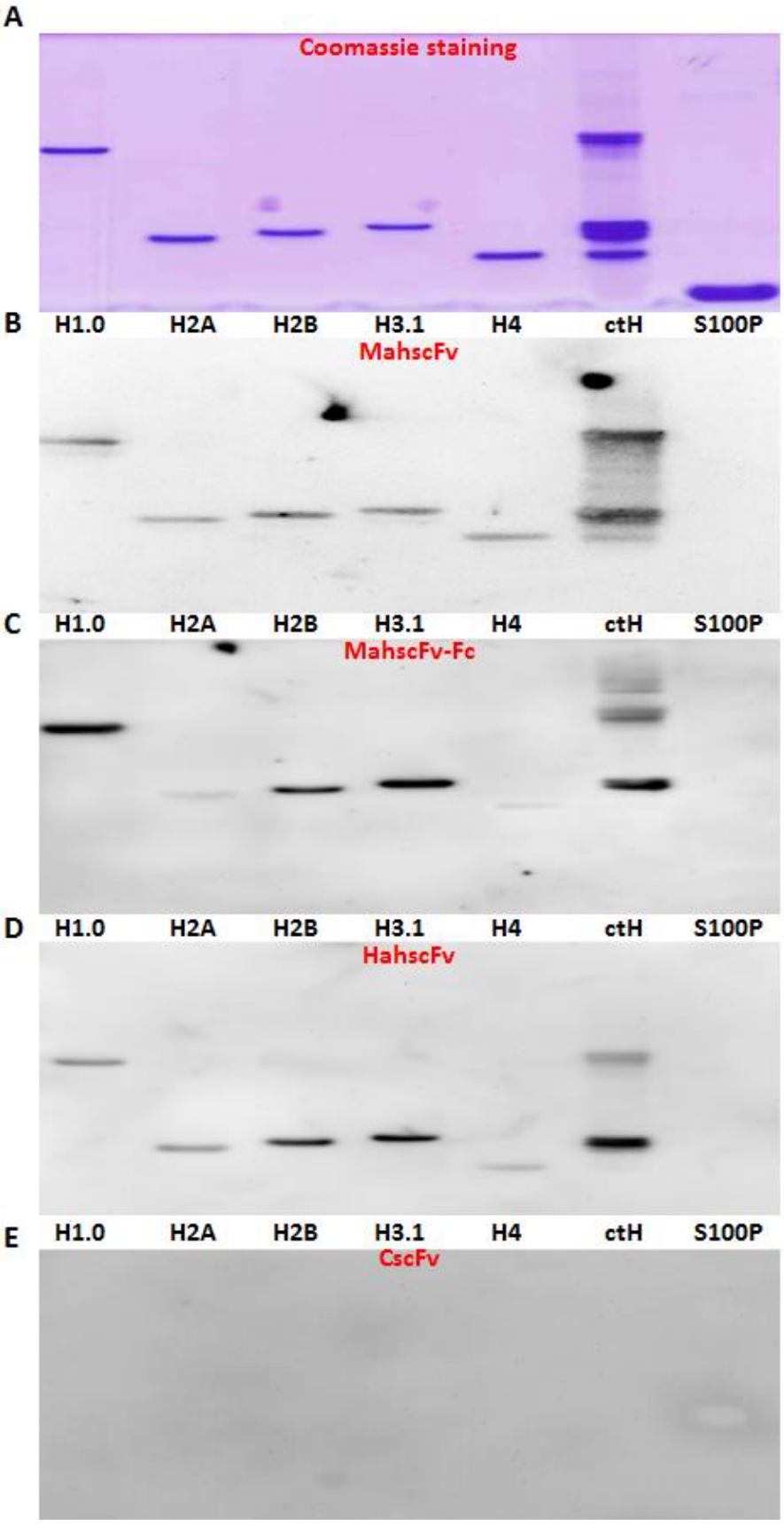
A
Coomassie staining
B
H1.0
H2A
H2B
H3.1
H4
ctH
S100P
MahscFv
C
H1.0
H2A
H2B
H3.1
H4
ctH
S100P
MahscFv-Fc
D
H1.0
H2A
H2B
H3.1
H4
ctH
S100P
HahscFv
E
H1.0
H2A
H2B
H3.1
H4
ctH
S100P
CscFv

Figure 2.4 Specificity of recombinant scFvs (**A**) 2 µg of recombinant histones H1.0, H2A, H2B, H3.1, H4, calf thymus histone and S100P were subjected to 15% SDS-PAGE. (**B**) The proteins were also transferred to PVDF membrane and probed with MahscFv-HRP, (**C**) MahscFv-Fc-HRP, (**D**) HascFv-HRP, or (**E**) CscFv-HRP.

To examine binding of HahscFv to histones under physiological conditions, the HahscFv was coated onto a 96 well plate and an ELISA was performed. Binding was determined using various concentrations of histones and streptavidin-HRP was used as a detector, since streptavidin can directly bind to histones [171]. The same concentrations of human histones H1, H2A and H2B were used, where by maximum binding at was seen at 100 nM histones. However, in this assay H1 showed a relatively low binding response compared to both H2A and H2B (Fig. 2.5A). In contrast, H3 and H4 required a much higher concentration to bind to the HahscFv, with maximal binding at 800 nM histones (Fig. 2.5B).

To determine the binding affinity of scFvs to histones, a surface plasmon resonance (SPR) system was used. Calf thymus histones were captured on sensor chip streptavidin (SA), and histone binding affinity to increasing concentrations (0.1, 0.3, 0.5, 0.8, 1.0, 1.5, 2.0 and 3.0 µM) of MahscFv, MahscFv-Fc and HahscFv, was determined. Following the Biacore™ X100 measurement, the affinity of MahscFv to Histones was determined to be 1.327×10^{-6} M (Fig. 2.6A), MahscFv-Fc to histones affinity was 2.045×10^{-6} M (Fig. 2.6B), and HahscFv to histones affinity was 3.529×10^{-6} M (Fig. 2.6C).

Taken together, these data demonstrate that all individual histones bound to HahscFv under both reducing and physiological conditions and thus merit further functional analysis.

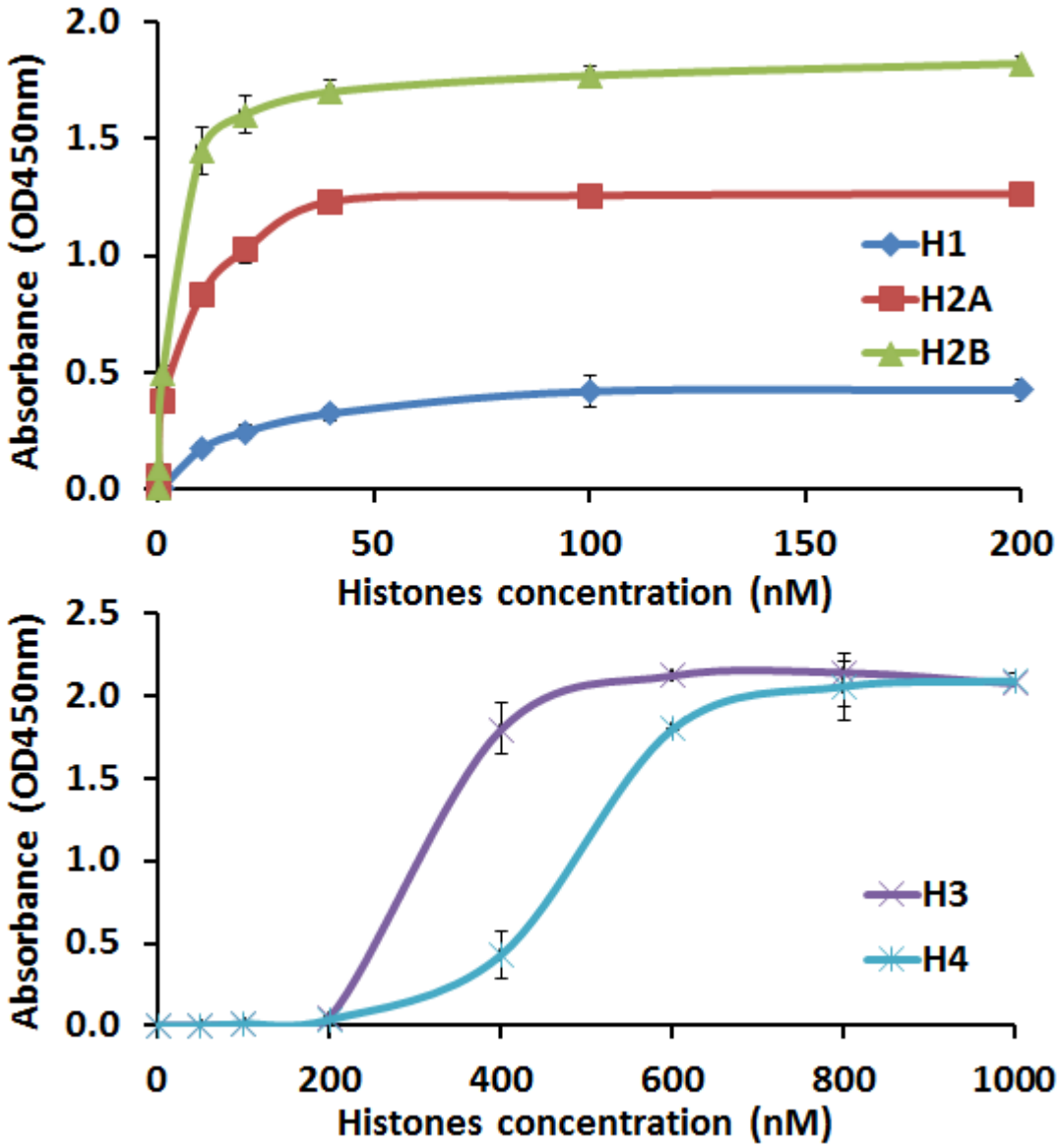

Figure 2.5 Binding of HahscFv to histones using ELISA. Binding of humanised ahscFv (HahscFv) to individual histones was determined by ELISA. (**A**) HahscFv was coated on a 96 well plate, and a series of concentration (1, 10, 20, 40, 100 and 200 nM) of H1, H2A and H2B were added and incubated for 3 hours. After extensive washing, streptavidin-HRP was added for 1 hour. (**B**) Following the same procedure as in (A), histone H3 and H4 binding to HahscFv was determined using increasing histone concentrations (50, 100, 200, 400, 600, 800 and 1,000 nM).

A

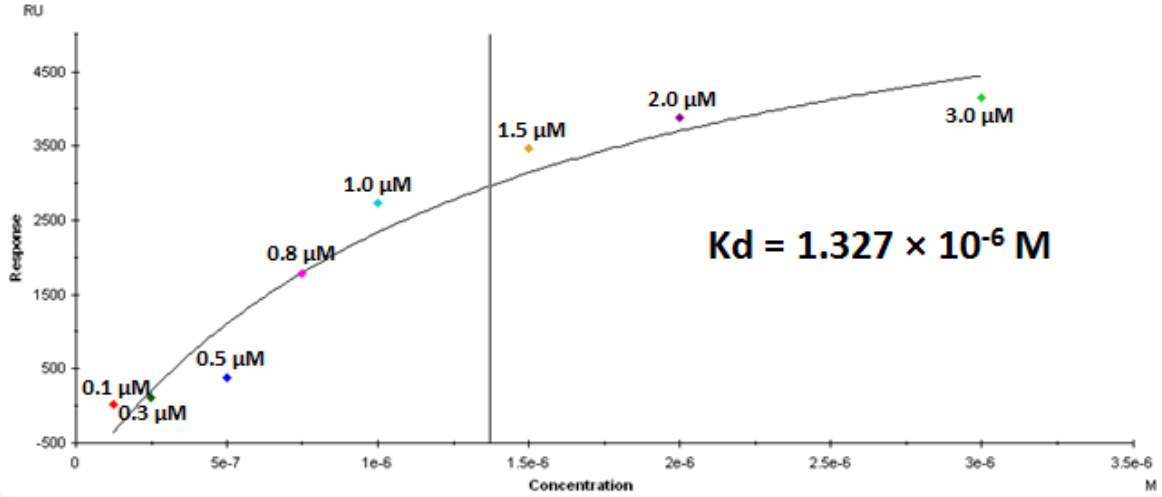
RU
Response
Concentration
M
0.1 µM
0.3 µM
0.5 µM
0.8 µM
1.0 µM
1.5 µM
2.0 µM
3.0 µM
Kd = 1.327 × 10-6 M

B

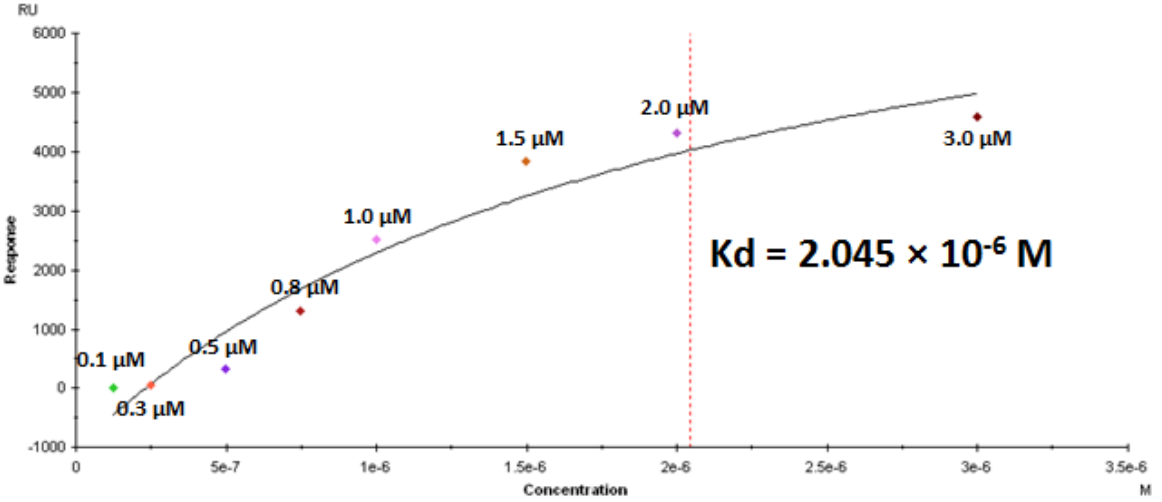
RU
Response
Concentration
M
0.1 µM
0.3 µM
0.5 µM
0.8 µM
1.0 µM
1.5 µM
2.0 µM
3.0 µM
Kd = 2.045 × 10-6 M

C

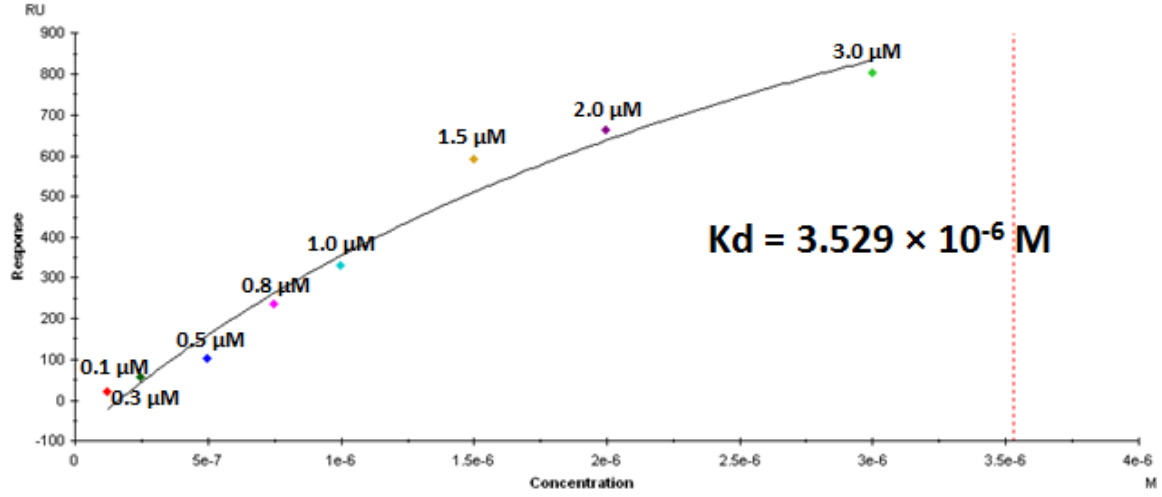
RU
Response
Concentration
M
0.1 µM
0.3 µM
0.5 µM
0.8 µM
1.0 µM
1.5 µM
2.0 µM
3.0 µM
Kd = 3.529 × 10-6 M

Figure 2.6 Affinities of scFvs to calf thymus histones. (**A**) Calf thymus histones were captured on sensor SA chip, and a series of MahscFv antibody concentrations (0.1, 0.3, 0.5, 0.8, 1.0, 1.5, 2.0 and 3.0 μM) were added. The affinity between MahscFv and histones was 1.327×10^{-6} M, (**B**) the affinity of MahscFv to histones was 2.045×10^{-6} M, and (**C**) HahscFv to histones was 3.529×10^{-6} M.

2.3.5 MahscFv inhibits histone-induced endothelial and cardiomyocyte cells toxicity *in vitro*

Since 2009, extracellular histones have been reported to be toxic to endothelial cells [14], which has further been characterized by our group [91]. In my experiments, EAhy926 cells (endothelial-like cells) [91] were treated with 50 μg/mL calf thymus histones, which showed significant toxicity to endothelial cells, compared with untreated cells, and this toxicity was significantly reduced by 100 μg/mL of MahscFv (Fig. 2.7A). To further demonstrate the protective effect of MahscFv and to investigate the possible translational relevance of this anti-histone treatment, HL-1 cells (cardiomyocytes) were treated with serum from septic patients. The serum from patients with circulating histone levels > 75 μg/mL was significantly toxic towards cardiomyocytes compared to normal serum and septic patient serum with histone levels < 75 μg/mL. Furthermore, this toxicity could be abrogated by 50 μg/mL of MahscFv (Fig. 2.7B). These data demonstrate that the major toxic effect within this patient serum was attributed to histones, and that this could be inhibited by MahscFv. In addition, this figure was also published in reference [37].

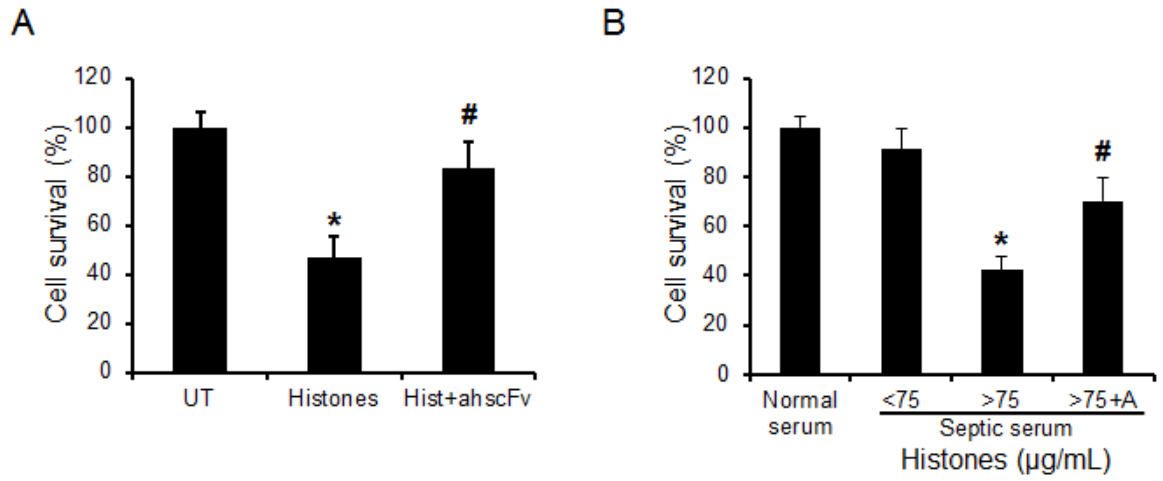

Figure 2.7 MahscFv protection against histone-induced endothelial and cardiomyocyte cell toxicity. (**A**) EAhy926 (Endothelial-like) cells were incubated in 2% FCS with or without 50µg/mL calf thymus histones, pre-incubated without or with 100 µg/mL MahscFv for one hour. Cells were stained with propidium iodide (PI) (10µg/mL) prior to flow cytometric analysis. The untreated (UT) cells were set as 100% (*p < 0.05 compared with untreated cell #p < 0.05 compared with histones treated cells n = 4). (**B**) HL-1 (cardiomyocytes) were treated with normal serum, septic serum (histones level < 75 µg/mL), septic serum (histones level > 75 µg/mL) and septic serum (histones level > 75 µg/mL) + 50 µg/mL MahscFv. The cell viability was measured by WST-8 assay. Cell survival of cells treated with normal serum was fixed as 100%. *p < 0.05 was compared with normal serum and #p < 0.05 compared with septic serum (histones level > 75 µg/mL). This figure had been presented in reference [37].

2.3.6 MahscFv abrogates cardiac injury in septic mice

Calf thymus histones infusion in mice had been tested in mice leading to lethality, and coinfusion of 10 mg/kg MahscFv had successfully rescued mice of which the mice had injected with a lethal-dose of histones [48].

To further characterize the protective effect MahscFv *in vivo*, septic mice were used. Induction of murine sepsis using intraperitoneal E.coli injection (1×10^8 CFU/mL) showed significantly elevated levels of circulating cardiac Troponin I (cTnI), a well-known clinical marker of cardiac injury, indicating cardiac injury in these septic mice. Furthermore, the levels of circulating cTnI were significantly correlated with circulating histone levels (data not shown) [37]. Taken together, this suggests that elevated circulating histones may play a role in inducing cardiac injury in these mice. To test this hypothesis MahscFv was infused into septic mice (8 and 16 hours after sepsis induction) and circulating cTnI was quantified. In fact, MahscFv infusion into septic mice significantly reduced cTnI levels, suggesting that histones play a role in cardiac injury and dysfunction during sepsis, which can be protected by MahscFv. This figure has also been presented in reference [37].

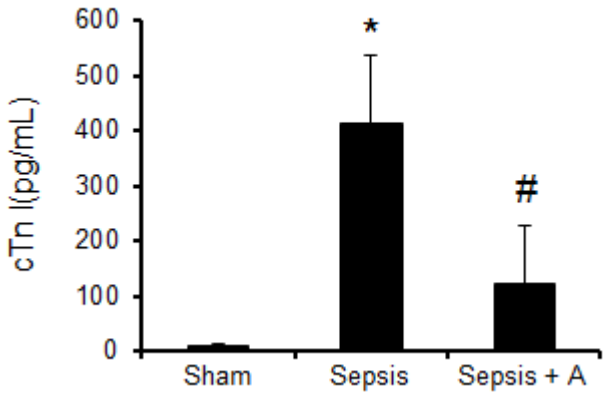

Figure 2.8 MahscFv protection of histone induced cardiac injury in mice. Cardiac troponin I (cTnI) levels shown in Sham mice (n = 6), septic mice (n = 6) and septic mice + 10 mg/kg MahscFv intervention (n = 6). Data is expressed as mean +/- S.D; *$p < 0.05$ when compared with Sham and #$p < 0.05$ compared with sepsis mice. This figure had been presented in reference [37].

2.3.7 Detoxifying histones *in vitro* with MahscFv-Fc

The MahscFv had been used to successfully reduce histone-induced cytotoxicity *in vitro*, and rescued mice in *in vivo* and is further characterized in this chapter. Therefore, I wanted to investigate the protective role of the novel mouse anti-histone scFv, used in this thesis, which is linked with Fc fragments from mouse IgG1 antibody. I have currently demonstrated that this antibody retains its specificity towards histones using Western blot and still binds with a high affinity as demonstrated by SPR. Therefore, I further investigated the functional relevance of this novel scFv reagent using endothelial cells as a model *in vitro* system, with cell toxicity determined by WST-8 assay. Endothelial cells (EAhy926) were treated with a series of calf thymus histone concentrations (10, 20, 50, 100, 200, 300 µg/mL). Histones were significantly toxic (200 µg/mL) to endothelial cells (EAhy926) (Fig. 2.9A), and the cytotoxicity of histones was dose-dependently reduced by MahscFv-Fc, which reached significance at 100 µg/mL (Fig. 2.9B).

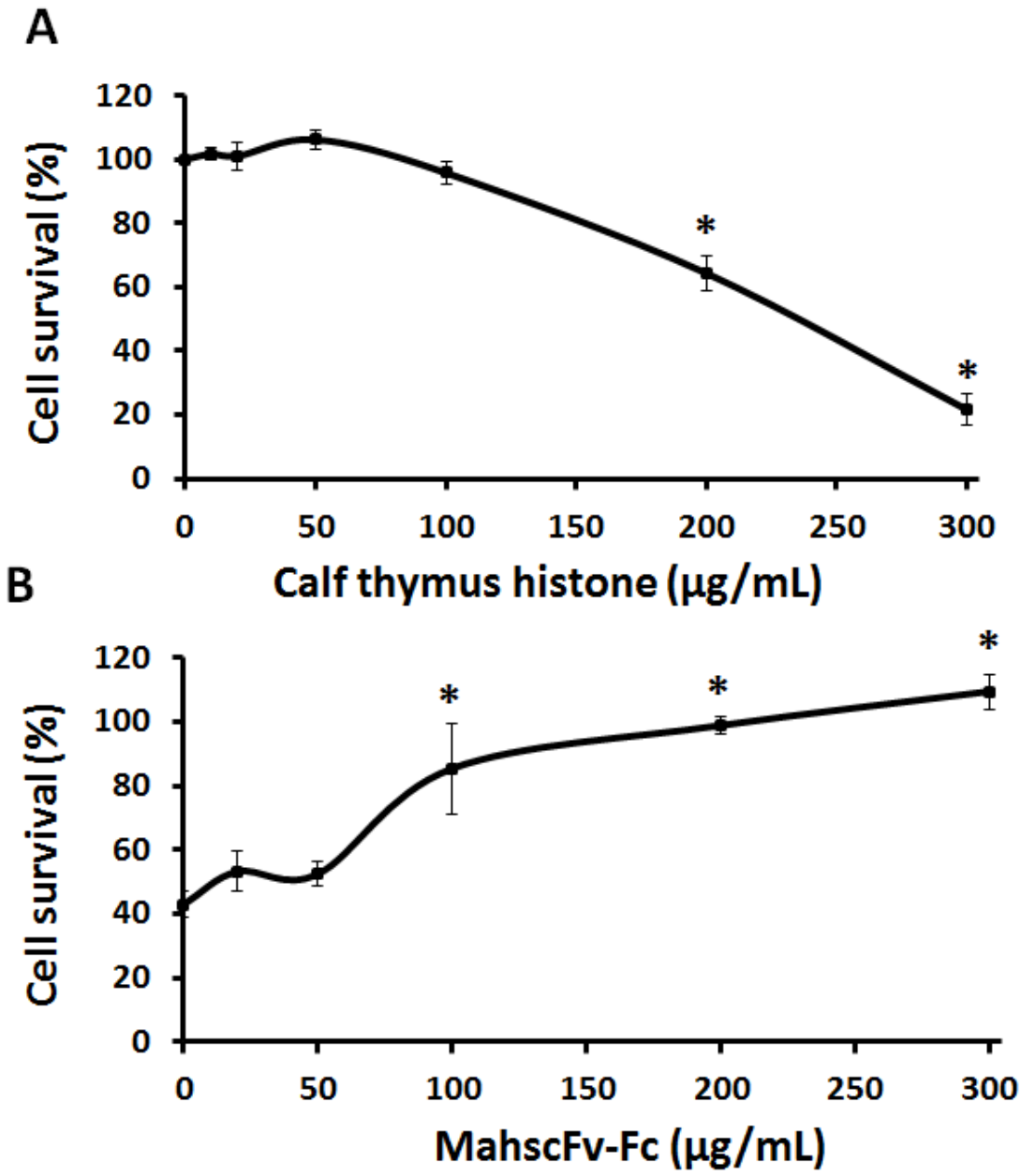

Figure 2.9 Effect of MahscFv-Fc on histone-induced endothelial toxicity to histones. (**A**) 1.5×10^4 of EA.hy926 cells were cultured on a 96-well-plate and treated with a series of calf thymus Histones concentrations (10, 20, 50, 100, 200, 300 µg/mL), (**B**) or cells were treated with 250 µg/mL of calf thymus Histones in the presence of MahscFv-Fc (20, 50, 100, 200 and 300 µg/mL) and incubated for 1 h. Cells were incubated with 10 µL of WST-8 for 4 h

and absorption read at OD_{450nm}. Means ± SD are shown. *$p < 0.05$ compared with untreated cells and without MahscFv-Fc using ANOVA test.

2.3.8 Detoxifying histones on endothelial cells *in vitro* with HahscFv

I utilized the *in vitro* endothelial cells (EAhy926) model system, using PI and flow cytometry to determine the effectiveness of HahscFv against histone-toxicity. Cells were cultured with 50 µg/mL histones, and increasing concentrations of HahscFv were used to investigate the protective effect of MahscFv (Fig. 2.10). The endothelial cell (EAhy926) viability was increased by 50 µg/mL Hahscfv (Fig. 2.10A). Further dose-dependent investigation showed that HahscFv reached significance at 50 µg/mL and the protective effect was even more apparent at higher doses (Fig. 2.10B).

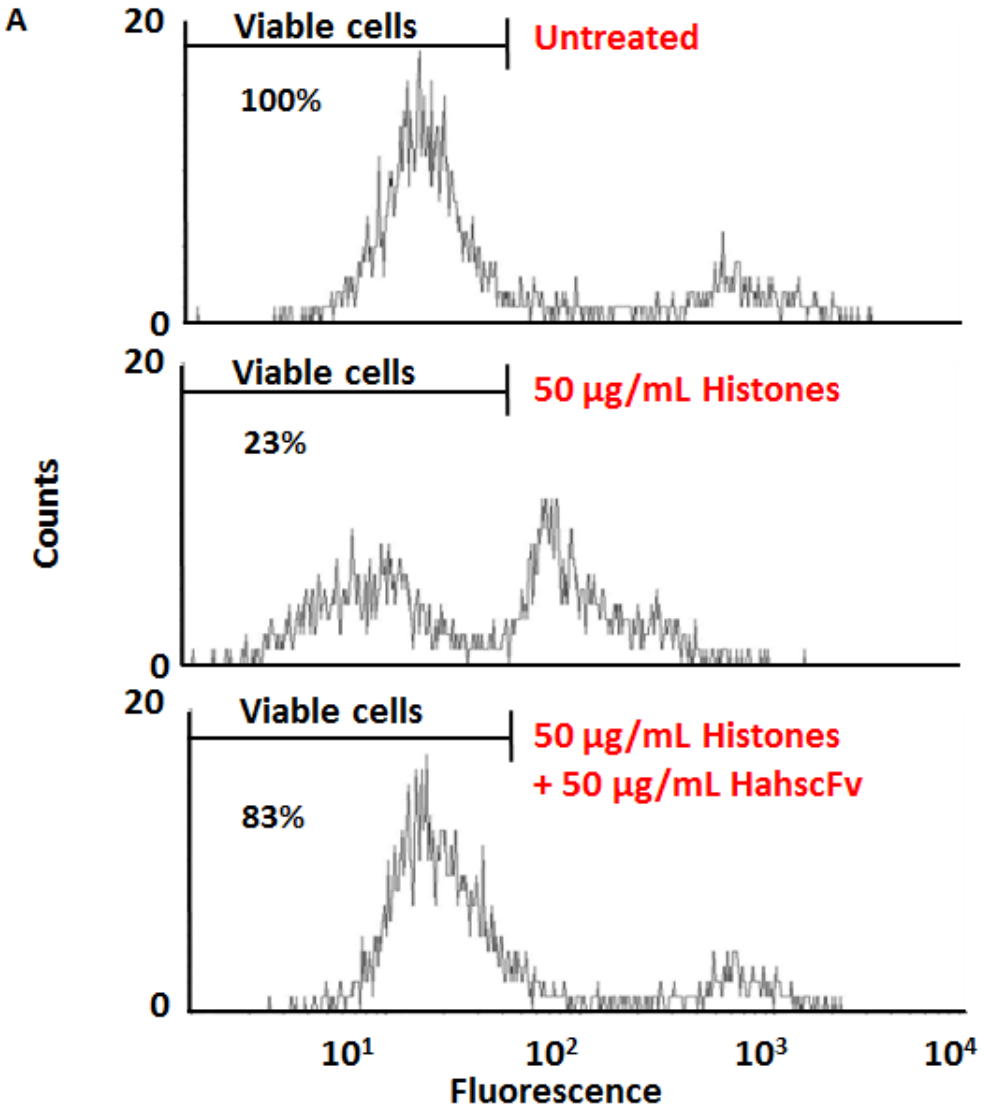
A
20
Viable cells
Untreated
100%
0
20
Viable cells
50 µg/mL Histones
23%
0
Counts
20
Viable cells
50 µg/mL Histones
+ 50 µg/mL HahscFv
83%
0
10¹
10²
10³
10⁴
Fluorescence

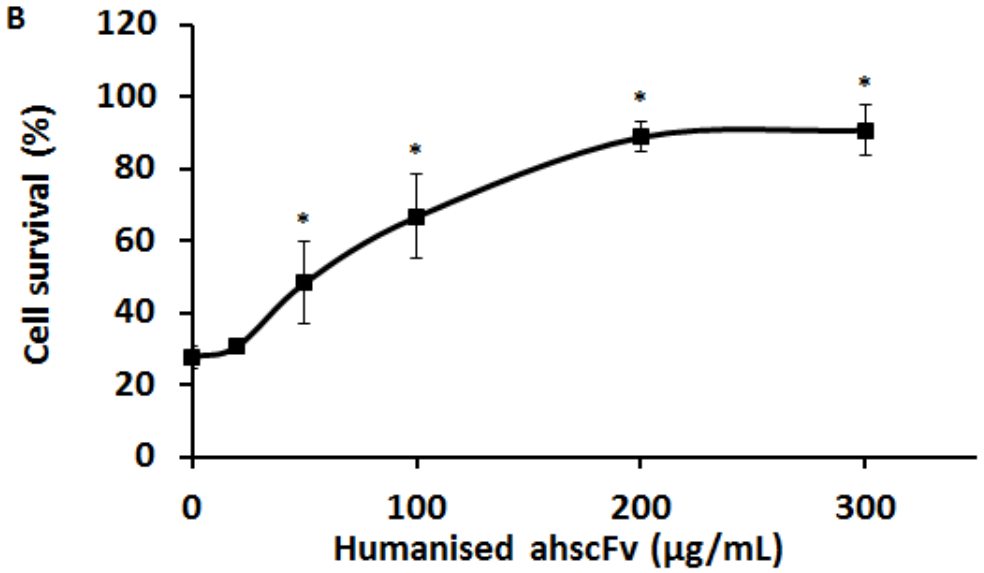
B
120
100
80
60
40
20
0
Cell survival (%)
*
*
*
*
0
100
200
300
Humanised ahscFv (µg/mL)

Figure 2.10 Typical flow cytometry diagrams of histone cytotoxicity and HahscFv protection. (**A**) EAhy926 Endothelial-like cells were incubated in 2% FBS with or without 50µg/mL calf thymus histones, pre-incubated without or with 50 µg/mL HahscFv for one hour. Cells were stained with propidium iodide (PI) (10µg/mL) prior to flow cytometric analysis. (**B**) EAhy926 cells were treated with 200 µg/mL histones with or without increasing concentrations of HahscFv for one hour (n=4). *$p < 0.05$ compared with untreated cells and without HahscFv using ANOVA test.

2.4 Discussion

Extracellular histones have been found to be toxic to endothelial cells and are a major mediator of death in sepsis. This toxicity could be reduced using both mouse monoclonal antibodies and activated protein C (APC) [173]. However, APC has been withdrawn from clinical trials [174]. Heparin is another reagent for detoxifying histones, but as observed with APC, carries the increased risk of bleeding. Although non-anticoagulant heparins have been developed and show some protective effects [92], the other side effects, such as heparin-induced thrombocytopenia, may prevent its application. Therefore, more effective reagents with fewer side effects are needed to detoxify histones. In addition, mouse anti-histone antibodies are also required for scientific research in mouse models. In this Chapter, I have developed MahcFv, MahscFv-Fc and HahscFv and tested their functions in reducing cytotoxicity of histones both *in vitro* and *in vivo*. These ahscFvs bind to nearly all individual histones but with different affinities. This may be due the nature of charges or sequence similarity of individual histones. These interactions are not non-specific, because they do not bind to S100P protein and control scFv does not interact with any of the individual histones (Fig. 2.4). Due to the limitation of the resources, I cannot measure the kinetics of each ahscFv to each individual histone. Instead, I have measured the kinetics of each ahscFv to calf thymus histones, a mixture of individual histones. Most of their Kds are in μM level and sufficient for functional analysis.

In vitro, I have tested their protective effects on endothelial cells exposed to histones and found that ≥ 50 μg/mL showed a protective effect to cells treated with 50 μg/mL histones, using molar ratio of approximately 1:2 (ahscFv:histones). With increased ahscFv concentrations, the protective effects are further increased. In addition, the MahscFv is able to protect cultured cardiomyocytes treated with histones *in vitro*. *In vivo*, the MahscFv is not only able to rescue the mice challenged with lethal dose of histones but also improve the

cardiac performance in septic mice models (Fig. 2.8). Those data strongly indicate that the MahscFv is an effective reagent to detoxify histones both *in vitro* and *in vivo*.

scFv, composed with a heavy and light linked by a flexible linker, not only retains the functions of intact antibody, but also had a number of advantages. For example, the relatively small size of scFv protiens make it easy to produce using recombinant DNA technology [140]. The disadvantage is that the most of the scFvs are not soluble when they are expressed in bacteria. As such, MahscFv, MahscFv-Fc and HahscFv were insoluble. Therefore, those proteins have to be denatured to make them soluble and refolding procedures were required. There may be two reasons for inclusion body formation, one is that expressed protein is deposited as aggregates because large amount of misfolded proteins are expressed. Another is that bacteria did not support post-translational modifications that are required to ensure correct protein folding [175]. In the future, we can utilize a mammalian expression system, such using Chinese hamster ovary (CHO) cells or human embryonic kidney 293 (HEK 293) cells to see if this can be improved.

We found that MahscFv could reduce the toxic effects of histones but cannot reduce the levels of histones. This is maybe due to the lack of Fc fragment so the complexes cannot be recognised by macrophages Fc receptors. Therefore, I added Fc fragments to scFv and generated MahscFv-Fc. The MahscFv-Fc antibody firstly showed the specificity to histones using Western blotting (Fig. 2.4C), and protection of endothelial cells from histone cytotoxicity (Fig. 2.9B). However, I have not had the opportunity to test this *in vivo*. This will be completed in the near future.

Exchanging the CDRs is one way to develop humanised scFv. I used mouse CDRs from MahscFv and human IgG1 heavy [176] and kappa light chains as a frame [177] to form a novel scFv, named HahscFv [141] which has been demonstrated to have similar binding

affinities to histones and are able to protect endothelial cells *in vitro* from histone toxicity. Further *in vivo* study will be carried out in the near future.

2.5 Conclusion

In conclusion, we are able to produce a functionally effective MahscFv, MahscFv-Fc and HahscFv to detoxify extracellular histones both *in vitro* and *in vivo*.

Chapter 3 Isolation, Identification, Production and Characterisation of Anti-Histone Antibodies from SLE Patients

3.1 Introduction

Humanised antibodies still retain sequences from animals i.e. murine CDRs from mice which are foreign to humans. Therefore, there is still a risk of triggering host antibody production against the therapeutic antibody. However, this chance is substantially lowered when using humanised compared to non-humanized antibodies. Therefore, a new approach is to use antibodies from patients with auto-immune diseases, although controversy still remains over the roles of auto-antibodies in human disease. Circulating autoantibodies against histones are present in more than 70% of SLE patients [178-183]. These anti-histone autoantibodies have previously been isolated and sequenced through labour intensive and costly approaches such as N-terminal peptide sequencing which require tailored chemical reactions, based on the amino acid composition [98].

In last two decades, human antibody libraries (from B cells) have been extensively studied. New screening methods, such as phage display, RNA display and even DNA display libraries (see section 1.5) have been developed. Therefore, it is practical to obtain the coding sequences for an antibody fragment against a specific antigen. However, it is labour intensive to construct a human antibody library from patients with anti-histone antibodies with no guarantee that the coding sequence for anti-histone antibodies will subsequently be included in the library. Another disadvantage is that many studies found that the coding sequences isolated from human B cell libraries only code antibodies with lower affinity to antigens [184]. Therefore, further modification of these antibodies is unavoidable and also labour intensive.

With the wide application and technological advancement of mass spectrometry in peptide sequencing, it is possible to map the CDR sequences of isolated antibodies [144]. Since it is relatively simple to isolate anti-histone antibodies using affinity chromatography, I decided to explore this novel proteomic approach to obtain the specific peptide sequences of anti-histone antibodies from SLE patients, and then produce a human scFv against histones. An outline of an experimental plan for isolation and production of the human anti-histone antibody is shown in Fig. 3.1.

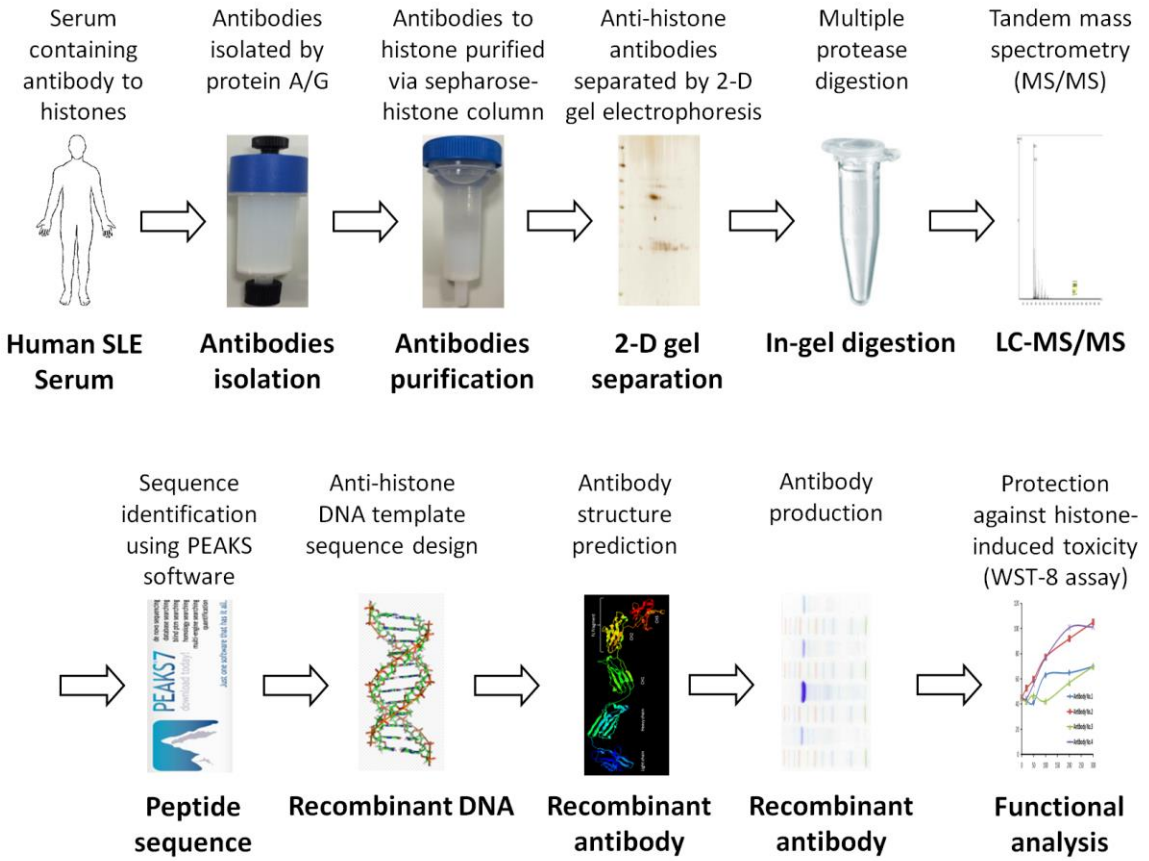

Figure 3.1 Outline of human anti-histone antibody production methodology.

3.2 Methods

3.2.1 Detection of anti-histone autoantibodies in serum from SLE patients

The detection of the presence of autoantibodies to histones in the sera taken from patients with SLE has been previously described [185], with several modifications in this study. Briefly, human recombinant histones (H1.0, H2A, H2B, H3.1 and H4) (NEB, USA), mixed calf thymus histones (ctH) (Roche, UK) and recombinant S100P (negative control) were subjected to 15% SDS-PAGE in reducing conditions and transferred onto 0.45 µm PVDF. The membrane was blocked for 1 h at room temperature in 30 mL blocking buffer (TBST with 5% (w/v) skimmed milk, 2% (w/v) bovine serum albumin (BSA)). The membrane was then probed in blocking buffer with serum from individual SLE patients acting as primary antibody ((1:200 (v/v) dilutions) at 4^{o}C overnight), and detected with goat anti-human IgG-HRP (secondary antibody 1:10,000 (v/v) dilution in blocking buffer, 1 h at room temperature). Bands were visualized using chemiluminescence (also see chapter 2, section 2.2.13). Normal healthy serum served as negative control. In addition, the membrane was directly probed with goat anti-human IgG-HRP to ensure no cross-reactivity (false positive) from the secondary antibody.

3.2.2 Isolation of total antibodies from serum

Antibody isolation was previously described [186] and used in this study. In brief, human serum was diluted by 2 × PBS and filtered with 0.45 µm filter. Human antibodies were then isolated using Pierce® Chromatography Cartridges Protein A/G (Thermo Fisher Scientific, USA) following manufacturer's instruction. The 5 mL column was first equilibrated with 50 mL PBS. Then the diluted and filtered serum was applied to the column. After washing with

100 mL PBS, the bound proteins were eluted with 20 mL of 0.1 M Glycine (pH 3.0), collected in small fractions (1 mL) and neutralised by adding 100 µL of 1 M Tris-HCl (pH 8.0).

3.2.3 Isolation of anti-histone antibodies from total antibodies

Calf thymus histone-conjugated CNBr-activated Sepharose 4B media (GE Healthcare, UK) were used. Briefly, 1 g of the Sepharose media was activated with 100 mL of 1 mM HCl for 1 h at 25°C, with 110 rpm rotation. The activated Sepharose was then transferred to a blank column and washed with 60 mL coupling buffer (0.1 M $NaHCO_3$, 0.5 M NaCl (pH 8.3)) and then coupled to 5 mg calf thymus histones in the coupling buffer overnight. Then the column was blocked with 0.1 M Tris-HCl (pH 8.0). The coupling efficiency was calculated as following:

$$\frac{\text{Total histone 5 mg} - \text{Unbound histone 0.1 mg}}{\text{Total histone 5 mg}} \times 100\% = 98\%$$

To isolate antibodies that bind to histones, the column was first equilibrated with 20 mL binding buffer (20 mM Tris-HCl, 150 mM NaCl, 2 mM $CaCl_2$, pH 7.4). The total antibodies isolated using Protein A/G beads from human SLE serum were then applied onto the column. After washing with 50 mL washing buffer (binding buffer + 0.05% (v/v) Tween-20) followed by 50 mL binding buffer without detergent, the column was eluted with elution buffer (0.1M glycine, pH 3.0), and neutralised with 1 M Tris-HCl (pH8.0).

3.2.4 Two-dimensional (2D) gel electrophoresis

The anti-histone antibody eluate from above was dialysed against PBS. After dialysis, the antibodies were precipitated using acetone (1:4) (v/v) overnight at -20°C and pelleted by centrifugation at 20,000 × g for 15 min. The pellet was washed with acetone twice and air dried on ice, and then re-suspended with 200 µL of rehydration buffer (8 M urea, 2% (w/v) CHAPS, 0.5% (v/v) IPG buffer, 20 mM DTT and Bromophenol blue trace). The suspended antibodies were uniformly loaded onto an 11 cm rehydration/equilibration tray with an 11 cm strip (pH 3-10 from Bio-Rad). The strip was conducted by passive rehydration at 250 V for 12 h at 20 °C in the PROTEAN IEF cell (Bio-Rad, USA), followed by isoelectric focusing (IEF) of a total of 55,000 volt hour using voltage stepping: 2.5 h at 8,000 volt, and 35,000 volt-hour at 8,000 volt. Then the strip was equilibrated with 2 mL of equilibration buffer (6 M urea, 30% (v/v) glycerol, 2% (w/v) SDS, 50 mM Tris-Cl pH 8.8, 1% (w/v) DTT) for 10 min at room temperature and placed on the top of a 1.5 mm thick, 16 × 18 cm SDS-gradient gel (7% – 18%) in a SE 600 Chroma vertical electrophoresis unit (GE healthcare, USA). After electrophoresis, the gel was stained using either Coomassie brilliant blue staining (see chapter 2, section 2.2.11) or silver staining.

3.2.6 Silver staining

After electrophoresis, the gel was silver stained [187]. In brief, the gel was firstly fixed with 40% (v/v) ethanol, 10% (v/v) acetic acid for 60 min and washed two times with 10 % (v/v) ethanol, then three times with H_2O for 5 min. After washing, the gel was stained using 0.2% (w/v) $AgNO_3$ for 30 min and rinsed in H_2O for 5 s. The gel was then developed in 2.5% (w/v) sodium carbonate containing 0.008% (v/v) formaldehyde until the solution turned brown. The reaction was terminated immediately by adding 1% (v/v) acetic acid for 5 min and then washed 6 times with H_2O for 5 min per each step. The gel was finally reduced with 0.3%

(w/v) sodium thiosulphate, 0.15% (w/v) potassium ferricyanide and 0.05% (w/v) sodium carbonate and washed for 5 min with water five times.

3.2.7 In-gel digestion for tandem mass spectrometry (MS/MS)

In-gel digestion was performed on coomassie stained gels, as described previously [188] with slight modification. Gel slices were incubated in following reagents sequentially, 200 µL MillQ H_2O, acetonitrile, 100 mM ammonium bicarbonate, 100 mM ammonium bicarbonate containing 50% (v/v) acetonitrile and acetonitrile, 15 min/per step. Gel pieces were then dried by speed-vac.

Alternatively, if the gel was silver stained, reduction and alkylation of the proteins was performed. Gel slices were then incubated with 200 µL of 10 mM DTT containing 20 mM Ammonium Bicarbonate for 60 min at 56°C. The tube was cooled to room temperature and 200 µL of 50 mM Iodoacetamide (IAA) was added and incubated in the dark for 30 min. The gel was incubated through a series of incubations with 200 µL 100 mM ammonium bicarbonate, 100 mM ammonium bicarbonate containing 50% (v/v) acetonitrile, 15 min/each step and dried using speed-vac. For the digestion, 12.5 µg/mL Trypsin, Chymotrypsin or Glu-C, 5 µg/mL Lys-C or 2 µg/mL Asp-N at 30°C for 16 h. After digestion, an equal volume of acetonitrile was added into the digestion mixture and incubated for 15 min. Then the digest was transferred to a new tube and dried using speed-vac. The dried powder was then resuspended with 50 µL 1% (v/v) formic acid and 15 µL of the peptide suspension was analysed using tandem mass spectrometry.

3.2.8 Antibody identification using nano-flow liquid chromatography coupled to mass spectrometry (LC-MS/MS)

The digested heavy and light chains of the anti-histone antibodies were identified using LC-MS/MS at the FingerPrints Proteomics Facility, Dundee University, as previously described [189]. Peptide analysis was carried out on a Velos orbitrap mass spectrometer coupled with a Dionex Ultimate 3000 Rapid Separator. Prior to loading of 15 µL samples containing digested peptides onto a trap column (100 µm × 2 cm, PepMap nanoViper C18 column, 5 µm, 100 Å, Thermo Scientific), the column was equilibrated in 98% buffer A (2% (v/v) acetonitrile and 0.1% (v/v) formic acid), and washed by the same buffer as above for 3 min. was connected after washing. Peptides were loaded on to a resolving C18 column (75 µm × 50 cm, PepMap RSLC C18 column, 2 µm, 100 Å, Thermo Scientific) and eluted with a gradient concentration of 98% buffer A and 40% buffer B (80% (v/v) acetonitrile, 0.08% (v/v) formic acid) with a 300 nL/min flow rate for 68 min. Peptides were then analysed with LTQ-Orbitap Velos with the resolution set at 60,000.

3.2.9 Peptide sequence analysing via PEAKS software

The raw data was processed in PEAKS 7. Briefly, a data search against UniProtKB/Swiss-Prot and National Center for Biotechnology Information (NCBI) nonredundant (nr) was performed with a precursor mass tolerance of 10.0 ppm, 0.5 Da fragment ion tolerances to specify each sample as raw data using various enzyme digestions. The fixed and variable modifications use carbamidomethylation of Cys, Oxidation of Met and Deamidation of Asn/Gln with a 1% false discovery rate (FDR). The peptide sequence was mapped using PEAKS SPIDER including posttranslational modifications (PTM). The antibody sequence was assembled by overlapping sequences obtained by digesting antibody fragments with different enzymes.

3.2.10 Recombinant human anti-histone antibody production

Based on the peptide sequence obtained above, the coding DNA sequence was simulated using the Phyre server [190]. The coding DNA for a scFv human sequence was synthesised by life technology containing BamHI and NdeI restriction sites. The DNA was amplified using polymerase chain reaction (PCR) and digested with NdeI and BamH1 restriction enzymes. The isolated insert was ligated with a digested pET-16b vector and sub-cloned into DH5α *E.coli*. The plasmids containing the correct coding DNA sequences were subsequently transformed into BL21 (DE strains), to express proteins at 18°C for 16 h. The production procedure was the same as described in Chapter 2, section 2.2.10.

3.2.11 No.2 human anti-histone antibody antibody affinity measurement

Surface plasmon resonance (SPR) is a commonly used method to measure the binding affinities [191-193]. Sensor Chip coated with streptavidin (SA) (GE Healthcare, UK) was used on the Biacore™ X100 (GE healthcare, UK) platform for the whole project. This is because that SA directly binds to histones with high affinities [171]. Briefly, calf thymus histones were captured on flow cell 2 of the SA chip with flow cell 1 as control and a series of concentrations of anti-histone antibodies were applied to the surfaces (0.125, 0.25, 0.5, 0.75, 1.0, 1.5, 2.0 and 3.0 μM) .

3.2.12 Recombinant human anti-histone antibody functional assay

EA.hy926 cell culture has been described in chapter 2, section 2.2.15. Briefly, confluent EA.hy926 cells were treated in 96 well plates with a series of anti-histone antibody

concentrations (0, 20, 50, 100, 200 and 300 μg/mL) for 10 min. 250 μg/mL calf thymus histone were added and incubated with the antibodies for 4 h. 10 μL of WST-8 dye was then added to 100 μL fresh media and incubated with the cells for a further 4 h. After incubation the OD_{450nm} reading was recorded.

3.2.13 Antibody-mediated protection against histones *in vivo*

C57BL/6 male mice were used to investigate the effect of human anti-histone antibody against calf thymus histone-induced toxicity; these procedures were performed according to state laws and operated in Southeast University in China, who holds a full animal license for using mice. 75 mg/kg calf thymus histones were infused through a tail vein, or 10 mg/kg of either heparin or No.2 human anti-histone antibody was injected 10 min prior to histones infusion. Mice survival was monitored over a 72 h period.

3.3 Results

3.3.1 Anti-histone antibodies are present in the sera of patients with SLE

The presence of anti-histone antibodies in SLE sera was determined using Western blotting. Human individual histones, calf thymus histones and S100P (negative control) were separated by SDS-PAGE and bands were observed after Coomassie brilliant blue staining (Fig. 3.2A). Proteins on duplicated gels were transferred onto PVDF membranes which were probed with either control human IgG (Fig. 3.2 B), healthy sera (Fig. 3.2C) or SLE sera (Fig. 3.2D) and detected with anti-human-HRP. Non-specific S100P bands appeared on all membranes (Fig. 3.2B-D). Antibodies that bind to histones were only present in SLE serum (Fig. 3.2D). Sera from 4 patients with SLE (From Dr. Andy Cross, Aintree Hospital) were detected, but only one (Fig 3.2D) showed a strong signal for histones (Data not shown). Only the serum containing anti-histone antibodies was used for further analysis.

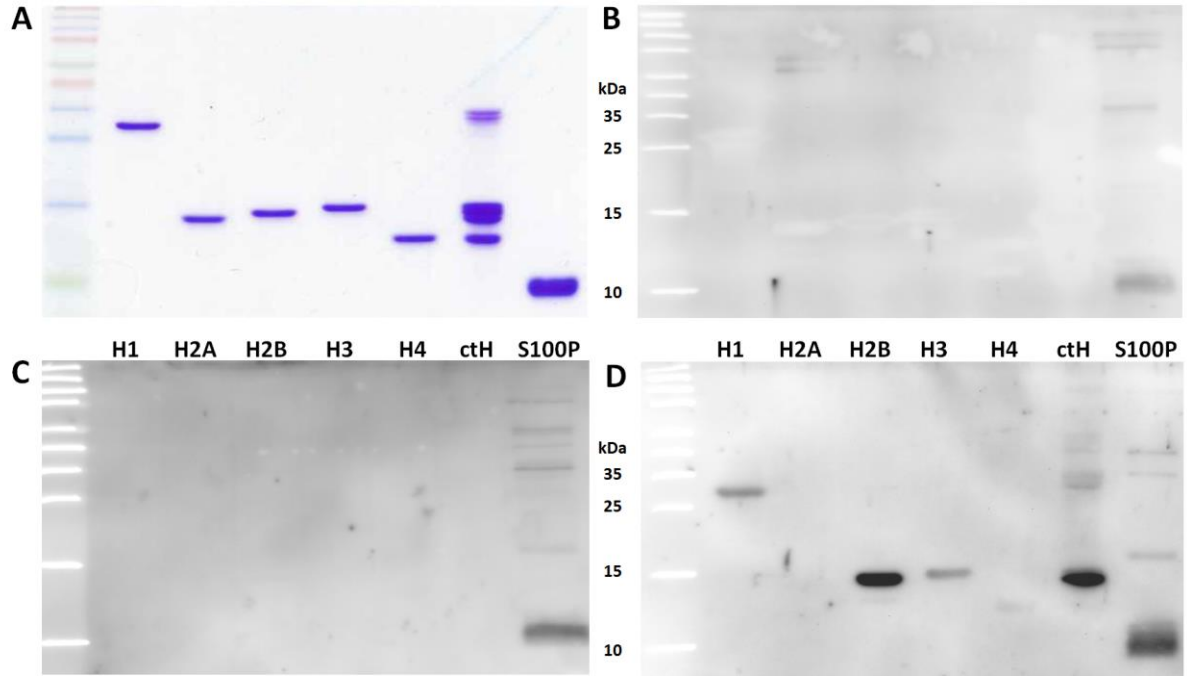

Figure 3.2 Screening for autoantibodies to histones in SLE sera. (**A**) 2 µg of recombinant human histones (H1, H2A, H2B, H3 and H4), calf thymus histones (ctH) and S100P

(negative control) were subjected to SDS-PAGE and stained with Coomassie Blue, (**B**) or probed with IgG antibodies after transfer onto a PVDF membrane, (**C**) probed with healthy sera, (**D**) probed with SLE sera.

3.3.2 Anti-histone antibodies were isolated from the SLE serum

Total antibodies were firstly isolated from the SLE serum using protein A/G resin. Next, polyclonal antibodies of anti-histone were purified using calf thymus histone-conjugated sepharose resin. The isolation procedures were monitored by Western blotting as described above. The isolated total antibodies (Fig. 3.3A) and histone specific antibodies (Fig. 3.3B) all recognised the same individual histones as that of the original serum.

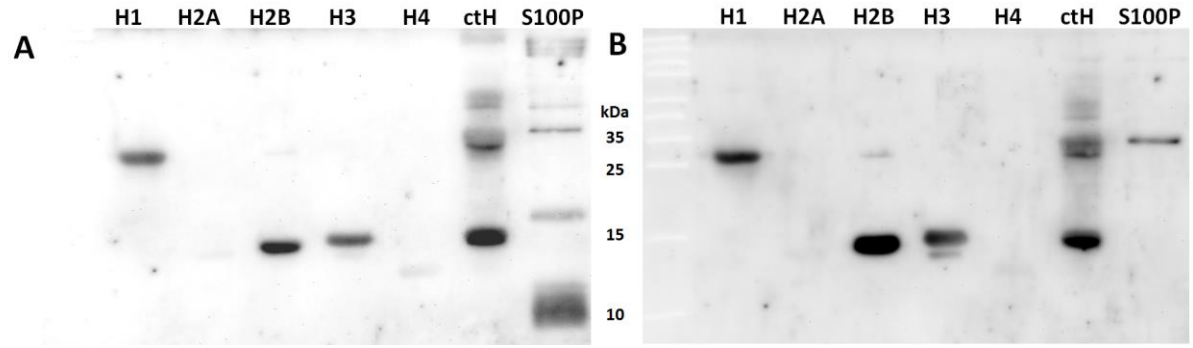

Figure 3.3 Purified human anti-histone antibodies from SLE serum were examined against histones. (**A**) 2 µg recombinant human histones, calf thymus histones (ctH) and S100P (negative control) were subjected to SDS-PAGE and probed with total antibodies isolated antibodies from SLE serum, or (**B**) probed with purified anti-histone antibodies using histones conjugated Sepharose resin.

3.3.3 Human anti-histone antibody sequences were identified

The purified human anti-histone polyclonal antibodies were run on a two-dimensional gel in order to separate the Heavy and Light chains (Fig. 3.4A). The subsequent spots containing heavy and light chain were excised and digested with Trypsin, Chymotrypsin, Glu-C, Lys-C and Asp-N and analysed using MS/MS. A typical spectrum of heavy (Fig. 3.4B) and light chain (Fig. 3.4C) are displayed following trypsin digestion. PEAKS software was used to analyse the spectra, for each specific enzymes. The peptide sequences of variable fragment of light (Fig. 3.4D) and heavy chain (Fig. 3.3E) were acquired after PEAKS analysis, with 100% peptide matching to the human IgG1template.

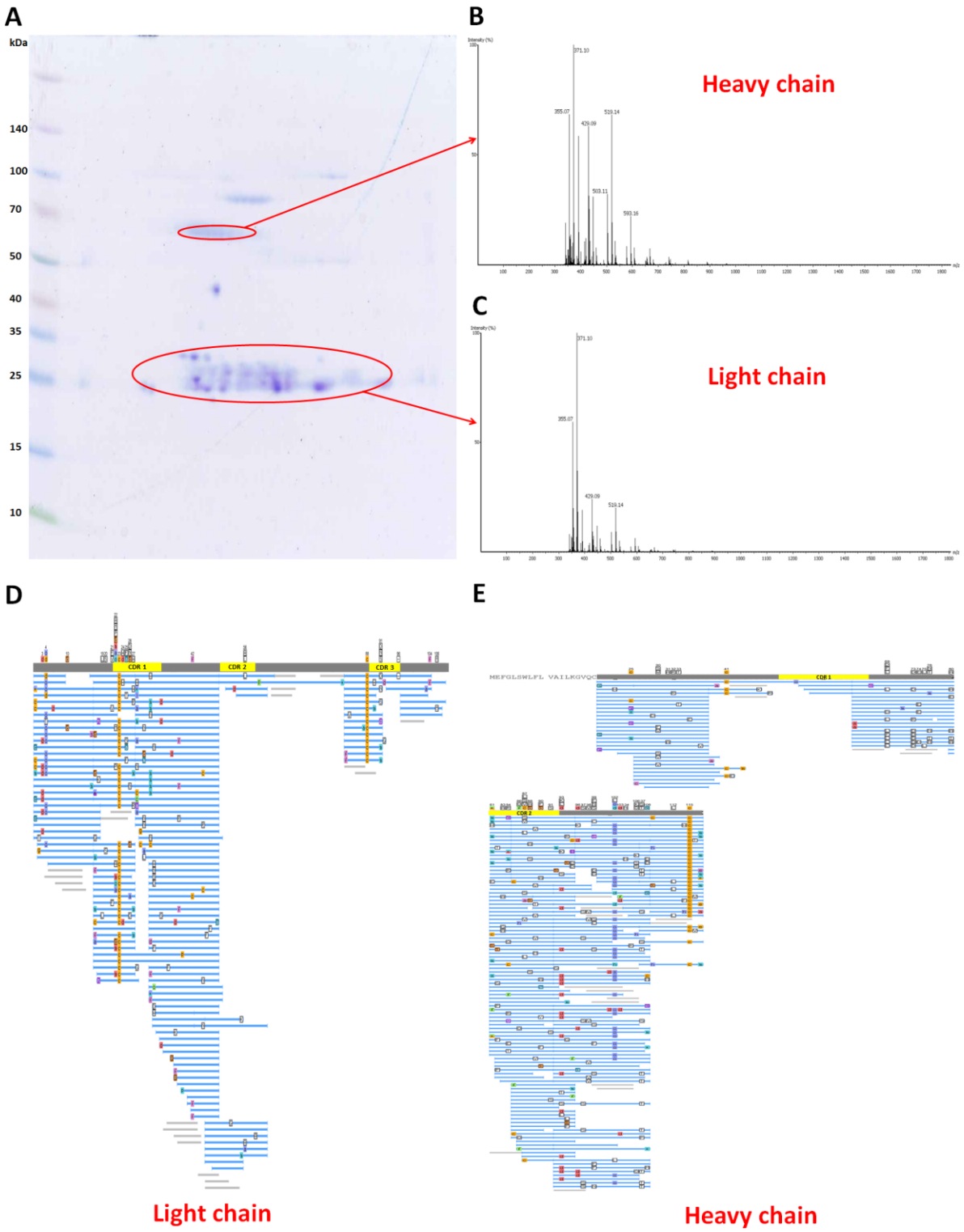

Figure 3.4 Identification of human anti-histone antibody sequences (**A**) Following a two steps purification, anti-histone antibodies were separated by two-dimension gel electrophoresis. (**B**) Typical heavy and (**C**) light chain spectra are presented. (**D**) The peptide

sequence of variable fragment of the light and (**E**) heavy chain are aligned based on specific spectra analysed using PEAKS 7 software, with post-translation modification (PTM). Blue lines represent sequence identity with the germline sequence and coloured residues represent differences between sequences. CDRs of heavy and light chains are highlighted. PTM legend: a: Amidation (K) (+42.01), c: Carbamidomethylation (+57.02), d: Deamidation (NQ) (+0.98) f:Formylation (+27.99), g: Glycidamide adduct (+87.03), h: Hydroxylation (+15.99), m: Methylation (+14.02), o: Oxidation (M) (+15.99), p: Phosphorylation (STY) (+79.97), s: Sodium adduct (+21.98) and ☒: Mutation.

3.3.4 Human anti-histone antibodies were successfully produced

The complete peptide sequences of the variable regions of both heavy and light chains were used to design a scFv with a commonly used linker (Fig. 3.5A) and the predicted structure is shown in Figure 3.5B. The sequences of both the light and heavy chains of the isolated human anti-histone antibodies were identical. However, there are 4 possible variable regions for the heavy chains. Therefore, 4 antibodies were designed based on different CDR sequences obtained from MS/MS and named No.1, No.2, No.3, and No.4 human anti-histone antibody. The coding DNA sequences were optimised, synthesised and subcloned into a pET-16b vector. The proteins were expressed in Shuffle® T7 express competent *E. coli*. After purification using on-column refolding, each scFv was separated by SDS-PAGE and stained with Coomassie brilliant blue (Fig. 3.5C – F). For each of the anti-histone antibodies, the purity was approximately 85%, which was likely due to antibody degradation.

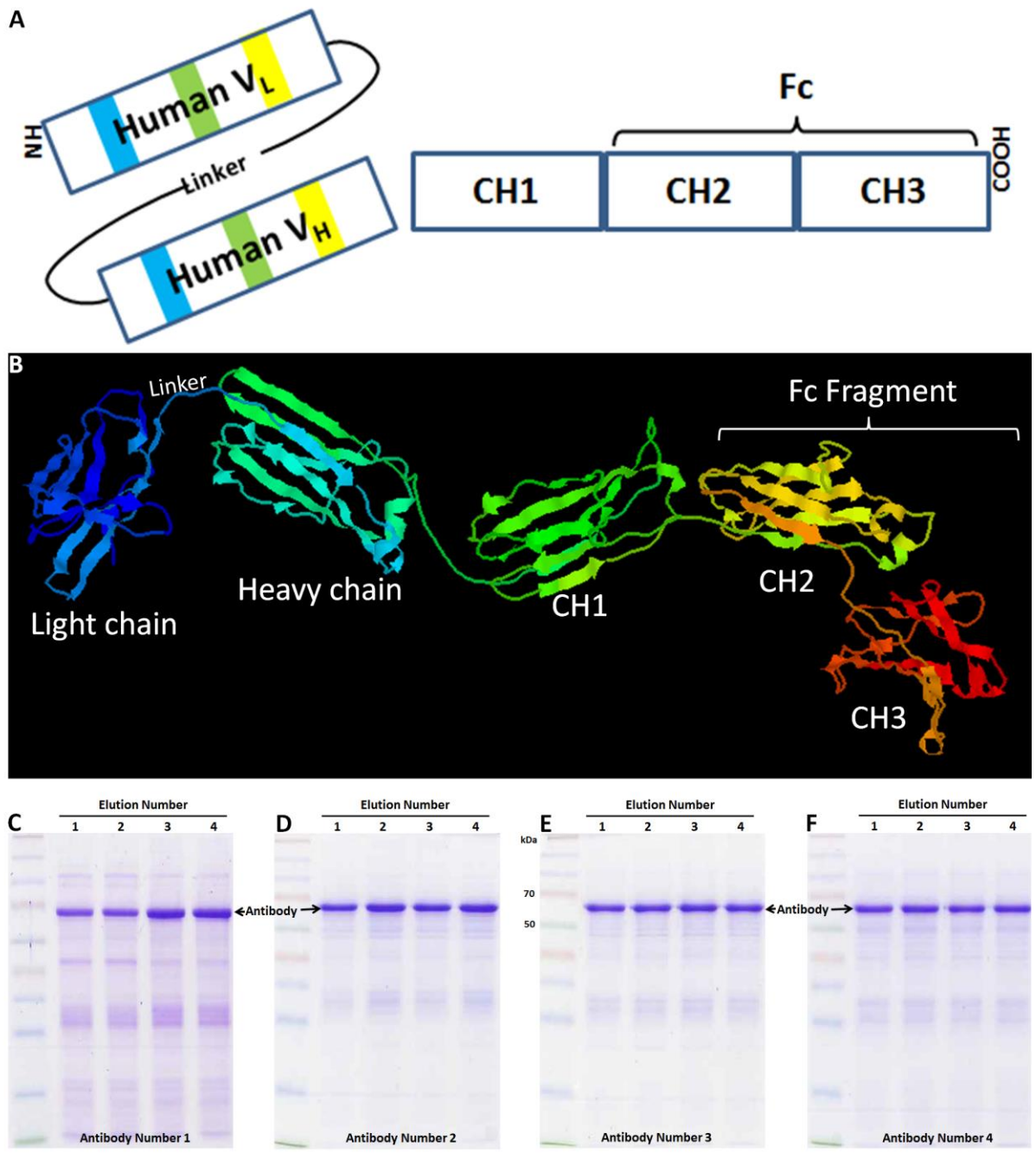

Figure 3.5 Recombinant human anti-histone antibody productions. (**A**) Antibody design template, including variable light and heavy chains with a flexible linker, and linked with CH1, CH2 and CH3 domains. (**B**) Template peptide sequence of a recombinant human anti-histone antibody was designed as illustrated. Four antibodies (**B**) Antibody No.1, (**C**) No.2, (**D**) No.3 and (**E**) No.4 were produced with integrated CDRs, specifically targeted against

histones. Four sequential column elution steps (Elution No. 1-4) for each antibody were separated by 12% SDS-PAGE and visualised by Coomassie brilliant blue staining.

3.3.5 Human anti-histone antibodies bind to histones with high affinity

To explore the specificity and affinity of the recombinant human anti-histone antibodies to histones, human histones and control proteins were subjected to Western blotting, and these antibodies were used as primary antibodies. I found that all 4 of the recombinant human anti-histone antibodies specifically bind to H1, H2B and H3 but not H2A (Fig. 3.5A – D). In contrast, a H4 band could only be clearly observed on the blot probed with No.2 human anti-histone antibody, with relatively weak bands in blots probed with the other three. The affinity of No.2 human anti-histone antibody to histones under native condition was investigated using SPR. Calf thymus histones were captured on sensor chip SA and various concentrations of human anti-histone antibodies were used in the kinetic assays. The average Kd of No.2 human anti-histone antibody was approximately 5.717×10^{-7} M (Fig 3.5E), whereas the affinity of No.4 antibody to histones was 3.197×10^{-6} M. Moreover, the Kds for No.1 and No.3 anti-histone antibodies were not able to be calculated due to their low binding affinity.

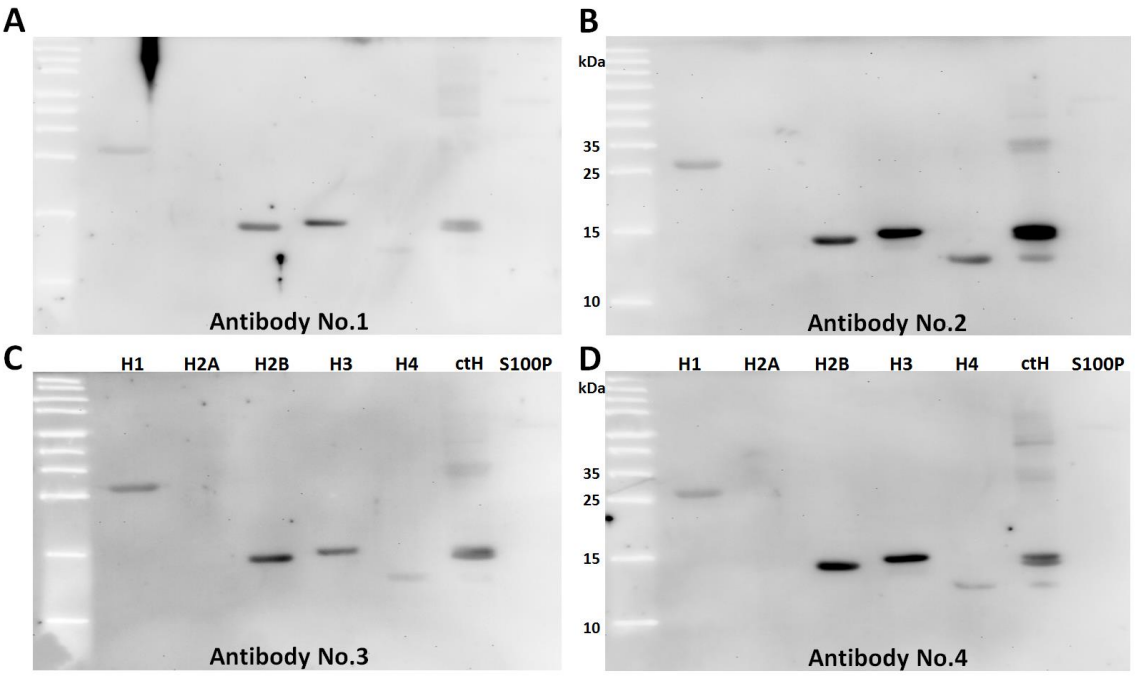

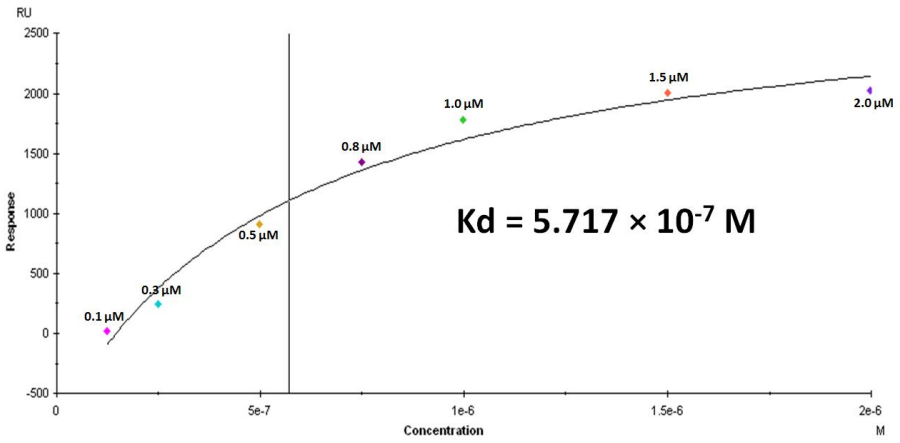

Antibody No.2

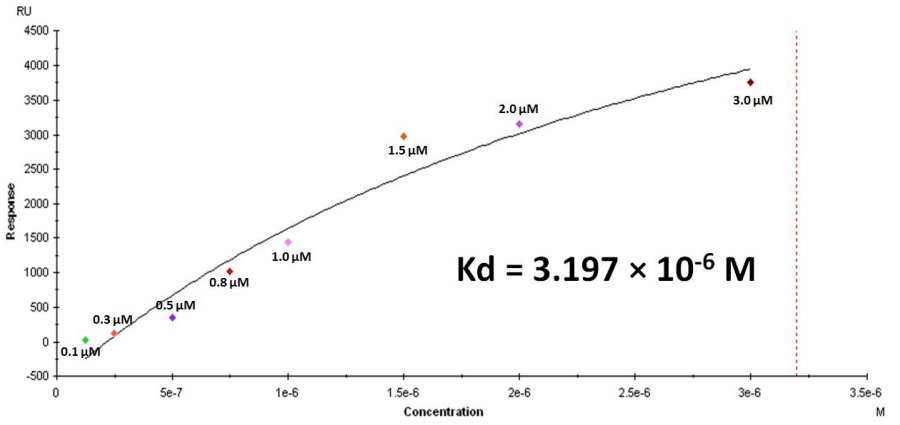

Antibody No.4

Figure 3.6 Human anti-histone antibody binding. (**A**) 2 μg of recombinant histones, mixed calf thymus histones and S100P (negative control) were subjected to 15% SDS-PAGE and probed with antibody (**A**) No.1, (**B**) No.2, (**C**) No.3 and (**D**) No.4 followed by transfer on to a PVDF membrane. (**E**) Calf thymus histones were captured on sensor chip SA, and a series of concentrations (0.1, 0.3, 0.5, 0.8, 1.0, 1.5, 2.0 and 3.0 μM) of No.2 antibody were used. The affinity between No.2 antibody and mixed histones is 5.717×10^{-7} M after the Biacore™ X100 measurement. (**F**) Using the same procedure as above for No.4 antibody, the affinity to calf thymus histones was determined to be 3.197×10^{-6} M.

3.3.6 Human anti-histone antibodies protect endothelial cells from histone toxicity

The cytotoxicity of histones to endothelial-like cells (EAhy926) has been shown in chapter 2, as well as in recent publications [91, 173]. I first determined that 250 μg/mL histones were cytotoxic to endothelial-like cells (EAhy926) using a WST-8 assay. Next, the protective effect of each human anti-histone antibody against histone-induced toxicity was investigated. Endothelial cells were significantly protected by all antibodies (Fig. 3.6A & B) with No.2 antibody showing a significant protective effect at concentrations as low as 50 μg/mL, demonstrating that this antibody is highly efficient in reduce the histone-induced toxicity.

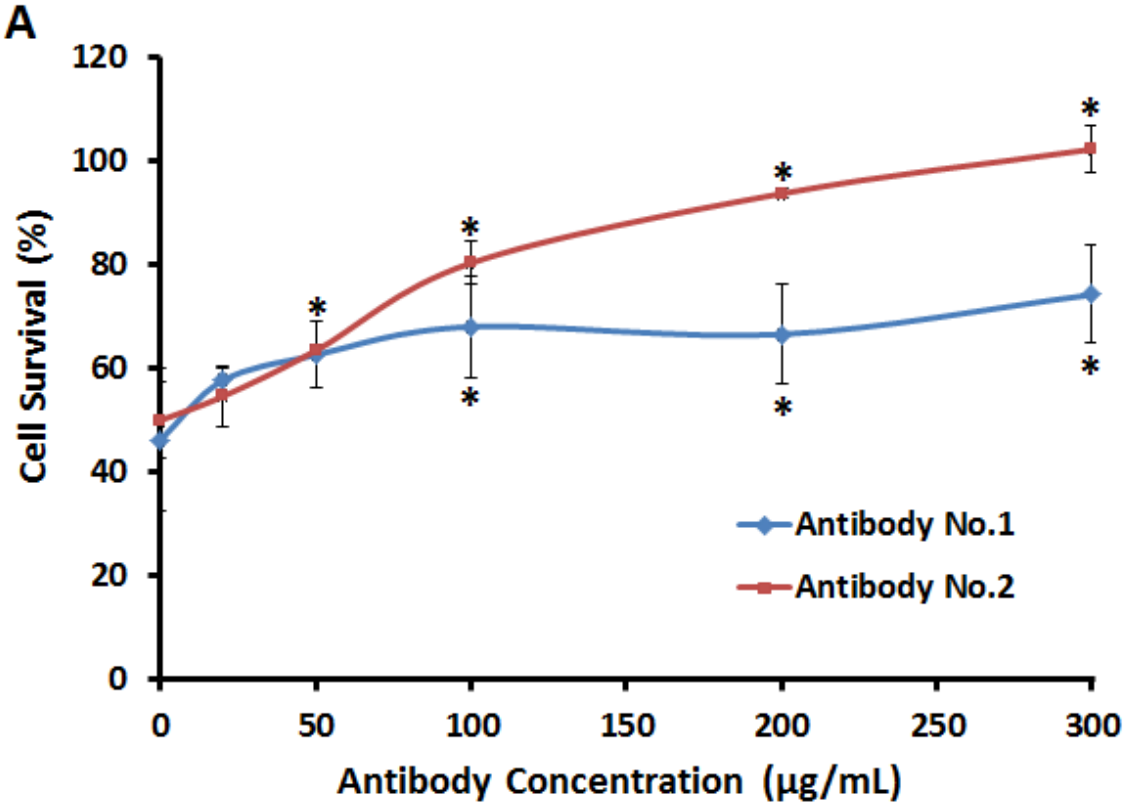
A
120
100
80
60
40
20
0
Cell Survival (%)
0
50
100
150
200
250
300
Antibody Concentration (μg/mL)
Antibody No.1
Antibody No.2

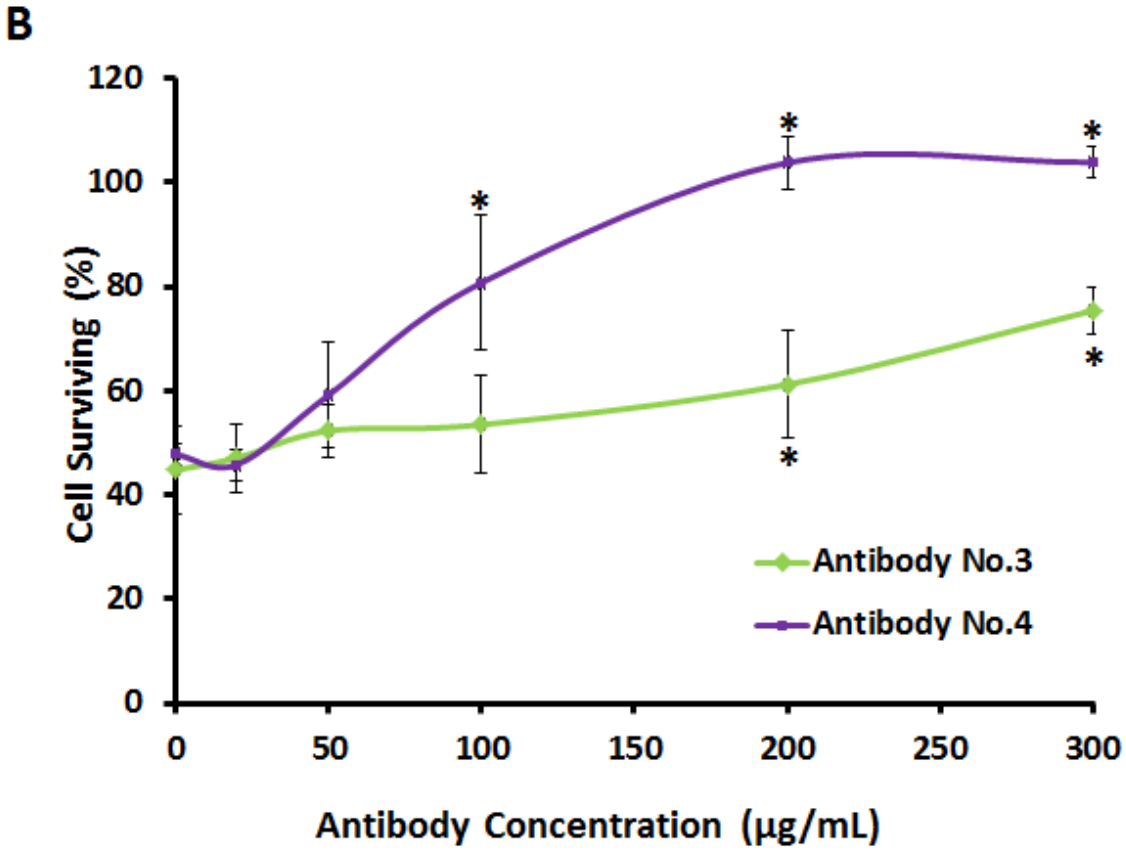
B
120
100
80
60
40
20
0
Cell Surviving (%)
0
50
100
150
200
250
300
Antibody Concentration (μg/mL)
Antibody No.3
Antibody No.4

Figure 3.7 Human anti-histone antibody protections *in vitro* against histone-induced cytoxicity. (A) In order to determine the protective effects, EA.hy926 cells were treated with calf thymus histones (250 μg/mL) in the absence of presence of different concentrations (20, 50, 100, 200 and 300 μg/mL) of the No.1 and No.2 recombinant antibodies. Cell survival (%) was determined by WST-8 toxicity assay. (**B**) The same method was used to show the protection to histones for No.3 and No.4 antibodies. Means ±SD are shown. *$p < 0.05$ compared with histones treated cells in the absence of antibodies using ANOVA test.

3.3.7 Human anti-histone antibodies rescue mice infused with histones

To further explore the protective effects of the No.2 antibody, calf thymus histones (75 mg/kg) were infused in to mice. At this lethal dose of histones all mice died within 4 h. However, pre-infusion of either 10 mg/kg No.2 antibody or heparin, 10 min prior to histone-infusion, significantly protected all mice from a lethal dose of histones (Fig 3.6C). These data demonstrate that No.2 antibody has an affinity to histones, and also inhibits histones-induced toxicity in mice. Taken together, No.2 human anti-histone antibody binds histones, inhibits histone-induced endothelial cell toxicity *in vitro*, and protects mice from histone-induced mortality.

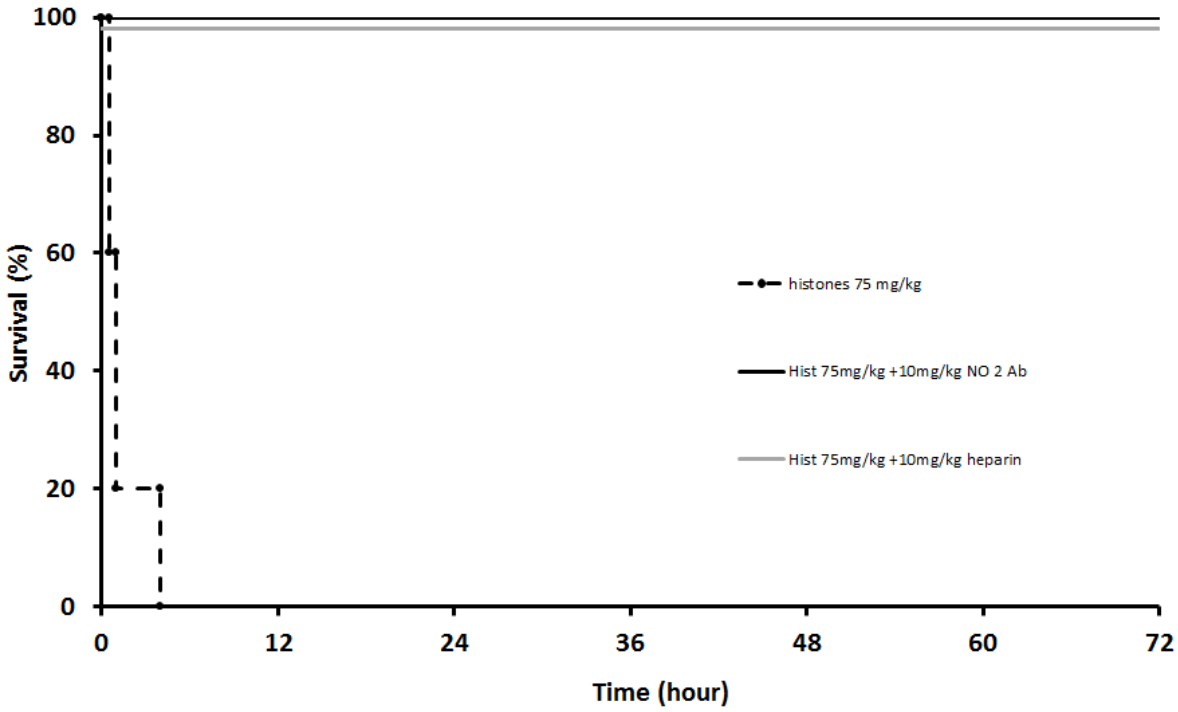

Figure 3.8 Effect of human anti-histone antibody against histone-induced toxicity in mice. Group 1; 75 mg/kg calf thymus histones were infused into 5 individual healthy mice, all mice died within 4 h. Group 2; 10 mg/kg No.2 antibody and 75 mg/kg histones (Hist) were infused into 5 healthy mice, these mice survived over 72 h. Group 3; 10 mg/kg heparin and 75 mg/kg histone were injected in 5 mice, these mice survived more than 72 h.

3.4 Discussion

A novel approach for producing human antibodies to specific antigens has been established in this study. This approach includes a two-step purification of human antibodies from sera, 2D gel electrophoresis, LC-MS/MS and PEAKS analysis, scFv coding sequence design and synthesis, recombinant antibody production and characterisation as outlined in Fig 3.1. To date, this approach has not been widely used, but the successful application in this study may encourage other groups to adopt this methodology. This may be of particular use when a neutralising antibody is urgently needed to treat a new outbreak of infectious diseases. Normally, neutralising antibodies exist in survivors of a viral or bacterial infection. Since this methodological approach is rapid and robust, identification and production of a novel therapeutic antibody may help to stop an outbreak of previously unknown infection. In addition, many auto-antibodies in human sera may be identified and produced in this way for both research and therapeutic benefit.

The human anti-histone antibodies isolated in this study recognise a spectrum of histones. This may be due to all histones having a strong positive charge or the presence of multiple lysine or arginine sequences. However further experiments are needed to clarify the reason behind this observation. Autoantibodies to H1, H2B and H3 in SLE sera also have been reported previously [194, 195]. Overall, due to the broad range of histones that these antibodies recognise, they may in fact be more effective in detoxifying histones than an antibody that only recognises a single histone isoform.

3.5 Conclusion

A proteomics approach for identification of human antibody sequence has been established. The recombinant human anti-histone antibodies are specific to histones and have high affinities. More importantly, those antibodies can reduce histone-induced toxicity to endothelial cells, and protect mice infused with lethal dose of histones. Therefore, there is a great potential to be developed as a clinically used anti-histone reagent.

Chapter 4 Identification of Histone-Binding Proteins in Human Serum Using Mass Spectrometry

4.1 Introduction

The toxic effects of histones include coagulation activation [38], platelet aggregation [39], pro-inflammatory cytokine release [40, 41] and endothelial damage [173]. Moreover, extracellular histones and DNA are released from neutrophils to form NETs, which facilitate thrombus formation and are relevant in models of deep vein thrombosis, transfusion-related acute lung injury, cancer, trauma and sepsis [14, 36, 42-44].

Histones-triggered harmful effects can be reduced by protein APC, an enzyme that cleaves histones, antibodies that neutralise histones [14], CRP [91], albumin [196] and heparin [92] that bind to histones. It is also reported that many plasma proteins could be co-precipitated with histones [93]. Moreover, we found that 20 μg/mL histones are significantly cytotoxic to endothelial cells in the absence of serum or plasma [91]. In contrast, >50 μg/mL histones in plasma show toxic effects on these cells [48]. However, the major proteins that strongly interact with histones in plasma are not fully clarified. In this study, I will isolate histone-binding proteins using a pull-down assay with high stringency and identify these proteins using mass spectrometry.

4.2 Methods

4.2.1 Isolation of histone-binding proteins from sera

Blank and histone-conjugated Sepharose columns were prepared as described in Chapter 3, section 3.2.3. Normal or acute phase sera from healthy and critically ill donors were diluted with 2 × PBS and centrifuged at 17,000 × g for 10 min at 4°C to remove the insoluble contents. The harvested supernatant was then applied to the blank Sepharose column in order to eliminate proteins that would non-specifically bind to Sepharose. For the sera from critically ill patients that contain high levels of CRP, a major acute phase protein that binds to and detoxifies histones [91], the pass through from blank Sepharose column were further applied to *p*-Aminophenyl Phosphoryl Choline-conjugated Agarose beads (Thermo Fisher Scientific, USA) to avoid the interference from CRP in the subsequent steps. The CRP-free sera were then applied to a histone-conjugated Sepharose column. After two washes (200 mL of PBS containing 0.5% (v/v) Tween 20 followed by 100 mL of PBS only), histone-binding proteins were finally eluted with 20 mL of 100 mM Glycine, pH 3.0 and immediately neutralised with 2 mL of 1 M Tris-HCl, pH8.0. The eluates were separated by SDS-PAGE or 2D gel electrophoresis which were then stained with Coomassie brilliant blue.

4.2.2 Spot in-gel digestion by trypsin

After 2-D gel electrophoresis, each spot was individually excised and digested using trypsin. The digested samples were then examined on LC-MS/MS, which is fully described in Chapter 3 sections 3.2..7 & 8.

4.2.3 Histone-binding protein analysis

The raw MS/MS data was analysed by PEAKS software using the same setting as described in Chapter 3 section 3.2.9.

4.2.4 Western blotting

The proteins that were identified using MS/MS mass spectrometry were further validated using Western blotting. The eluates together with human antithrombin and prothrombin (as positive controls) were subjected to Western blotting and probed with anti-prothrombin and anti-antithrombin antibodies. The detailed procedures were described in details in Chapter 2 section 2.2.13.

4.3 Results

4.3.1 CRP has been completely removed from acute phase patient sera

CRP levels are normally less than 10 mg/L in serum, but may increase up to 1,000 fold in severe disease conditions [197]. CRP interacts with histones [91]. Therefore, high levels of CRP may interfere with the isolation of other histone-binding proteins [91]. As such, the CRP in the serum from patients was removed by phosphocholine-conjugated beads. Figure 4.1A shows that the CRP was retained in the column and can be eluted using free phosphocholine. However, when the pass through was applied to second phosphocholine-conjugated column, the CRP band was not present (Fig. 4.1A right), suggesting that CRP was completely removed from the serum. In addition, CRP was not identified after PEAKS analysis (Table 4.1). The CRP-free pass through from second column was used for isolation of histone-binding proteins.

4.3.2 Histone-binding proteins can be pulled down using histone-conjugated Sepharose

The sera proteins isolated using histone-conjugated beads were separated by 2-D gel electrophoresis. Following Coomassie brilliant blue staining, 7 identifiable spots were observed in patient (Fig. 4.1B) and normal sera (Fig. 4.1C). Taken together, histone binding proteins were eluted from both acute phase and normal sera and showed a similar pattern when separated using 2-D gel electrophoresis.

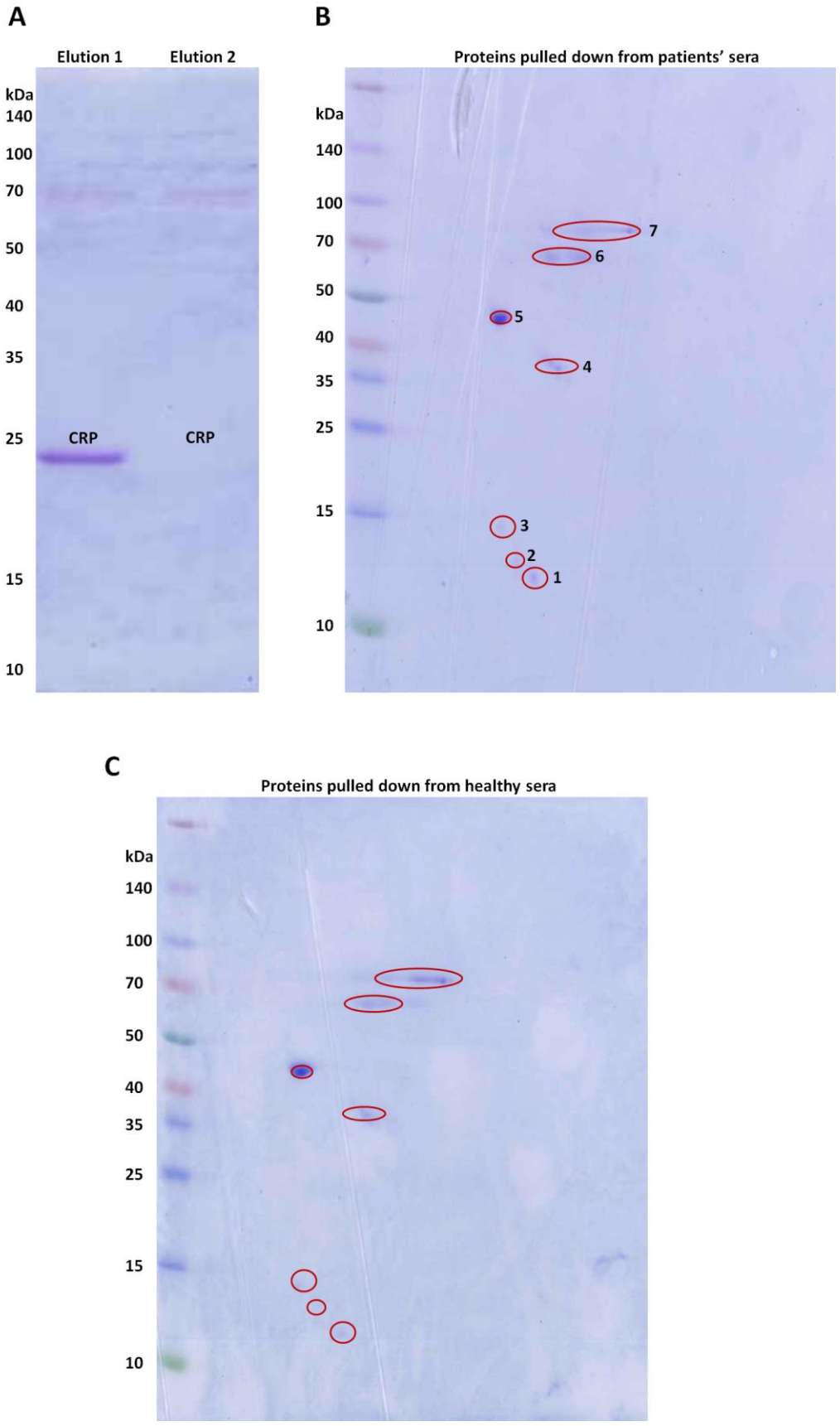
A
Elution 1
Elution 2
kDa
140
100
70
50
40
35
25
15
10
CRP
CRP
B
Proteins pulled down from patients' sera
kDa
140
100
70
50
40
35
25
15
10
7
6
5
4
3
2
1
C
Proteins pulled down from healthy sera
kDa
140
100
70
50
40
35
25
15
10

Figure 4.1 Histone binding protein isolation from both critically ill patient and normal sera. (**A**) CRP was twice isolated from critically ill patient sera during the acute phase of disease using phosphoryl Choline-conjugated beads, and then the first and second eluates were subjected to 15% SDS-PAGE. (**B**) Following CRP elimination, histone binding proteins were captured using affinity chromatography with a histone conjugated sepharose column from sera. The column eluate was separated by 2-D gradient gel (8 – 18%) electrophoresis, and stained with coomassie brilliant blue. Each spot (red circle) was digested by trypsin, and investigated using LC-MS/MS. (**C**) Histone binding proteins were also eluted from normal sera separated by 2-D gradient gel (8 – 18%) electrophoresis, and stained with coomassie brilliant blue.

4.3.3 Identification of the isolated histone-binding proteins using mass spectrometry

Following 2-D gel electrophoresis, each spot was excised and digested by trypsin, and subsequently analysed by LC-MS/MS. The raw data was processed using PEAKS software and the IDs of each of the 7 spot are listed in Table 4.1. A strong spot in Figure 4.1C (red circle No.5), suggesting both high abundance within the serum and high affinity for histones, was identified using mass spectrometry, and with the raw spectrum data is displayed in figure 4.2A. Upon analysis using PEAKS software, human antithrombin (protein identification in UniProt is P01008 and molecular weight is 52.6 kDa) was identified and confirmed by sequence alignment (Fig. 4.2B), which showed a peptide coverage of 74% when compared to the template sequence. Spot No. 7 in figure 4.1C was also identified by MS/MS and the raw data is displayed in figure 4.2C. Following PEAKS analysis, human prothrombin (protein identification in UniProt is P00734 and molecular weight is 70 kDa) was identified and confirmed by sequence alignment (Fig. 4.2D), with 40% peptide coverage compared to the template sequence.

Table 4.1 Histone binding protein identification with MS/MS.

Accession	Gene name	Description	Coverage (%)	Peptides matched	MW in NCBI (kDa)	MW on the gel (kDa)	Spot No.
P62805	H4	Human Histone H4	51	6	11.4	12	1
P58876	H2B1D	Human histone H2B	38	6	13.9	12	1
P62805	H4	Human Histone H4	51	6	11.4	13	2
P58876	H2B	Human histone H2B	46	6	13.9	13	2
Q99879	H2B1M	Human histone H2B	30	4	14.0	14	3
P16104	H2AX	Human Histone H2A	24	3	15.1	14	3
P10909	CLUS	HUMAN Clusterin	77	88	52.5	32	4
P01008	ANT3	HUMAN Antithrombin-III	74	59	52.6	47	5
P00734	THRB	HUMAN Prothrombin	37	57	70.0	47	5
P04004	VTNC	HUMAN Vitronectin	75	75	54.3	47	5
P04004	VTNC	HUMAN Vitronectin	69	86	54.3	65	6

P01876	IGHA1	HUMAN Ig alpha-1 chain C region	67	32	37.7	65	6
P01877	IGHA2	HUMAN Ig alpha-2 chain C region	44	23	36.5	65	6
P01019	ANGT	HUMAN Angiotensinogen	39	13	53.2	65	6
P00734	THRB	HUMAN Prothrombin	40	117	70.0	75	7

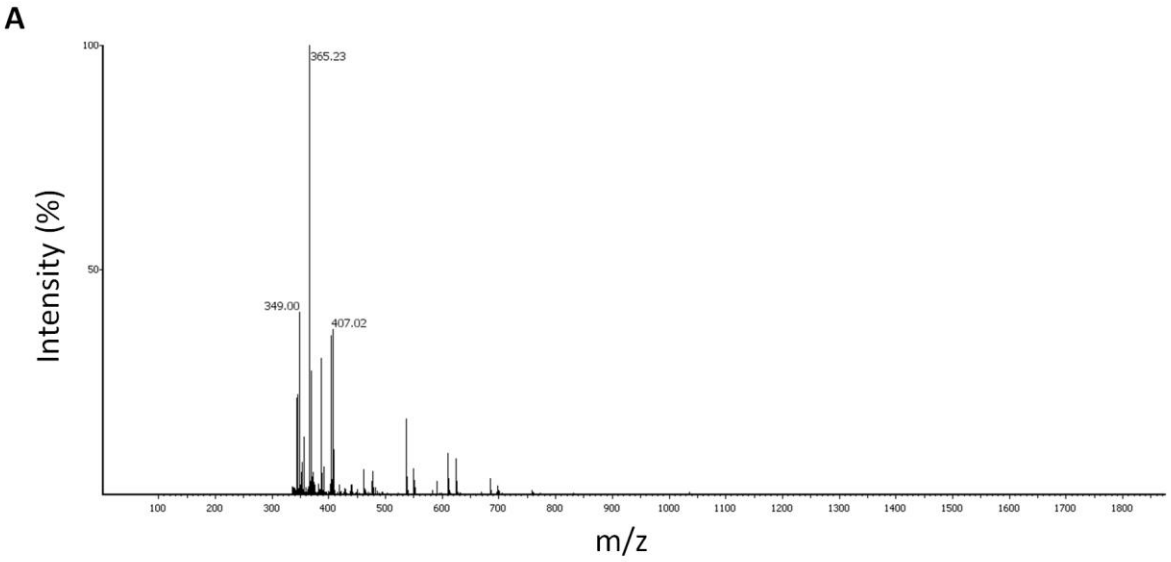
A
Intensity (%)
m/z
365.23
349.00
407.02


B
1 MYSNVIGTVT SGKRKVYLLS LLLIGFWDCV TCHGSPVDIC TAKPRDIPMN PMCIYRSPEK KATEDEGSEQ KIPEATNRRV WELSKANSRF ATTFYQHLAD SKNDNDNIFL
111 SPLSISTAFA MTKLGACNDT LQQLMEVFKF DTISEKTSDQ IHFFFAKLNC RLYRKANKSS KLVSANRLFG DKSLTFNETY QDISELVYGA KLQPLDFKEN AEQSRAAINK
221 WVSNKTEGRI TDVIPSEAIN ELTVLVLVNT IYFKGLWKSK FSPENTRKEL FYKADGESCS ASMMYQEGKF RYRRVAEGTQ VLELPFKGDD ITMVLILPKP EKSLAKVEKE
331 LTPEVLQEWL DELEEMMLVV HMPRFRIEDG FSLKEQLQDM GLVDLFSPEK SKLPGIVAEG RDDLYVSDAF HKAFLEVNEE GSEAAASTAV VIAGRSLNPN RVTFKANRPF
441 LVFIREVPLN TIIFMGRVAN PCVK

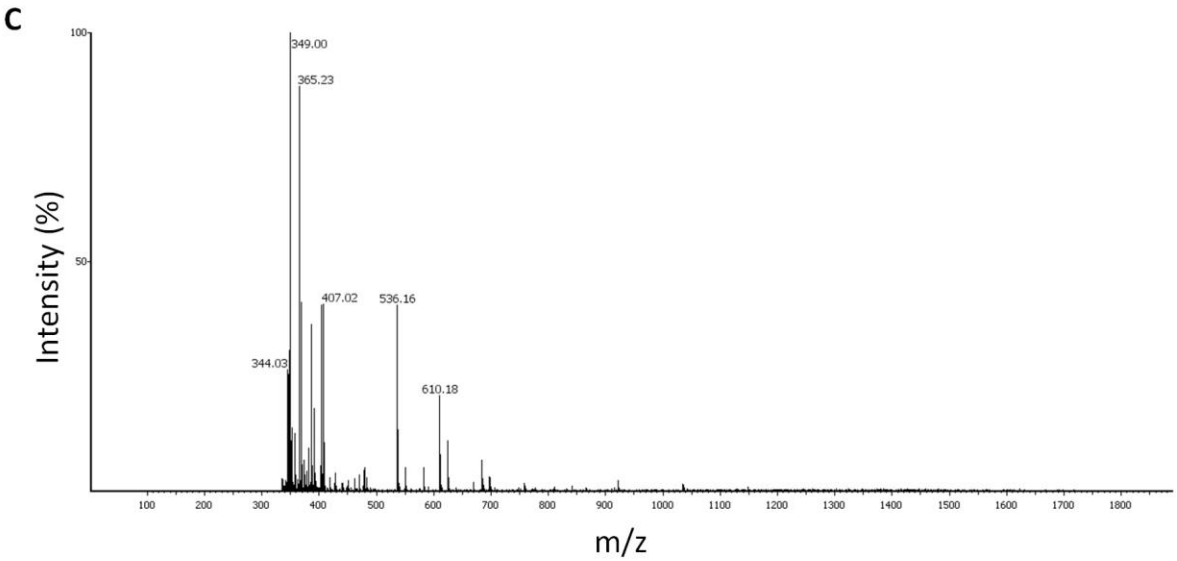
C
Intensity (%)
m/z
349.00
365.23
407.02
536.16
344.03
610.18

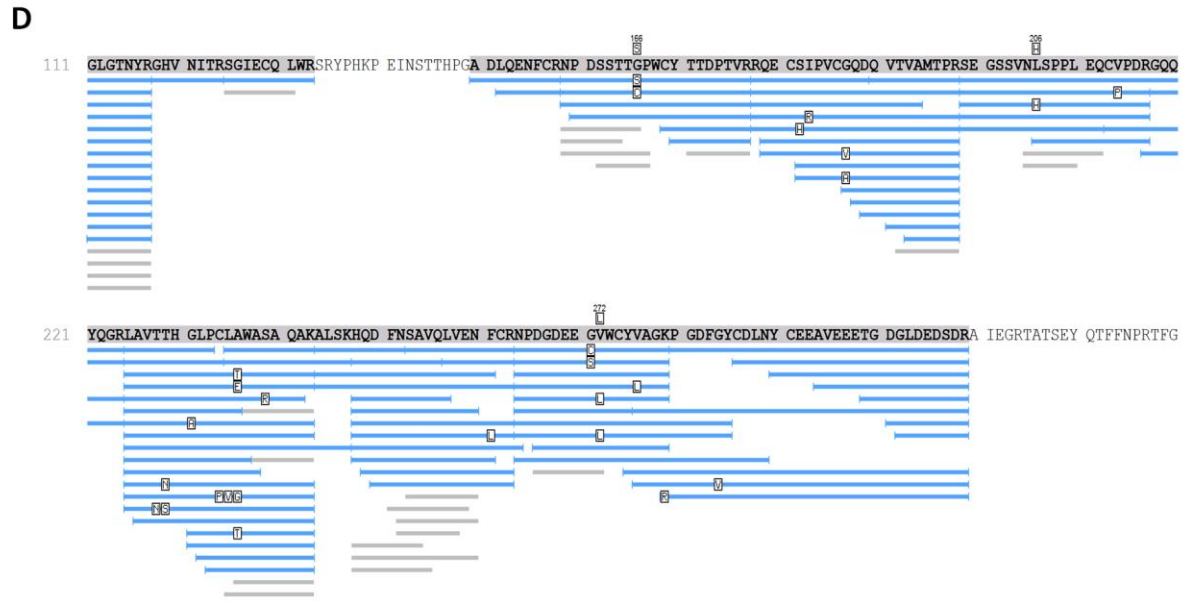

Figure 4.2 Human antithrombin and prothrombin identification using MS/MS and PEAKS. (**A**) A spectrum raw data of spot No. 5 was defined and the spectrum is displayed. (**B**) The raw data was analysed by PEAKS, and human antithrombin was identified with 74% peptide coverage using the NCBInr database. (**C**) A mass spectrum was acquired from spot No.7. (**D**) After PEAKS analysis, prothrombin could be identified (with 40% peptide coverage).

4.3.4 Western blotting verifies these identified histone-binding proteins

To further confirm that the isolated histone-binding protein eluate contains antithrombin and prothrombin, the histone binding-protein elution was subjected to Western blotting and probed with either anti-antithrombin (Fig. 4.3A) or anti-prothrombin (Fig. 4.3A) antibodies, using the respective human proteins as positive controls.

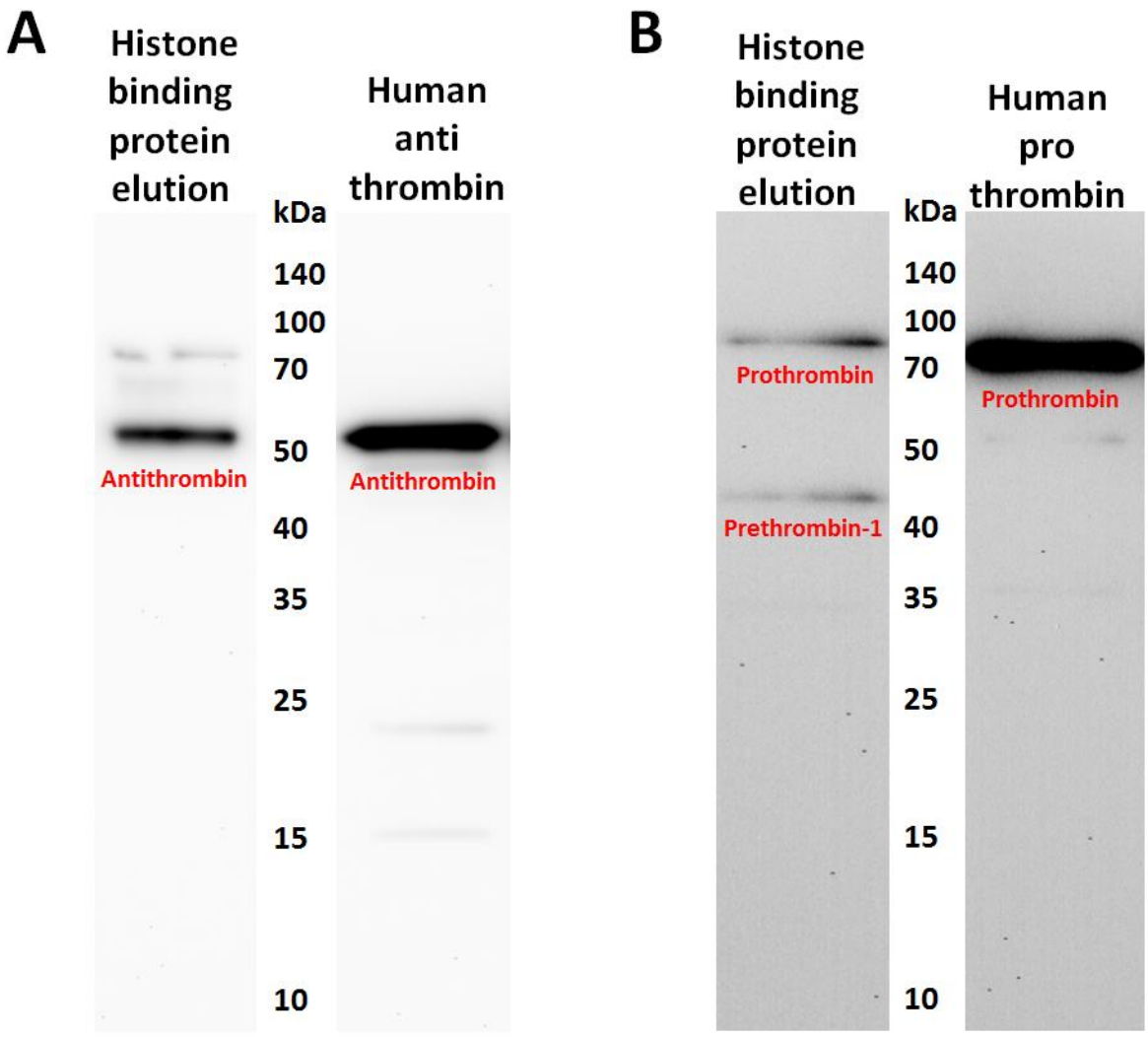

Figure 4.3 Confirmation that human antithrombin and prothrombin are histone-binding proteins present in serum. (**A**) The eluate from histone-conjugated sepharose beads was separated by SDS-PAGE and probed with an ant-antithrombin antibody (left panel), with purified human anit-thrombin as a positive control (right panel). (**B**) Western blotting was performed on the eluate with an anti-prothrombin antibody (left panel), with purified prothrombin as a positive control (right panel).

4.4 Discussion

In this study, I used a highly stringent approach to isolate histone-binding proteins in sera. This is different from previous publications [93]. With the high stringency, only the proteins that tightly bind to histones are isolated or those pursent at high concentrations. Therefore, previously reported histone-binding proteins such as albumin and complement components [93], were not pulled down. Histones were also bound and isolated using this method due to their high binding affinities within the nucleosome. If histones are present in the serum it would therefore be expected that histone H3, when conjugated on the Sepharose beads, could pull-down H4 and vice versa. Similarly, H2A would be able to bind to H2B and thus be present in my data analysis. Since this is a well-known fact, I did not pursue this investigation further.

The most interesting finding is that antithrombin and prothrombin were pulled down using this highly stringent method. Although these proteins have previously been shown to interact with histones, this is the first report that they can be directly pulled down from human serum. This finding also provides further evidence as to why high levels of circulating histones cause significant coagulation abnormalities [48]. By confirming these data using Western blot, I am confident that these findings are robust. Therefore, in the next Chapter I will investigate the functional role of the interaction between histones and prothrombin.

4.5 Conclusion

Histone-binding proteins have been identified using mass spectrometry and analysed using PEAKS software. Human antithrombin and prothrombin bind to histones, which had been confirmed by Western blot. Further characterization of the binding between histones and

prothrombin, as well as the role of this binding in enhanced prothrombin activation will be studied in the next chapter.

Chapter 5 Extracellular Histone Enhanced Prothrombin Activation is Reduced by Anti-Histone Treatment

5.1 Introduction

Extracellular histones have been characterised in the promotion of coagulation and thrombosis. The pro-coagulant properties of histones include endothelial damage with release of vWF, platelet activation and thrombin generation from loss of thrombomodulin (TM)-dependent protein C anticoagulant effects [14, 45, 46]. *In vivo* histone infusion in mice results in rapid thrombocytopenia and platelet consumption in thrombi. Further evidence to support the role of histones in the activation of coagulation has been demonstrated by our group. In mouse models, plasma TAT complexes were significantly elevated following either trauma (endogenous histone model) or histone infusion (exogenous histone model) [48]. Pathologically, the lungs were the predominantly affected organ with neutrophil infiltration, pulmonary edema, haemorrhage, and microvascular thrombosis. The formation of thrombi in lungs strongly supports the hypothesis that histone-triggered coagulation activation is involved in lung injury and possibly MOF.

Thrombin is a pivotal molecule in the coagulation cascade. The regulation of thrombin generation is critical to the balance of bleeding and vascular occlusion [198]. Prothrombin is a zymogen form and its assembly factor (F) Xa, co-factor FVa in the presence of calcium ions and phospholipids constitutes the prothrombinase complex that facilitates thrombin generation. The relationship between prothrombin levels and thrombin generation is strikingly different from other coagulation factor. The rate of thrombin generation, peak activity reached and free total amount of thrombin produced are proportional to free thrombin levels [199].

Prothrombin or coagulation factor II, is a single chain protein composed of fragment 1 (F1) (residues 1 – 155), F2 (residues 156 – 271) and protease domain (α-thrombin) (residues 272 – 579). There are two cleavage pathways in the prothrombinase complex [25]. Prothrombin is initially cleaved at Arg-271 to split into two parts; Fragment 1.2 complex, and prethrombin-2. Moreover, prothrombin is cleaved at Arg-320 to form meizothrombin, because A and B chain are connected by a disulphide bond (Cys-293 and Cys-439). In addition, prothrombin can be activated via cleaving residue Arg-271 on the platelet surface under physiological conditions [25].

Histone H4 has been recently found to promote prothrombin autoactivation [20]. In this study fluorescent titrations were used to demonstrate that H4 directly binds to prothrombin. Furthermore, they demonstrate that this has functional relevance through H4-induced prothrombin cleavage. However, since this reaction took up to 8 hours to occur, its physiological relevance needs to be further explored. In Chapter 4, I have directly pulled down prothrombin using histone-conjugated beads from serum under highly stringent conditions, indicating a strong integration between histones and prothrombin. However, the interaction between histones and prothrombin and its functional roles have not been fully characterised and moreover, the role of prothrombin cofactors had not been taken into account. **In this study, I will** investigate the effect of histones on prothrombin cleavage to understand the mechanism of histone-enhanced thrombin generation.

5.2 Methods

5.2.1 Recombinant HPT fragment 1 and 2 production

Recombinant human prothrombin fragment 1 and 2 were produced in BL21 *E. coli* and purified using affinity chromatography, which has been fully described in Chapter 2, section 2.2.9 & 10.

5.2.2 Mapping the binding sites using gel overlay

Prothrombin, prothrombin fragment 1, prothrombin fragment 2 and human α-thrombin were subjected to 12% SDS-PAGE and transferred to a 0.45 µm PVDF membrane. After transfer, the membrane was incubated with 5 µg of H3 suspended in gel overlay buffer (100 mM NaCl, 50 mM Tris-HCl, 2 mM $CaCl_2$, 2 mM DTT, 0.5% (w/v) BSA, 0.25% (w/v) gelatin (Sigma, USA) and 0.5% (v/v) IGEPAL® CA-630 (Sigma, USA)) overnight at 4°C. The membrane was then washed the following day with overlay washing buffer (100 mM NaCl, 50 mM Tris-HCl, 2 mM DTT, and 0.5% (v/v) IGEPAL® CA-630) twice and TBS-T three times, which was continually blocked with blocking reagent (TBST, 2% (w/v) BSA and 5% (w/v) milk) for two hours. Primary (anti-H3 antibody) and secondary (anti-IgG-HRP antibody) were used as per western blot protocol which was described in Chapter 2, section 2.2.13.

5.2.3 Predicted interaction between Prothrombin and H4 using the ZDOCK server

Prediction of the interaction between prothrombin and H4 was performed by docking, using ZDOCK server as described in reference [200]. Briefly, the ZDOCK server website (http://zdock.umassmed.edu/) was used to simulate the protein-protein interaction. The input

receptor was prothrombin (4NZQ in protein data bank (PDB)) and the input ligand was H4.1 (Q757K0 in PDB). The job ID is 80836.

5.2.4 Determination of binding affinity and the effects of anti-histone reagents

The SPR system with Sensor Chip SA has been described in chapter 3 to measure the antibody-antigen affinity. In this chapter, histones were captured on Sensor Chip SA to investigate the affinity between histone and prothrombin.

Biosensor system including Sensor Chip SA was primed with suspending buffer (100 NaCl, 20 mM Tris-HCl, pH 7.4). 20 µg/mL of each recombinant histone H1, H2A, H2B, H3 and H4 was captured on flow cell 2 (Fc2) with Fc1 set as blank. Increasing concentrations of prothrombin (0.125, 0.25, 0.5, 0.75, 1.0, 1.5, 2.0 and 3.0 µM) were loaded on sensor Chip SA through Fc1 (blank) and Fc2 (histone) with a regeneration step (20 mM HCl) between each histone concentration. Kd values were calculated using the binding to Fc2 (histone) – Fc (blank).

When testing the effect of blocking H4 binding to prothrombin using either ahscFv or heparin, H4 was first coated on to Fc2. 1.5 µM of heparin, control scFv and MahscFv were individually added to Fc 2, with Fc1 as a blank. 1.5 µM of prothrombin was then applied on both Fc2 and Fc1. Response unit was calculated by Fc2 – Fc1.

5.2.5 Prothrombin cleavage

Prothrombin cleavage assay was performed, as described previously [25]. Briefly, prothrombin was dialysed in cleavage buffer (20 mM HEPES, 150 mM NaCl, 5 mM $CaCl_2$, 0.1% (v/v) PEG-8000, pH7.4) for 24 h at 4°C. The cleavage assay was performed in cleavage

buffer, containing 1.5 µM hPT, +/-5 nM FXa and +/- 50 µg/mL H1, H2A, H2B, H3 or H4. When inhibitors were used heparin (6 µM) (Sigma Aldrich, UK) or ahscFv (100 µg/mL) were pre-incubated with histones for 10 min. All reactions were initiated upon the addition of prothrombin and terminated by the addition of 4 × Laemmli buffer and heated at 95°C for 10 min. Proteins were then subjected to SDS-PAGE and visualised using Coomassie blue staining.

5.2.6 Density quantification

To determine the effect of each treatment on prothrombin cleavage, densitometry was performed. Images of coomassie-stained SDS-PAGE gels were captured on a G:BOX (Syngene) using GeneSnap software (Syngene) and further analysed using GeneTools software (Syngene). Densitometry was performed for each prothrombin band in triplicate using equal sized boxes for each treatment. Background was subtracted from the region surrounding each band to account for intra-assay variations in staining, whereas inter-assay variability was corrected by taking a background reading in a blank region of each gel. The corrected density of the untreated prothrombin was assigned the value of 100 percent and the density of each treatment on that gel was expressed as a percentage thereafter.

5.2.7 Thrombin generation assay

Thrombin generation measurements were performed in a 96-well plate fluorimeter (SpectraMax Gemini) equipped with a 360/460 nm filter set, using a fluorogenic thrombin substrate (Technoclone, Austria), Z-Gly-Gly-Arg-AMC. The assay was performed in prothrombin cleavage buffer (total volume=100 µL), containing 1.5 µM prothrombin, +/-0.5 nM Factor Xa and +/- 50 µg/mL H1, H2A, H2B, H3 or H4. When inhibitors were used,

heparin (6 µM) (Sigma Aldrich, UK) or ahscFv (100 µg/mL) were pre-incubated with histones for 10 min. The reaction was initiated upon the addition of prothrombin and the fluorogenic thrombin substrate (50 µL) and fluorescent emissions measured at 37°C every min for 120 min. Sample analysis was performed using Microsoft Excel and thrombin concentrations (nM) were calculated using a thrombin calibration curve (10, 3 and 1 nM thrombin).

For Factor X and Factor V deficient plasma, 32 µL of plasma (Haematologic Technologies Inc) was mixed with 50 µg/mL H4, to a total volume 40 µL. The reaction was then initiated by the addition of 10 µL TGA reagent C (RC) Low (containing tissue factor and phospholipids) (Technoclone, Austria) and 50µL Z-Gly-Gly-Arg-AMC fluorogenic substrate. Fluorescent measurements were taken at 1 min intervals for 60 min at 37°C. Sample analysis was conducted on Technothrombin TGA evaluation software (Technoclone, Austria) using a thrombin calibration curve and data are expressed as thrombin (nM) generation per min.

5.3 Results

5.3.1 Histones H3 and H4 bind to prothrombin

To clarify which histones interact with prothrombin, Biacore X100 SPR system was used. Histones H4 and H3 showed much higher binding responses to prothrombin than equimolar concentration of H1, H2A or H2B. The binding affinities with H3, was Kd = 6.8 x 10^{-7} M and Kd = 7.0 x 10^{-7} M for H4 (Figure 5.1A). However, the Kd values for H1, H2A and H2B were unable to be calculated due to their very low responses. To determine which regions of prothrombin were the histone binding sites, the potential interaction models was first simulated using published 3D structures and they predicted that histones H3 and H4 may interact with fragments 1 and 2 of prothrombin (Figure 5.1B). To confirm this, human

recombinant prothrombin fragment 1 and 2 proteins were produced and a gel overlay assay was used to confirmed that that H3 bound to both fragments 1 and 2 of prothrombin but not to thrombin (B-chain) (Figure 5.1C). However, H4 bound to both fragment 1 and 2 as well as to thrombin, which showed slightly different binding to that of H3.

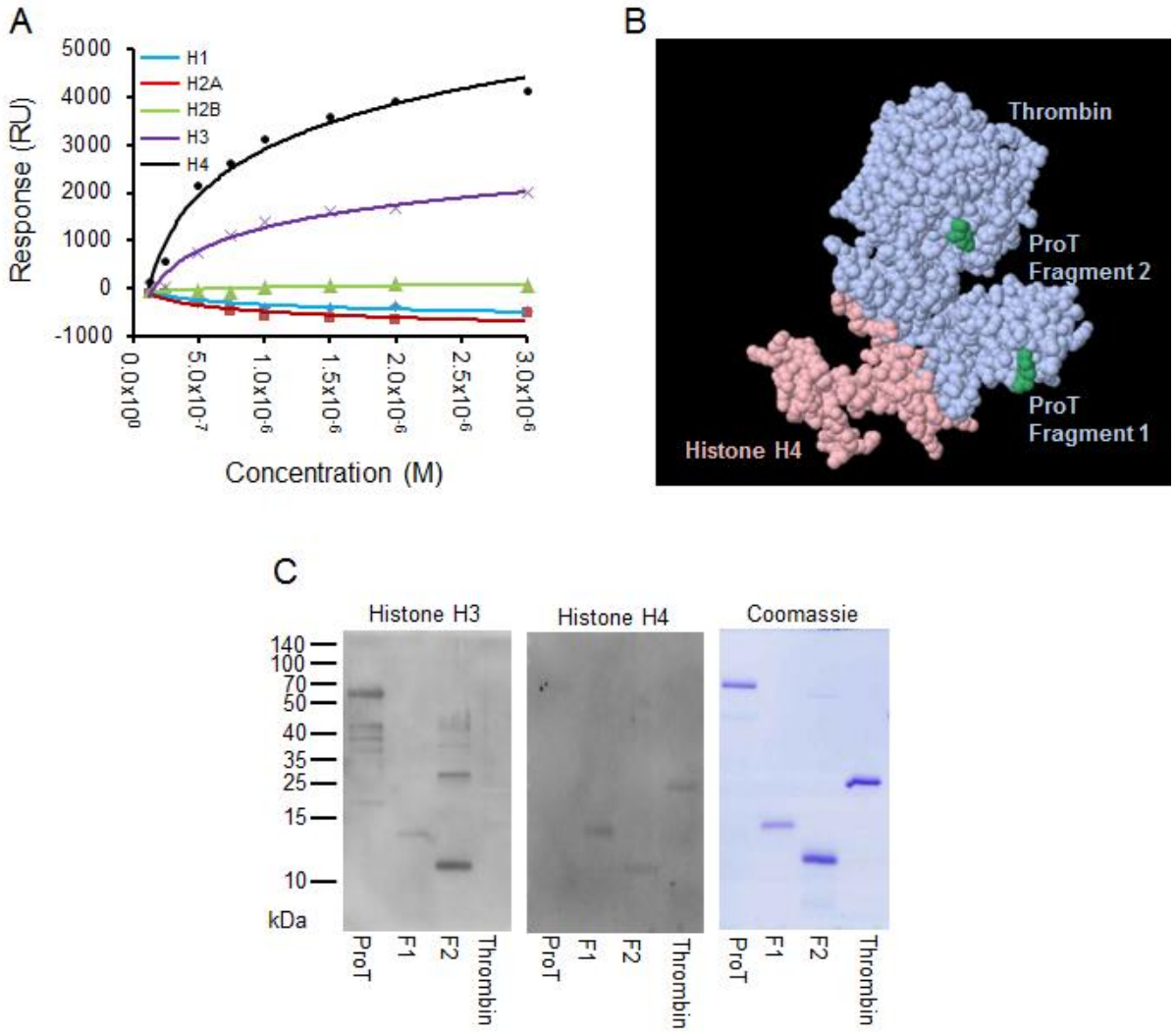

Figure 5.1 The binding of histones to prothrombin. (**A**) 20 µg/mL of recombinant histone H1, H2A, H2B, H3 or H4 was captured on flow cell 2 and flow cell 1 set as control. Various concentrations (0.125, 0.25, 0.5, 0.75, 1.0, 1.5, 2.0 and 3.0 µM) of prothrombin was then added to both Fc1 and Fc2. (**B**) Docking prediction using ZDOCK server (Job ID: 80836),

predicted that H4 binds to prothrombin. Specifically, H4 recognised prothrombin fragment 1 (peptide sequence: STATDVFWAKYTACETARTPRDKLAACLEG) and fragment 2 (peptide sequence: WASAQAKALSKHQDFNS). (**C**) Equimolar concentrations of prothrombin (ProT), prothrombin fragment 1 (F1), prothrombin fragment 2 (F2), α-thrombin, antithrombin and S100P were subjected to a 12% SDS-PAGE, stained with Coomassie brilliant blue (right panel), and transferred to PVDF membrane and overlaid with H3 (left panel) or H4 (middle panel).

5.3.2 Histones H3 and H4 facilitate the cleavage of prothrombin by factor Xa

H4 has previously been shown to induce prothrombin autoactivation, which takes up to 8 hours to occur, with H3 taking three times longer than H4 [20]. It is known that Factor Va interacts with both fragment 1 and 2 of prothrombin within the coagulation cascade acting as a co-factor to facilitate prothrombin cleavage by Factor Xa, generating active thrombin rapidly [201]. Given the binding data above, histones H3 and H4 may therefore behave similarly to that of Factor Va in promoting prothrombin cleavage by Factor Xa. Using a prothrombin cleavage assay, prothrombin was not cleaved in the absence of Factor Xa within 1 h (Figure 5.2A) but enhanced cleavage occurred from 1 min when prothrombin was co-incubated with Factor Xa (Figure 5.2A) and either histone H4 or H3 (Figure 5.2B). Without histones, little prothrombin was cleaved by Factor Xa because in the absence of co-factor, Factor Va was missing (Figure 5.2C). Histone H4 was much more effective than H3 in enhancing prothrombin cleavage by Factor Xa (Figure 5.2D). In contrast, the other histones did not show a significant effect (Figure 5.3A). H3 and H4 significantly enhanced the cleavage of prothrombin (Figure 5.3B).

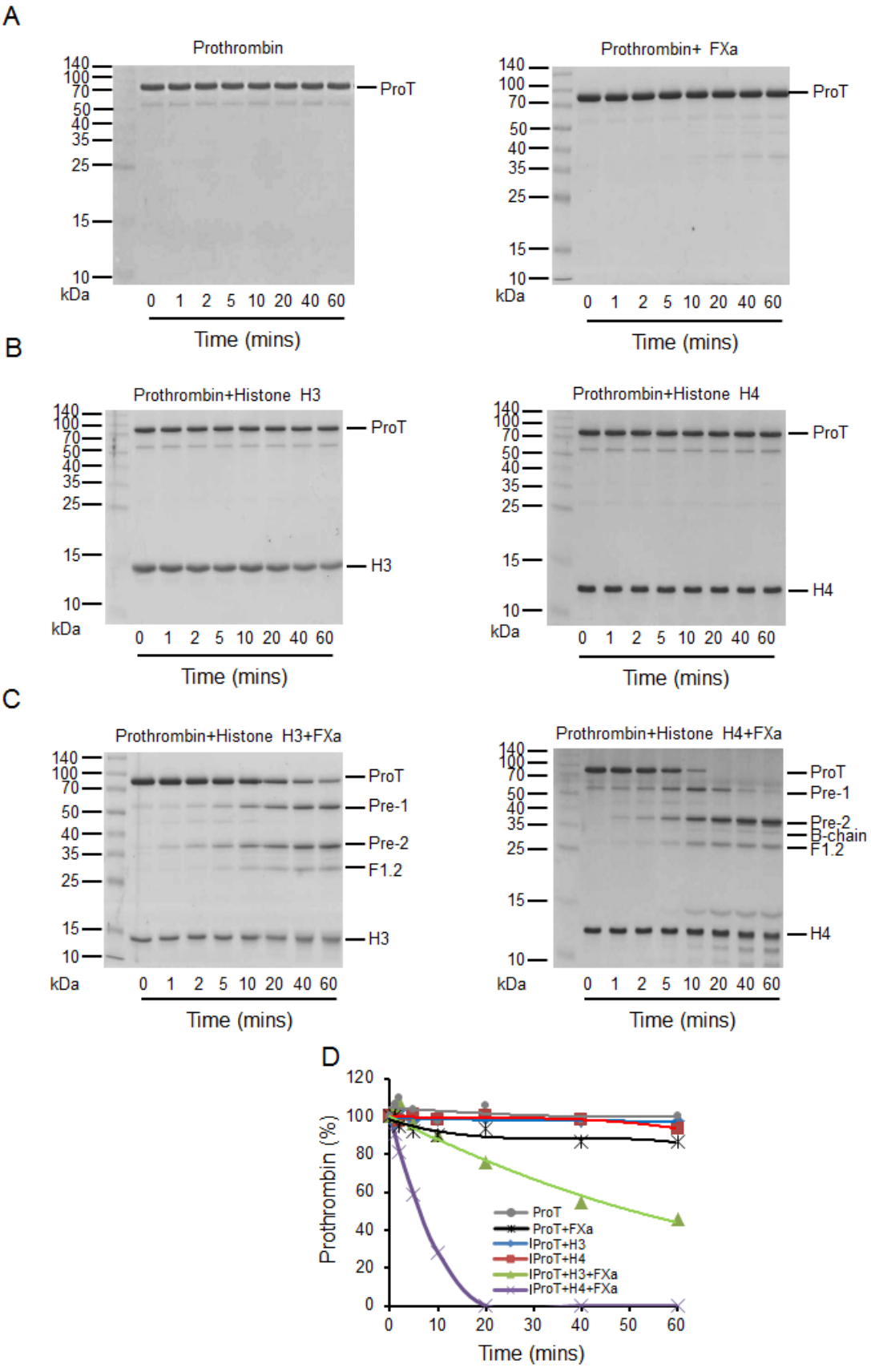
A
Prothrombin
Prothrombin+ FXa
ProT
kDa
Time (mins)
B
Prothrombin+Histone H3
Prothrombin+Histone H4
H3
H4
C
Prothrombin+Histone H3+FXa
Prothrombin+Histone H4+FXa
Pre-1
Pre-2
F1.2
B-chain
D
Prothrombin (%)
ProT
ProT+FXa
IProT+H3
IProT+H4
IProT+H3+FXa
IProT+H4+FXa

Figure 5.2 Effect of histones H3 and H4 on prothrombin cleavage in the presence of FXa. (**A**) Prothrombin (1.5 µg/mL) was incubated without (left panel) or with factor Xa (FXa) (5nM) (right panel) at 37°C. Aliquots were removed at various times, as indicated, and subject to 15% SDS-PAGE. The gels were stained in Coomassie blue for 1 h and destained overnight. (**B**) Prothrombin (1.5 µg/mL) was incubated at 37°C for indicated time points in the presence of either H3 (left panel) or H4 (50 µg/mL) (right panel), subject to SDS-PAGE and visualized using coomassie blue. (**C**) Prothrombin (1.5 µg/mL) was incubated with FXa (5nM) with either H3 (50 µg/mL) (left panel) or H4 (50 µg/mL) (right panel) for indicated time points and visualized using coomassie blue. (**D**) Prothrombin bands from A-C were quantified by densitometry and expressed as a percentage compared to T=0. The mean values for each time point over 3 independent experiments are shown.

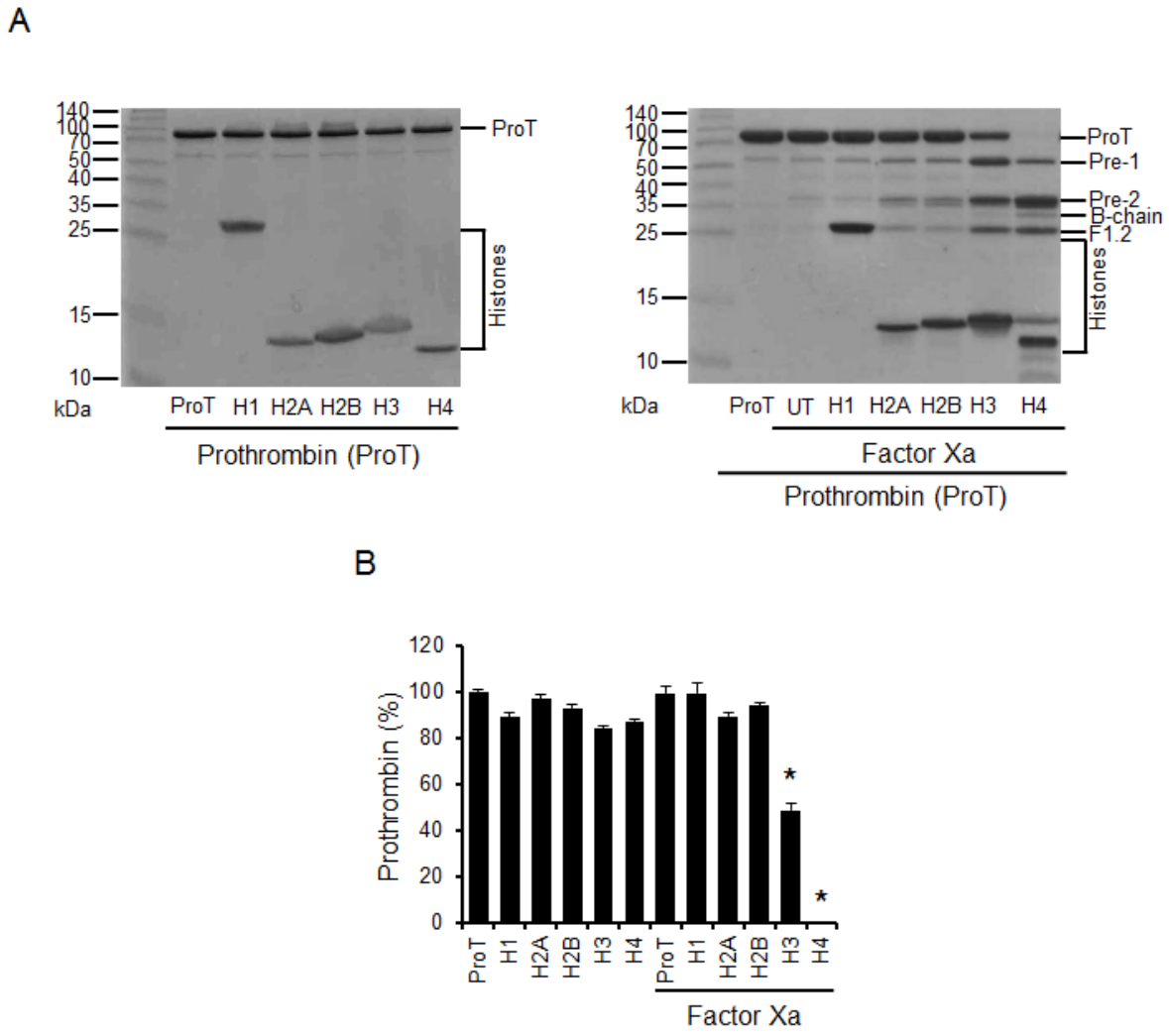

Figure 5.3 Effect of individual histones on prothrombin cleavage. (**A**) Prothrombin (1.5 µg/mL) was incubated with histone H1, H2A, H2B, H3 or H4 (50 µg/mL) without (left panel) or with factor Xa (FXa) (5nM) (right panel) for 1 h at 37°C, subject to 15% SDS-PAGE and visualized using Coomassie blue. (**B**) Prothrombin bands from gels in (A) were quantified using densitometry and represent as mean +/- 1 S.D for 3 independent experiments. *ANOVA test shows significant increase in prothrombin cleavage compared with Prothrombin + FXa alone (P<0.05).

5.3.3 Histone H4 more effectively enhances thrombin generation

To generate active thrombin, Factor Xa needs to cleave 3 sites of prothrombin to generate fragments that include Prethrombin 1, Prethrombin 2 and the B-chain of thrombin. Mature thrombin contains two fragments linked by a disulfide bound (Fig. 1.2). Under reducing gel conditions, a 34 kDa band, i.e. the size of the B chain would represent active thrombin. Interestingly, this band was clearly visualised by Coomassie brilliant blue staining only in the lane where prothrombin was incubated with both FXa and histone H4, but not as evident with H3 (Fig. 5.3). To investigate whether the enhanced FXa cleavage of prothrombin generates active thrombin, a fluorogenic thrombin substrate, Z-Gly-Gly-Arg-AMC, was used to monitor the enzyme activity of thrombin. The substrate was cleaved in the presence of H4 but not H3 (Fig. 5.4A). In fact, H4 in the presence of FXa was the only histone able to result in the generation of active thrombin (Fig. 5.4B).

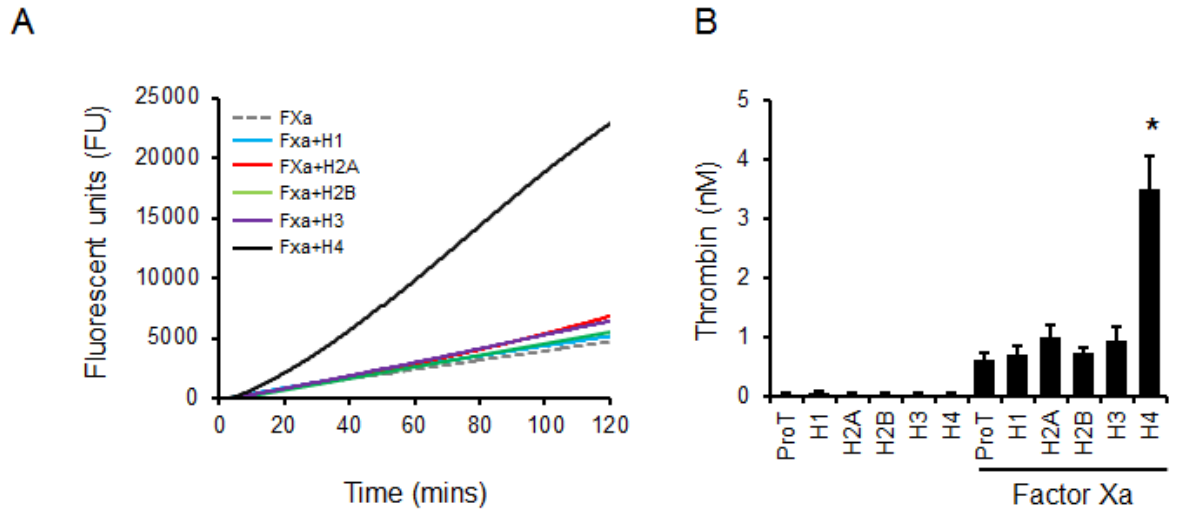

Figure 5.4 Effect of individual histones on thrombin generation. (**A**) Thrombin generation was performed in prothrombin cleavage buffer (20 mM HEPES, 150 mM NaCl, 5 mM $CaCl_2$) containing Prothrombin (1.5 µM), +/- FXa (0.5 nM) and +/- Histone (H)1, HA, H2B,

H3 or H4 (50 µg/mL). The reaction was initiated upon the addition of prothrombin and the fluorogenic thrombin substrate, Z-Gly-Gly-Arg-AMC. Fluorescent emissions (Ex 360/Em 460nm) were measured at 37°C every minute for 120 minutes. Data are representative fluorescent units (FU) curves generated for 3 independent experiments. (**B**) Graphical representation (Mean +/-1 S.D) of thrombin generation in (A) using a thrombin calibration curve to determine the concentration of thrombin (nM) generated for each treatment. *ANOVA test shows significant increase in generation compared with Prothrombin + FXa alone (P<0.05).

5.3.4 Anti-histone antibodies and heparin block histone H4-enhanced prothrombin cleavage and thrombin generation

To demonstrate the specificity of histone H4-enhanced prothrombin cleavage and thrombin generation, I used HahscFv and heparin that have been demonstrated to detoxify histones both *in vitro* and *in vivo*. Both HahscFv and heparin abolished the binding of H4 to prothrombin in the SPR assay (Fig. 5.5A & B) and inhibited H4-enhancement of prothrombin cleavage (Figure 5.5C & D) and consequent thrombin generation (Figure 5.5E & F). These data demonstrate that the effect on prothrombin cleavage and thrombin generation appears specific to histone H4.

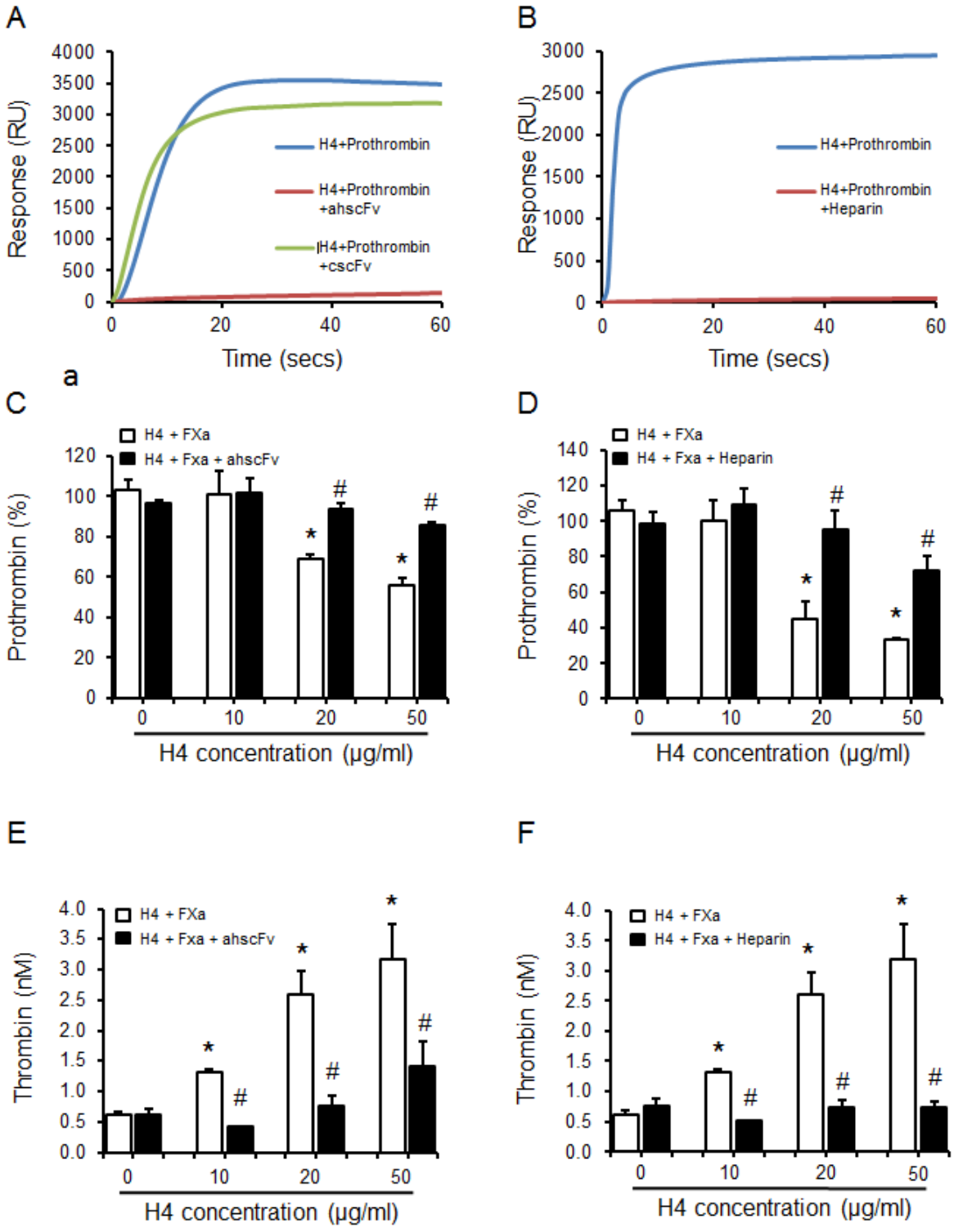

Figure 5.5 The effect of anti-histone reagents against histone H4 binding to prothrombin, prothrombin cleavage and thombin generation. (**A** and **B**) H4 was captured on sensor chip SA and either incubated with 1.5 of µM HahscFv, control scFv (**A**) or heparin (**B**), then prothrombin (1.5 µM) added to the flow cell and binding curves were obtained for

60 seconds. Curves are representative of 3 independent experiments. (**C** and **D**) Prothrombin (1.5 µg/mL) was incubated with FXa (5 nM) and H4 (0, 10, 20 or 50 µg/mL), (**C**) with or without HahscFv (100 µg/mL) or (**D**) Heparin (6 µM) at 37°C for 60 min. Samples were subject to 15% SDS-PAGE and gels stained with Coomassie blue. Prothrombin bands were then quantified by densitometry and expressed as a percentage of undigested prothrombin on the same gel. The mean +/- 1 S.D for >3 independent experiments are shown. (**E** and **F**) Prothrombin (1.5 µg/mL) was incubated with factor Xa (FXa) (0.5nM) with H 4 (0, 10, 20 or 50µ/mL), (**E**) with or without ahscFv (100 µg/mL) or (**F**) Heparin (6 µM). Upon initiation of the reaction changes in fluorescence were monitored at 37°C every minute for 120 minutes. Mean +/- 1 S.D of thrombin generated at the end of the reaction is shown. *ANOVA test shows significant increase compared with Prothrombin + FXa alone (P<0.05). $^{\#}$ANOVA test shows significant reduction in the presence of ahscFv or heparin compared to that without ahscFv or heparin (P<0.05).

5.3.5 Histone H4 replaces FVa to stimulate thrombin generation in FV deficient plasma but not for FX deficiency

Since histone H4 interacts with both fragment 1 and 2 of prothrombin to enhance prothrombin cleavage and thrombin generation by FXa in a similar manner to FVa, I used FV deficient plasma to investigate whether histone H4 could replace FVa within the coagulation cascade. The addition of 50 µg/mL histone H4 to FV deficient plasma restored thrombin generation (Fig. 5.6A). In contrast, histone H4 did not restore the cascade when added to FX deficient plasma (Fig. 5.6A). However, adding H4 to FX deficient plasma supplemented with FXa enhanced thrombin generation, indicating histone H4 has an additive effect in the presence of FV (Fig. 5.6B).

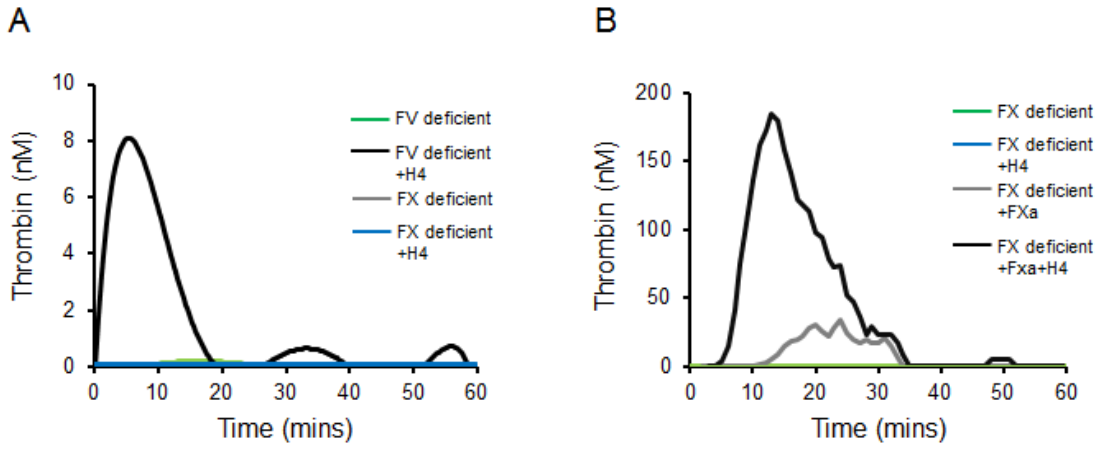

Figure 5.6 Effect of histone H4 in the generation of thrombin in FV and FX deficient plasmas. (**A**) Thrombin generation in FV and FX deficient plasma was performed with or without H4 (50 µg/mL). (**B**) Thrombin generation was performed in FX deficient plasma in the presence or absence of FXa (0.5 nM) +/- H4 (50 µg/mL). The reactions were initiated by the addition of TGA reagent C (RC) Low (containing tissue factor and phospholipids) and fluorescence generated by the cleavage of the fluorogenic thrombin substrate, Z-Gly-Gly-

Arg-AMC. Measurements were taken at 1 min intervals for 60 min at 37°C. Representative curves are shown from 3 independent experiments.

5.4 Discussion

This work demonstrates that extracellular histones can enhance prothrombin activation. Specifically, histone H4 increases Factor Xa-induced prothrombin cleavage, which results in thrombin activation. In this way, H4 could replace Factor Va in the coagulation cascade and facilitate thrombin generation.

Previously, pro-coagulant properties of histones have partly been attributed to the loss of thrombomodulin (TM)-dependent protein C anticoagulant effects [38], which could lead to the cleavage of FVa and FVIIIa in reducing thrombin generation. However, these observations do not take into account more recent findings demonstrating the role of H4 in promoting prothrombin autoactivation. Since this process takes up to 8 hours to occur and thrombin generation occurs within minutes, this prompted me to investigate the role of co-factors in histone-induced prothrombin activation. FVa interacts with both fragment 1 and 2 of prothrombin and facilitates prothrombin cleavage and thrombin generation by FXa. H4 binds to fragments 1 and 2 of prothrombin and, in a manner that appears similar to that of FVa, facilitates FXa-induced prothrombin cleavage and thrombin generation.

Histones H4 and H3 showed higher binding responses to prothrombin than the other histones, with H4 having the greatest affinity. This was also shown to have functional significance whereby only H4 and H3 were able to facilitate the cleavage of prothrombin in the presence of Factor Xa. However, there was a marked difference in the ability of histone H4 and H3 to generate thrombin. This could be due to the ability of different histones facilitating the cleavage of different sites in the presence of FXa. In fact, only H4 was able to produce a 34 kDa band when incubated with prothrombin in the presence of Factor Xa. Since prothrombin has 3 cleavage sites (Arg-155, Arg-271 and Arg-320), that upon cleavage lead to the generation of active thrombin; this would suggest that only H4 is able to facilitate the sufficient cleavage of each of these three sites. H1, H2A and H2B could not facilitate the

cleavage of prothrombin by FXa. H3 and H4 with FXa generate bands for the correct molecular weight of prethrombin-1 and prethrombin-2, which would be consistent with cleavage at Arg-155 and Arg-271 respectively. Only H4 was able to generate a 34 kDa B-chain, band which would be formed through cleavage of Arg-320 of prothrombin, resulting in the generation of active thrombin.

Coagulation activation is a major feature of histone-induced toxicity observed *in vitro* and *in vivo*. Our group have demonstrated a link between extracellular histones and a marker of thrombin generation, plasma thrombin–anti-thrombin (TAT) complexes, in both histone-infusion and trauma mouse models [48]. Moreover, TAT levels could be significantly reduced upon infusion of MahscFv. Furthermore, this was shown to have translational relevance to trauma patients, whereby plasma TAT levels were significantly increased and also correlated with circulating histone levels. This chapter highlights a potential functional link between elevated histone levels and increased thrombin generation previously demonstrated *in vivo* and sheds light on the role of extracellular histones in the coagulation cascade.

5.5 Conclusion

In conclusion, both anti-histone antibodies and heparin are able to significantly reduce histone-induced prothrombin cleavage and thrombin generation. Although more striking results are obtained using heparin than anti-histone scFvs, the side effects of heparins, particularly on platelets, may become an obstacle for its clinical use. Therefore, further improvement of the anti-histone scFvs may hold a promise for anti-histone therapy.

Chapter 6 General Discussion

6.1 Discussion

The toxicity of extracellular histones is now well documented and it is likely to play an important role in disease progression whenever there is extensive cell death and this can lead to multiple organ failure [14, 48]. However, the reagents suitable as anti-histone therapy are very limited. It is known that APC [14] and heparin [92] are able to detoxify histones. However, they are anticoagulant and likely to cause bleeding and therefore cannot be used in critical illness especially when there is thrombocytopenia. Non-anticoagulant APC or heparin is under development but they may have other side effects, for example heparin-induced thrombocytopenia [202]. In contrast, anti-histone antibodies are specific and may have fewer side effects and therefore hold particular promise as suitable anti-histone reagents for clinical use.

For therapeutic purposes, large quantities of anti-histone antibodies are required. The whole intact antibody is difficult to produce to match these requirements. The scFv has greatly simplified the structure compared to the whole antibody [140]. This makes it practical to produce a functional antibody fragment using recombinant DNA technology [140]. However, most scFvs have solubility problems and have to be denatured and refolded. In this work, I have successfully overcome this problem by on-column refolding and produced sufficient, soluble and functional anti-histone scFvs for both *in vitro* and *in vivo* experiments.

It is well documented that antibodies have species specificity. As such, if a therapeutic antibody contains a sequence from a different species then this antibody could serve as an antigen, whereby the host response would be to produce an antibody against this therapeutic agent, i.e. a human anti-mouse antibody can be induced. For clinical use, humanised

antibodies are essential to avoid the immune response [203]. In this work, I first used the traditional methodology of replacing the CDRs of human IgG1 with CDRs from mouse anti-histone antibodies, to generate a humanised anti-histone scFv and its anti-histone properties have been proven. However, the mouse CDRs may also have the risk, albeit much lower, risk of inducing an immune response to produce anti-mouse CDR antibodies. To overcome this disadvantage, I chose another approach to generate human anti-histone antibodies.

As it is known that anti-histone antibodies exist in the sera from patients with SLE or other autoimmune diseases [204], these human anti-histone antibodies are theoretically less likely to cause an immune response when used in patients. There are many methodologies to generate human antibodies based on B cell libraries, such as phage display, RNA-display and DNA-display [149]. However, these techniques are fairly labour intensive and time consuming. In this work, I explored a new approach, which is to pull down anti-histone antibodies directly from patients' sera and then to determining its peptide sequences using MS/MS, and finally reproduced the antibody on a large scale using recombinant DNA technology. In this thesis, I have demonstrated that this approach is a simple, fast and practical way of reproducing human antibodies. The new human anti-histone antibody I produced has great potential to be developed as a clinically useful anti-histone reagent.

Work from our group has already highlighted the potential benefits of the blocking histone cytotoxicity to reduce ALI in trauma [48] and cardiac dysfunction in sepsis [37]. Central to their pathologies is the role of excessive thrombin generation and our finding on H4 induced prothrombin activation into thrombin lends support to the concept of blocking histones, especially when thrombin generation becomes maladaptive and spills into DIC. The challenge is to design and undertake much needed clinical studies in the timing of antithrombin intervention as well as the duration of such treatments. Future work will be

along these lines to realise the promise of saving lives and reducing the poor outcome in critical illness.

In this work, I have also applied the pull down technique to the identification of histone-binding proteins in human sera, both normal and during critical illness. Using highly stringent conditions, I have identified some interesting proteins, such as prothrombin and anti-thrombin. Since it is well documented that extracellular histones are potent pro-coagulation reagents, this finding may explain why histones can trigger blood clotting cascades. Through a thorough study, I find that histones, particularly H4, bind to fragment 1 and 2 of prothrombin, which facilitates the cleavage of prothrombin by Factor Xa to generate active thrombin, the latter activates coagulation. This is the first study that elucidates the molecular mechanism behind histone-enhanced thrombin generation.

6.2 Conclusion

In summary, my work not only creates new methodologies in producing human anti-histone antibodies, which have been used in many *in vitro* and *in vivo* experiments, but also gains new scientific findings in understanding how extracellular histones promote thrombin generation. However, due to the limitation of time and resources, much work is needed to further characterize both the biological and clinical impact of these findings.

6.3 Further work

1. The functional roles of human anti-histone scFv was only tested *in vitro*. In the near future, we will use the antibody fragment in different animal models, such sepsis and pancreatitis to evaluate its protective roles in diseases with high levels of circulating histones.

2. The roles of the interaction between histones and anti-thrombin will be explored. In conjunction with the roles of histones in affecting prothrombin and fibrinogen, I will try to dissect the fundamental roles and mechanisms of histones in thrombosis, DIC and organ failure.

3. I will further optimise the new approach to producing human antibodies to establish a standard system in order to apply this approach to other diseases, particularly for epidemics of infectious diseases which require fast production of neutralising antibodies to control these outbreaks.

References

1. Lone, N.I. and T.S. Walsh, *Impact of intensive care unit organ failures on mortality during the five years after a critical illness.* Am J Respir Crit Care Med, 2012. **186**(7): p. 640-7.
2. Welch, C.A., D.A. Harrison, and K.M. Rowan, *Trends in outcomes from adult general critical care units: potential outcome-based quality indicators other than case-mix adjusted mortality.* Journal of the Intensive Care Society, 2008. **9**(3): p. 220-223.
3. Garcia-Leme, J. and S.P. Farsky, *Hormonal control of inflammatory responses.* Mediators Inflamm, 1993. **2**(3): p. 181-98.
4. van Diepen, J.A., et al., *Interactions between inflammation and lipid metabolism: relevance for efficacy of anti-inflammatory drugs in the treatment of atherosclerosis.* Atherosclerosis, 2013. **228**(2): p. 306-15.
5. Yin, K. and D.K. Agrawal, *Vitamin D and inflammatory diseases.* J Inflamm Res, 2014. **7**: p. 69-87.
6. Levy, M.M., et al., *2001 SCCM/ESICM/ACCP/ATS/SIS International Sepsis Definitions Conference.* Crit Care Med, 2003. **31**(4): p. 1250-6.
7. Stearns-Kurosawa, D.J., et al., *The pathogenesis of sepsis.* Annu Rev Pathol, 2011. **6**: p. 19-48.
8. de Jong, H.K., T. van der Poll, and W.J. Wiersinga, *The systemic pro-inflammatory response in sepsis.* J Innate Immun, 2010. **2**(5): p. 422-30.
9. Bone, R.C., et al., *Definitions for sepsis and organ failure and guidelines for the use of innovative therapies in sepsis. The ACCP/SCCM Consensus Conference*

Committee. American College of Chest Physicians/Society of Critical Care Medicine. Chest, 1992. **101**(6): p. 1644-55.

10. Taniguchi, T., et al., *Change in the ratio of interleukin-6 to interleukin-10 predicts a poor outcome in patients with systemic inflammatory response syndrome.* Crit Care Med, 1999. **27**(7): p. 1262-4.
11. Ueda, S., et al., *Increased plasma levels of adrenomedullin in patients with systemic inflammatory response syndrome.* Am J Respir Crit Care Med, 1999. **160**(1): p. 132-6.
12. Hietaranta, A., et al., *Extracellular phospholipases A2 in relation to systemic inflammatory response syndrome (SIRS) and systemic complications in severe acute pancreatitis.* Pancreas, 1999. **18**(4): p. 385-91.
13. Takala, A., et al., *Systemic inflammatory response syndrome without systemic inflammation in acutely ill patients admitted to hospital in a medical emergency.* Clin Sci (Lond), 1999. **96**(3): p. 287-95.
14. Xu, J., et al., *Extracellular histones are major mediators of death in sepsis.* Nat Med, 2009. **15**(11): p. 1318-21.
15. Toh, C.H., W.K. Hoots, and S.S.C.o.D.I.C.o.t. ISTH, *The scoring system of the Scientific and Standardisation Committee on Disseminated Intravascular Coagulation of the International Society on Thrombosis and Haemostasis: a 5-year overview.* J Thromb Haemost, 2007. **5**(3): p. 604-6.
16. Toh, C.H. and Y. Alhamdi, *Current consideration and management of disseminated intravascular coagulation.* Hematology Am Soc Hematol Educ Program, 2013. **2013**: p. 286-91.
17. Esmon, C.T., *The protein C pathway.* Chest, 2003. **124**(3 Suppl): p. 26S-32S.

18. Macias, W.L., et al., *New insights into the protein C pathway: potential implications for the biological activities of drotrecogin alfa (activated).* Crit Care, 2005. **9 Suppl 4**: p. S38-45.

19. Esmon, C.T., *The normal role of Activated Protein C in maintaining homeostasis and its relevance to critical illness.* Crit Care, 2001. **5**(2): p. S7-12.

20. Barranco-Medina, S., et al., *Histone H4 promotes prothrombin autoactivation.* J Biol Chem, 2013. **288**(50): p. 35749-57.

21. Pozzi, N., et al., *Autoactivation of thrombin precursors.* J Biol Chem, 2013. **288**(16): p. 11601-10.

22. Walker, R.K. and S. Krishnaswamy, *The activation of prothrombin by the prothrombinase complex. The contribution of the substrate-membrane interaction to catalysis.* J Biol Chem, 1994. **269**(44): p. 27441-50.

23. Butenas, S., C. van't Veer, and K.G. Mann, *"Normal" thrombin generation.* Blood, 1999. **94**(7): p. 2169-78.

24. Pozzi, N., et al., *Crystal structure of prothrombin reveals conformational flexibility and mechanism of activation.* J Biol Chem, 2013. **288**(31): p. 22734-44.

25. Wood, J.P., et al., *Prothrombin activation on the activated platelet surface optimizes expression of procoagulant activity.* Blood, 2011. **117**(5): p. 1710-8.

26. Yasuhara, S., et al., *Mitochondria, endoplasmic reticulum, and alternative pathways of cell death in critical illness.* Crit Care Med, 2007. **35**(9 Suppl): p. S488-95.

27. Bantel, H. and K. Schulze-Osthoff, *Cell death in sepsis: a matter of how, when, and where.* Crit Care, 2009. **13**(4): p. 173.

28. Holdenrieder, S. and P. Stieber, *Clinical use of circulating nucleosomes.* Crit Rev Clin Lab Sci, 2009. **46**(1): p. 1-24.

29. Holdenrieder, S., et al., *Nucleosomes in serum as a marker for cell death.* Clin Chem Lab Med, 2001. **39**(7): p. 596-605.

30. Wu, D., et al., *Apoptotic release of histones from nucleosomes.* J Biol Chem, 2002. **277**(14): p. 12001-8.

31. Logters, T., et al., *Diagnostic accuracy of neutrophil-derived circulating free DNA (cf-DNA/NETs) for septic arthritis.* J Orthop Res, 2009. **27**(11): p. 1401-7.

32. Gauthier, V.J., L.N. Tyler, and M. Mannik, *Blood clearance kinetics and liver uptake of mononucleosomes in mice.* J Immunol, 1996. **156**(3): p. 1151-6.

33. Marino-Ramirez, L., et al., *Histone structure and nucleosome stability.* Expert Rev Proteomics, 2005. **2**(5): p. 719-29.

34. Luger, K., et al., *Crystal structure of the nucleosome core particle at 2.8 A resolution.* Nature, 1997. **389**(6648): p. 251-60.

35. Woodcock, C.L., A.I. Skoultchi, and Y. Fan, *Role of linker histone in chromatin structure and function: H1 stoichiometry and nucleosome repeat length.* Chromosome Research, 2006. **14**(1): p. 17-25.

36. Abrams, S.T., et al., *Circulating Histones are Mediators of Trauma-Associated Lung Injury.* Am J Respir Crit Care Med, 2012.

37. Alhamdi, Y., et al., *Circulating Histones Are Major Mediators of Cardiac Injury in Patients With Sepsis.* Crit Care Med, 2015.

38. Ammollo, C.T., et al., *Extracellular histones increase plasma thrombin generation by impairing thrombomodulin-dependent protein C activation.* J Thromb Haemost, 2011. **9**(9): p. 1795-803.

39. Fuchs, T.A., A.A. Bhandari, and D.D. Wagner, *Histones induce rapid and profound thrombocytopenia in mice.* Blood, 2011. **118**(13): p. 3708-14.

40. Xu, J., et al., *Extracellular histones are mediators of death through TLR2 and TLR4 in mouse fatal liver injury.* J Immunol, 2011. **187**(5): p. 2626-31.

41. Huang, H., et al., *Endogenous histones function as alarmins in sterile inflammatory liver injury through Toll-like receptor 9 in mice.* Hepatology, 2011. **54**(3): p. 999-1008.

42. Fuchs, T.A., et al., *Extracellular DNA traps promote thrombosis.* Proc Natl Acad Sci U S A, 2010. **107**(36): p. 15880-5.

43. Caudrillier, A., et al., *Platelets induce neutrophil extracellular traps in transfusion-related acute lung injury.* J Clin Invest, 2012. **122**(7): p. 2661-71.

44. Demers, M., et al., *Cancers predispose neutrophils to release extracellular DNA traps that contribute to cancer-associated thrombosis.* Proc Natl Acad Sci U S A, 2012. **109**(32): p. 13076-81.

45. Savchenko, A.S., et al., *VWF-mediated leukocyte recruitment with chromatin decondensation by PAD4 increases myocardial ischemia/reperfusion injury in mice.* Blood, 2014. **123**(1): p. 141-8.

46. Kowalska, M.A., et al., *Modulation of protein C activation by histones, platelet factor 4, and heparinoids: new insights into activated protein C formation.* Arterioscler Thromb Vasc Biol, 2014. **34**(1): p. 120-6.

47. Nakahara, M., et al., *Recombinant thrombomodulin protects mice against histone-induced lethal thromboembolism.* PLoS One, 2013. **8**(9): p. e75961.

48. Abrams, S.T., et al., *Circulating histones are mediators of trauma-associated lung injury.* Am J Respir Crit Care Med, 2013. **187**(2): p. 160-9.

49. Longstaff, C., et al., *Mechanical stability and fibrinolytic resistance of clots containing fibrin, DNA, and histones.* J Biol Chem, 2013. **288**(10): p. 6946-56.

50. Adams, R.L. and R.J. Bird, *Review article: Coagulation cascade and therapeutics update: relevance to nephrology. Part 1: Overview of coagulation, thrombophilias and history of anticoagulants.* Nephrology (Carlton), 2009. **14**(5): p. 462-70.

51. Semeraro, F., et al., *Extracellular histones promote thrombin generation through platelet-dependent mechanisms: involvement of platelet TLR2 and TLR4.* Blood, 2011. **118**(7): p. 1952-61.

52. Caen, J. and Q. Wu, *Hageman factor, platelets and polyphosphates: early history and recent connection.* J Thromb Haemost, 2010. **8**(8): p. 1670-4.

53. Witko-Sarsat, V., et al., *Neutrophils: molecules, functions and pathophysiological aspects.* Lab Invest, 2000. **80**(5): p. 617-53.

54. Di Carlo, E., et al., *The intriguing role of polymorphonuclear neutrophils in antitumor reactions.* Blood, 2001. **97**(2): p. 339-45.

55. Barletta, K.E., K. Ley, and B. Mehrad, *Regulation of neutrophil function by adenosine.* Arterioscler Thromb Vasc Biol, 2012. **32**(4): p. 856-64.

56. Li, P., et al., *PAD4 is essential for antibacterial innate immunity mediated by neutrophil extracellular traps.* J Exp Med, 2010. **207**(9): p. 1853-62.

57. Douda, D.N., et al., *Akt is essential to induce NADPH-dependent NETosis and to switch the neutrophil death to apoptosis.* Blood, 2014. **123**(4): p. 597-600.

58. Papayannopoulos, V., et al., *Neutrophil elastase and myeloperoxidase regulate the formation of neutrophil extracellular traps.* J Cell Biol, 2010. **191**(3): p. 677-91.

59. Nakashima, K., et al., *PAD4 regulates proliferation of multipotent haematopoietic cells by controlling c-myc expression.* Nat Commun, 2013. **4**: p. 1836.

60. Pilsczek, F.H., et al., *A novel mechanism of rapid nuclear neutrophil extracellular trap formation in response to Staphylococcus aureus.* J Immunol, 2010. **185**(12): p. 7413-25.

61. Lippolis, J.D., et al., *Neutrophil extracellular trap formation by bovine neutrophils is not inhibited by milk.* Vet Immunol Immunopathol, 2006. **113**(1-2): p. 248-55.

62. Ermert, D., et al., *Mouse neutrophil extracellular traps in microbial infections.* J Innate Immun, 2009. **1**(3): p. 181-93.

63. Ramos-Kichik, V., et al., *Neutrophil extracellular traps are induced by Mycobacterium tuberculosis.* Tuberculosis (Edinb), 2009. **89**(1): p. 29-37.

64. Juneau, R.A., et al., *Nontypeable Haemophilus influenzae initiates formation of neutrophil extracellular traps.* Infect Immun, 2011. **79**(1): p. 431-8.

65. Brinkmann, V., et al., *Neutrophil extracellular traps kill bacteria.* Science, 2004. **303**(5663): p. 1532-5.

66. Remijsen, Q., et al., *Dying for a cause: NETosis, mechanisms behind an antimicrobial cell death modality.* Cell Death Differ, 2011. **18**(4): p. 581-8.

67. Fuchs, T.A., A. Brill, and D.D. Wagner, *Neutrophil extracellular trap (NET) impact on deep vein thrombosis.* Arterioscler Thromb Vasc Biol, 2012. **32**(8): p. 1777-83.

68. Berends, E.T., et al., *Nuclease expression by Staphylococcus aureus facilitates escape from neutrophil extracellular traps.* J Innate Immun, 2010. **2**(6): p. 576-86.

69. Hentzer, M., et al., *Alginate overproduction affects Pseudomonas aeruginosa biofilm structure and function.* J Bacteriol, 2001. **183**(18): p. 5395-401.

70. Yousefi, S., et al., *Viable neutrophils release mitochondrial DNA to form neutrophil extracellular traps.* Cell Death Differ, 2009. **16**(11): p. 1438-44.

71. Pignatti, P., et al., *Downmodulation of CXCL8/IL-8 receptors on neutrophils after recruitment in the airways.* J Allergy Clin Immunol, 2005. **115**(1): p. 88-94.

72. Marcos, V., et al., *CXCR2 mediates NADPH oxidase-independent neutrophil extracellular trap formation in cystic fibrosis airway inflammation.* Nat Med, 2010. **16**(9): p. 1018-23.

73. Nishinaka, Y., et al., *Singlet oxygen is essential for neutrophil extracellular trap formation.* Biochem Biophys Res Commun, 2011. **413**(1): p. 75-9.

74. Yost, C.C., A.S. Weyrich, and G.A. Zimmerman, *The platelet activating factor (PAF) signaling cascade in systemic inflammatory responses.* Biochimie, 2010. **92**(6): p. 692-7.

75. Gupta, A.K., et al., *Induction of neutrophil extracellular DNA lattices by placental microparticles and IL-8 and their presence in preeclampsia.* Hum Immunol, 2005. **66**(11): p. 1146-54.

76. Parker, H., et al., *Requirements for NADPH oxidase and myeloperoxidase in neutrophil extracellular trap formation differ depending on the stimulus.* J Leukoc Biol, 2012. **92**(4): p. 841-9.

77. Remijsen, Q., et al., *Neutrophil extracellular trap cell death requires both autophagy and superoxide generation.* Cell Res, 2011. **21**(2): p. 290-304.

78. Doring, Y., et al., *Lack of neutrophil-derived CRAMP reduces atherosclerosis in mice.* Circ Res, 2012. **110**(8): p. 1052-6.

79. Dwivedi, N., et al., *Felty's syndrome autoantibodies bind to deiminated histones and neutrophil extracellular chromatin traps.* Arthritis Rheum, 2012. **64**(4): p. 982-92.

80. Rohrbach, A.S., et al., *PAD4 is not essential for disease in the K/BxN murine autoantibody-mediated model of arthritis.* Arthritis Res Ther, 2012. **14**(3): p. R104.

81. Kessenbrock, K., et al., *Netting neutrophils in autoimmune small-vessel vasculitis.* Nat Med, 2009. **15**(6): p. 623-5.

82. Hakkim, A., et al., *Impairment of neutrophil extracellular trap degradation is associated with lupus nephritis.* Proc Natl Acad Sci U S A, 2010. **107**(21): p. 9813-8.

83. Liu, C.L., et al., *Specific post-translational histone modifications of neutrophil extracellular traps as immunogens and potential targets of lupus autoantibodies.* Arthritis Res Ther, 2012. **14**(1): p. R25.

84. Neeli, I., S.N. Khan, and M. Radic, *Histone deimination as a response to inflammatory stimuli in neutrophils.* J Immunol, 2008. **180**(3): p. 1895-902.

85. Bagavant, H. and S.M. Fu, *Pathogenesis of kidney disease in systemic lupus erythematosus.* Curr Opin Rheumatol, 2009. **21**(5): p. 489-94.

86. Davies, M.J., *Myeloperoxidase-derived oxidation: mechanisms of biological damage and its prevention.* J Clin Biochem Nutr, 2011. **48**(1): p. 8-19.

87. Nakazawa, D., U. Tomaru, and A. Ishizu, *Possible implication of disordered neutrophil extracellular traps in the pathogenesis of MPO-ANCA-associated vasculitis.* Clin Exp Nephrol, 2013. **17**(5): p. 631-3.

88. Bosmann, M., et al., *Extracellular histones are essential effectors of C5aR- and C5L2-mediated tissue damage and inflammation in acute lung injury.* FASEB J, 2013. **27**(12): p. 5010-21.

89. Abakushin, D.N., I.A. Zamulaeva, and A.M. Poverenny, *Histones evoke thymocyte death in vitro; histone-binding immunoglobulins decrease their cytotoxicity.* Biochemistry (Mosc), 1999. **64**(6): p. 693-8.

90. Pereira, L.F., et al., *Histones interact with anionic phospholipids with high avidity; its relevance for the binding of histone-antihistone immune complexes.* Clin Exp Immunol, 1994. **97**(2): p. 175-80.

91. Abrams, S.T., et al., *Human CRP defends against the toxicity of circulating histones.* J Immunol, 2013. **191**(5): p. 2495-502.

92. Wildhagen, K.C., et al., *Nonanticoagulant heparin prevents histone-mediated cytotoxicity in vitro and improves survival in sepsis.* Blood, 2014. **123**(7): p. 1098-101.

93. Pemberton, A.D., J.K. Brown, and N.F. Inglis, *Proteomic identification of interactions between histones and plasma proteins: implications for cytoprotection.* Proteomics, 2010. **10**(7): p. 1484-93.

94. Alcantara, F.F., D.J. Iglehart, and R.L. Ochs, *Heparin in plasma samples causes nonspecific binding to histones on Western blots.* J Immunol Methods, 1999. **226**(1-2): p. 11-8.

95. Morita, S., et al., *High affinity binding of heparin by necrotic tumour cells neutralises anticoagulant activity--implications for cancer related thromboembolism and heparin therapy.* Thromb Haemost, 2001. **86**(2): p. 616-22.

96. Tan, E.M., J. Robinson, and P. Robitaille, *Studies on antibodies to histones by immunofluorescence.* Scand J Immunol, 1976. **5**(6-7): p. 811-8.

97. Fishbein, E., D. Alarcon-Segovia, and J.M. Vega, *Antibodies to histones in systemic lupus erythematosus.* Clin Exp Immunol, 1979. **36**(1): p. 145-50.

98. Monestier, M., et al., *Structure and binding properties of monoclonal antibodies to core histones from autoimmune mice.* Mol Immunol, 1993. **30**(12): p. 1069-75.

99. Allam, R., et al., *Histones from dying renal cells aggravate kidney injury via TLR2 and TLR4.* J Am Soc Nephrol, 2012. **23**(8): p. 1375-88.

100. Allam, R., et al., *Histones trigger sterile inflammation by activating the NLRP3 inflammasome.* Eur J Immunol, 2013. **43**(12): p. 3336-42.

101. Murphy, K., et al., *Janeway's immunobiology*. 8th ed. 2012, New York: Garland Science. xix, 868 p.

102. Eales, L.-J., *Immunology for life scientists : a basic introduction : a student-centered learning approach*. 1997, Chichester ; New York: John Wiley & Sons. vii, 304 p.

103. Lipman, N.S., et al., *Monoclonal versus polyclonal antibodies: distinguishing characteristics, applications, and information resources.* ILAR J, 2005. **46**(3): p. 258-68.

104. Schroeder, H.W., Jr. and L. Cavacini, *Structure and function of immunoglobulins.* J Allergy Clin Immunol, 2010. **125**(2 Suppl 2): p. S41-52.

105. Ohno, S., N. Mori, and T. Matsunaga, *Antigen-binding specificities of antibodies are primarily determined by seven residues of VH.* Proc Natl Acad Sci U S A, 1985. **82**(9): p. 2945-9.

106. Al-Lazikani, B., A.M. Lesk, and C. Chothia, *Standard conformations for the canonical structures of immunoglobulins.* J Mol Biol, 1997. **273**(4): p. 927-48.

107. Duncan, A.R. and G. Winter, *The binding site for C1q on IgG.* Nature, 1988. **332**(6166): p. 738-40.

108. Elluru, S.R., S.V. Kaveri, and J. Bayry, *The protective role of immunoglobulins in fungal infections and inflammation.* Semin Immunopathol, 2015. **37**(2): p. 187-97.

109. Dunkelberger, J.R. and W.C. Song, *Complement and its role in innate and adaptive immune responses.* Cell Res, 2010. **20**(1): p. 34-50.

110. Mc, K.C., *THe prevention and modification of measles.* Journal of the American Medical Association, 1937. **109**(25): p. 2034-2038.

111. Barandun, S., et al., *Intravenous administration of human gamma-globulin.* Vox Sang, 1962. **7**: p. 157-74.

112. Newcombe, C. and A.R. Newcombe, *Antibody production: polyclonal-derived biotherapeutics.* J Chromatogr B Analyt Technol Biomed Life Sci, 2007. **848**(1): p. 2-7.

113. Kohler, G. and C. Milstein, *Continuous cultures of fused cells secreting antibody of predefined specificity.* Nature, 1975. **256**(5517): p. 495-7.

114. Cohen, S.N., et al., *Construction of biologically functional bacterial plasmids in vitro.* Proc Natl Acad Sci U S A, 1973. **70**(11): p. 3240-4.

115. Better, M., et al., *Escherichia coli secretion of an active chimeric antibody fragment.* Science, 1988. **240**(4855): p. 1041-3.

116. McCafferty, J., et al., *Phage antibodies: filamentous phage displaying antibody variable domains.* Nature, 1990. **348**(6301): p. 552-4.

117. Liang, P. and A.B. Pardee, *Differential display of eukaryotic messenger RNA by means of the polymerase chain reaction.* Science, 1992. **257**(5072): p. 967-71.

118. Yonezawa, M., et al., *DNA display for in vitro selection of diverse peptide libraries.* Nucleic Acids Res, 2003. **31**(19): p. e118.

119. Asano, R., et al., *Efficient construction of a diabody using a refolding system: anti-carcinoembryonic antigen recombinant antibody fragment.* J Biochem, 2002. **132**(6): p. 903-9.

120. Takemura, S., et al., *Construction of a diabody (small recombinant bispecific antibody) using a refolding system.* Protein Eng, 2000. **13**(8): p. 583-8.

121. Chames, P., et al., *Therapeutic antibodies: successes, limitations and hopes for the future.* Br J Pharmacol, 2009. **157**(2): p. 220-33.

122. Wootla, B., A. Denic, and M. Rodriguez, *Polyclonal and Monoclonal Antibodies in Clinic,* in *Human Monoclonal Antibodies*, M. Steinitz, Editor. 2014, Humana Press. p. 79-110.

123. Casadevall, A., E. Dadachova, and L.A. Pirofski, *Passive antibody therapy for infectious diseases.* Nat Rev Microbiol, 2004. **2**(9): p. 695-703.

124. Casadevall, A. and M.D. Scharff, *Return to the past: the case for antibody-based therapies in infectious diseases.* Clin Infect Dis, 1995. **21**(1): p. 150-61.

125. Orange, J.S., et al., *Use of intravenous immunoglobulin in human disease: a review of evidence by members of the Primary Immunodeficiency Committee of the American Academy of Allergy, Asthma and Immunology.* J Allergy Clin Immunol, 2006. **117**(4 Suppl): p. S525-53.

126. Dunbar, B.S. and E.D. Schwoebel, *[49] Preparation of polyclonal antibodies.* Methods in enzymology, 1990. **182**: p. 663-670.

127. Lonberg, N., *Human antibodies from transgenic animals.* Nat Biotechnol, 2005. **23**(9): p. 1117-25.

128. Kuroiwa, Y., et al., *Antigen-specific human polyclonal antibodies from hyperimmunized cattle.* Nat Biotechnol, 2009. **27**(2): p. 173-81.

129. Bradbury, A. and A. Pluckthun, *Reproducibility: Standardize antibodies used in research.* Nature, 2015. **518**(7537): p. 27-9.

130. Midtvedt, K., et al., *Individualized T cell monitored administration of ATG versus OKT3 in steroid-resistant kidney graft rejection.* Clin Transplant, 2003. **17**(1): p. 69-74.

131. Leavy, O., *Therapeutic antibodies: past, present and future.* Nat Rev Immunol, 2010. **10**(5): p. 297.

132. Schroff, R.W., et al., *Human anti-murine immunoglobulin responses in patients receiving monoclonal antibody therapy.* Cancer Res, 1985. **45**(2): p. 879-85.

133. Legouffe, E., et al., *Human anti-mouse antibody response to the injection of murine monoclonal antibodies against IL-6.* Clin Exp Immunol, 1994. **98**(2): p. 323-9.

134. Roder, J.C., S.P. Cole, and D. Kozbor, *The EBV-hybridoma technique.* Methods Enzymol, 1986. **121**: p. 140-67.

135. Winter, G. and C. Milstein, *Man-made antibodies.* Nature, 1991. **349**(6307): p. 293-9.

136. Ishida, I., et al., *Production of human monoclonal and polyclonal antibodies in TransChromo animals.* Cloning Stem Cells, 2002. **4**(1): p. 91-102.

137. Michnick, S.W. and S.S. Sidhu, *Submitting antibodies to binding arbitration.* Nat Chem Biol, 2008. **4**(6): p. 326-9.

138. Hughes, S.S., *Making dollars out of DNA. The first major patent in biotechnology and the commercialization of molecular biology, 1974-1980.* Isis, 2001. **92**(3): p. 541-75.

139. Johnson, I.S., *Human insulin from recombinant DNA technology.* Science, 1983. **219**(4585): p. 632-7.

140. Bird, R.E., et al., *Single-chain antigen-binding proteins.* Science, 1988. **242**(4877): p. 423-6.

141. Jones, P.T., et al., *Replacing the complementarity-determining regions in a human antibody with those from a mouse.* Nature, 1986. **321**(6069): p. 522-5.

142. Biocca, S., M.S. Neuberger, and A. Cattaneo, *Expression and targeting of intracellular antibodies in mammalian cells.* EMBO J, 1990. **9**(1): p. 101-8.

143. Dodev, T.S., et al., *A tool kit for rapid cloning and expression of recombinant antibodies.* Sci Rep, 2014. **4**: p. 5885.

144. Cheung, W.C., et al., *A proteomics approach for the identification and cloning of monoclonal antibodies from serum.* Nat Biotechnol, 2012. **30**(5): p. 447-52.

145. Smith, G.P. and V.A. Petrenko, *Phage Display.* Chem Rev, 1997. **97**(2): p. 391-410.

146. Winter, G., et al., *Making antibodies by phage display technology.* Annu Rev Immunol, 1994. **12**: p. 433-55.

147. Mandecki, W., Y.C. Chen, and N. Grihalde, *A mathematical model for biopanning (affinity selection) using peptide libraries on filamentous phage.* J Theor Biol, 1995. **176**(4): p. 523-30.

148. Roberts, R.W. and J.W. Szostak, *RNA-peptide fusions for the in vitro selection of peptides and proteins.* Proc Natl Acad Sci U S A, 1997. **94**(23): p. 12297-302.

149. Amstutz, P., et al., *In vitro display technologies: novel developments and applications.* Curr Opin Biotechnol, 2001. **12**(4): p. 400-5.

150. Liu, R., et al., *Optimized synthesis of RNA-protein fusions for in vitro protein selection.* Methods Enzymol, 2000. **318**: p. 268-93.

151. Seelig, B., *mRNA display for the selection and evolution of enzymes from in vitro-translated protein libraries.* Nat. Protocols, 2011. **6**(4): p. 540-552.

152. Fukuda, I., et al., *In vitro evolution of single-chain antibodies using mRNA display.* Nucleic Acids Res, 2006. **34**(19): p. e127.

153. Eidhammer, I., *Computational methods for mass spectrometry proteomics*. 2007, Chichester, England ; Hoboken, NJ: John Wiley & Sons. x, 284 p.

154. Bell, A.W., et al., *The protein microscope: incorporating mass spectrometry into cell biology.* Nat Methods, 2007. **4**(10): p. 783-4.

155. Beretta, L., *Proteomics from the clinical perspective: many hopes and much debate.* Nat Methods, 2007. **4**(10): p. 785-6.

156. Kocher, T. and G. Superti-Furga, *Mass spectrometry-based functional proteomics: from molecular machines to protein networks.* Nat Methods, 2007. **4**(10): p. 807-15.

157. Ferguson, P.L. and R.D. Smith, *Proteome analysis by mass spectrometry.* Annu Rev Biophys Biomol Struct, 2003. **32**: p. 399-424.

158. Shevchenko, A., et al., *In-gel digestion for mass spectrometric characterization of proteins and proteomes.* Nat Protoc, 2006. **1**(6): p. 2856-60.

159. Perkins, D.N., et al., *Probability-based protein identification by searching sequence databases using mass spectrometry data.* Electrophoresis, 1999. **20**(18): p. 3551-67.

160. Eng, J.K., A.L. McCormack, and J.R. Yates, *An approach to correlate tandem mass spectral data of peptides with amino acid sequences in a protein database.* J Am Soc Mass Spectrom, 1994. **5**(11): p. 976-89.

161. Ma, B., et al., *PEAKS: powerful software for peptide de novo sequencing by tandem mass spectrometry.* Rapid Commun Mass Spectrom, 2003. **17**(20): p. 2337-42.

162. Frank, A.M., et al., *De novo peptide sequencing and identification with precision mass spectrometry.* J Proteome Res, 2007. **6**(1): p. 114-23.

163. Pisitkun, T., et al., *Tandem mass spectrometry in physiology.* Physiology (Bethesda), 2007. **22**: p. 390-400.

164. Froger, A. and J.E. Hall, *Transformation of plasmid DNA into E. coli using the heat shock method.* J Vis Exp, 2007(6): p. 253.

165. Diezel, W., G. Kopperschlager, and E. Hofmann, *An improved procedure for protein staining in polyacrylamide gels with a new type of Coomassie Brilliant Blue.* Anal Biochem, 1972. **48**(2): p. 617-20.

166. Desjardins, P., J.B. Hansen, and M. Allen, *Microvolume protein concentration determination using the NanoDrop 2000c spectrophotometer.* J Vis Exp, 2009(33).

167. Riccardi, C. and I. Nicoletti, *Analysis of apoptosis by propidium iodide staining and flow cytometry.* Nat Protoc, 2006. **1**(3): p. 1458-61.

168. Claycomb, W.C., et al., *HL-1 cells: a cardiac muscle cell line that contracts and retains phenotypic characteristics of the adult cardiomyocyte.* Proc Natl Acad Sci U S A, 1998. **95**(6): p. 2979-84.

169. White, S.M., P.E. Constantin, and W.C. Claycomb, *Cardiac physiology at the cellular level: use of cultured HL-1 cardiomyocytes for studies of cardiac muscle cell structure and function.* Am J Physiol Heart Circ Physiol, 2004. **286**(3): p. H823-9.

170. Nagaoka, M. and T. Akaike, *Single amino acid substitution in the mouse IgG1 Fc region induces drastic enhancement of the affinity to protein A.* Protein engineering, 2003. **16**(4): p. 243-5.

171. Bailey, L.M., et al., *Artifactual detection of biotin on histones by streptavidin.* Anal Biochem, 2008. **373**(1): p. 71-7.

172. Sørensen, H.P. and K.K. Mortensen, *Advanced genetic strategies for recombinant protein expression in Escherichia coli.* Journal of biotechnology, 2005. **115**(2): p. 113-128.

173. Xu, J., et al., *Extracellular histones are major mediators of death in sepsis.* Nature medicine, 2009. **15**(11): p. 1318-21.

174. Ranieri, V.M., et al., *Drotrecogin alfa (activated) in adults with septic shock.* The New England journal of medicine, 2012. **366**(22): p. 2055-64.

175. Baneyx, F. and M. Mujacic, *Recombinant protein folding and misfolding in Escherichia coli.* Nat Biotechnol, 2004. **22**(11): p. 1399-408.

176. Menon, S., et al., *The production, binding characteristics and sequence analysis of four human IgG monoclonal antiphospholipid antibodies.* Journal of autoimmunity, 1997. **10**(1): p. 43-57.

177. Dong, L., et al., *Cloning and expression of two human recombinant monoclonal Fab fragments specific for EBV viral capsid antigen.* International immunology, 2007. **19**(3): p. 331-6.

178. Fishbein, E., D. Alarcon-Segovia, and J.M. Vega, *Antibodies to histones in systemic lupus erythematosus.* Clinical and experimental immunology, 1979. **36**(1): p. 145-50.

179. Tan, E.M., J. Robinson, and P. Robitaille, *Studies on antibodies to histones by immunofluorescence.* Scandinavian journal of immunology, 1976. **5**(6-7): p. 811-8.

180. O'Dell, J.R., A. Bizar-Schneebaum, and B.L. Kotzin, *In vitro anti-histone antibody production by peripheral blood cells from patients with systemic lupus erythematosus.* Clinical immunology and immunopathology, 1988. **47**(3): p. 343-53.

181. Liu, C.L., et al., *Specific post-translational histone modifications of neutrophil extracellular traps as immunogens and potential targets of lupus autoantibodies.* Arthritis research & therapy, 2012. **14**(1): p. R25.

182. Yung, R.L., K.J. Johnson, and B.C. Richardson, *New concepts in the pathogenesis of drug-induced lupus.* Laboratory investigation; a journal of technical methods and pathology, 1995. **73**(6): p. 746-59.

183. Hess, E., *Drug-related lupus.* The New England journal of medicine, 1988. **318**(22): p. 1460-2.

184. Swers, J.S., Y.A. Yeung, and K.D. Wittrup, *Integrated mimicry of B cell antibody mutagenesis using yeast homologous recombination.* Mol Biotechnol, 2011. **47**(1): p. 57-69.

185. Pratesi, F., et al., *Antibodies from patients with rheumatoid arthritis target citrullinated histone 4 contained in neutrophils extracellular traps.* Ann Rheum Dis, 2014. **73**(7): p. 1414-22.

186. Cheung, W.C., et al., *A proteomics approach for the identification and cloning of monoclonal antibodies from serum.* Nature biotechnology, 2012. **30**(5): p. 447-52.

187. Heukeshoven, J. and R. Dernick, *Simplified Method for Silver Staining of Proteins in Polyacrylamide Gels and the Mechanism of Silver Staining.* Electrophoresis, 1985. **6**(3): p. 103-112.

188. Shevchenko, A., et al., *In-gel digestion for mass spectrometric characterization of proteins and proteomes.* Nature protocols, 2006. **1**(6): p. 2856-60.

189. Atrih, A., et al., *Quantitative proteomics in resected renal cancer tissue for biomarker discovery and profiling.* Br J Cancer, 2014. **110**(6): p. 1622-33.

190. Kelley, L.A. and M.J. Sternberg, *Protein structure prediction on the Web: a case study using the Phyre server.* Nat Protoc, 2009. **4**(3): p. 363-71.

191. Malmqvist, M., *Surface plasmon resonance for detection and measurement of antibody-antigen affinity and kinetics.* Curr Opin Immunol, 1993. **5**(2): p. 282-6.

192. Abdiche, Y.N., D.S. Malashock, and J. Pons, *Probing the binding mechanism and affinity of tanezumab, a recombinant humanized anti-NGF monoclonal antibody, using a repertoire of biosensors.* Protein Sci, 2008. **17**(8): p. 1326-35.

193. Hearty, S., P. Leonard, and R. O'Kennedy, *Measuring antibody-antigen binding kinetics using surface plasmon resonance.* Methods Mol Biol, 2012. **907**: p. 411-42.

194. Sun, X.Y., et al., *Anti-histones antibodies in systemic lupus erythematosus: prevalence and frequency in neuropsychiatric lupus.* J Clin Lab Anal, 2008. **22**(4): p. 271-7.

195. Burlingame, R.W. and R.L. Rubin, *Drug-induced anti-histone autoantibodies display two patterns of reactivity with substructures of chromatin.* J Clin Invest, 1991. **88**(2): p. 680-90.

196. Lam, F.W., et al., *Histone induced platelet aggregation is inhibited by normal albumin.* Thromb Res, 2013. **132**(1): p. 69-76.

197. Wang, R.E., L. Tian, and Y.H. Chang, *A homogeneous fluorescent sensor for human serum albumin.* J Pharm Biomed Anal, 2012. **63**: p. 165-9.

198. Brummel-Ziedins, K.E., *Developing individualized coagulation profiling of disease risk: thrombin generation dynamic models of the pro and anticoagulant balance.* Thromb Res, 2014. **133 Suppl 1**: p. S9-S11.

199. Allen, G.A., et al., *Impact of procoagulant concentration on rate, peak and total thrombin generation in a model system.* J Thromb Haemost, 2004. **2**(3): p. 402-13.

200. Pierce, B.G., et al., *ZDOCK server: interactive docking prediction of protein-protein complexes and symmetric multimers.* Bioinformatics, 2014. **30**(12): p. 1771-3.

201. Deguchi, H., et al., *Prothrombin kringle 1 domain interacts with factor Va during the assembly of prothrombinase complex.* Biochem J, 1997. **321 (Pt 3)**: p. 729-35.

202. Linkins, L.-A., *Heparin induced thrombocytopenia*. Vol. 350. 2015.

203. Scott, A.M., J.D. Wolchok, and L.J. Old, *Antibody therapy of cancer*. Nat Rev Cancer, 2012. **12**(4): p. 278-287.

204. Kubo, M., et al., *Prevalence and Antigen Specificity of Anti-Histone Antibodies in Patients with Polymyositis//Dermatomyositis.* 1999. **112**(5): p. 711-715.

Appendix 1 Reagents

Reagent	Company
10 × PBS	Fisher Scientific (Hampton, USA)
10 × TBE	Geneflow Ltd (Staffordshire, UK)
10 × Tris/Glycine	Geneflow Ltd (Staffordshire, UK)
10 × Tris/Glycine/SDS	Geneflow Ltd (Staffordshire, UK)
2-Log DNA Ladder (0.1-10.0 kb)	New England Biolabs (Massachusetts, USA)
2-macaptoethanol	Sigma-Aldrich (St. Louis, Missouri, USA)
2-Propanol (Isopropanol)	Sigma-Aldrich (St. Louis, Missouri, USA)
Acetic Acid	Thermo Fisher Scientific (Waltham, USA)
Acetone	Thermo Fisher Scientific (Waltham, USA)
Acrylamide	Geneflow Ltd (Staffordshire, UK)
Activated Protein C (APC)	Haematologic Technologies Inc. (Cambridge, UK)
Ammonium Persulfate	Sigma-Aldrich (St. Louis, Missouri, USA)
Ampicillin sodium salt	Sigma-Aldrich (St. Louis, Missouri, USA)
Anti-Histone H3 antibody	abcam (Cambridge, UK)
Asp-N	Promega (Madison, WI USA)
BamHI	New England Biolabs (Massachusetts, USA)
Bovine Serum Albumin (BSA)	Sigma-Aldrich (St. Louis, Missouri, USA)
Brilliant Blue R	Sigma-Aldrich (St. Louis, Missouri, USA)
Bromophenol Blue	Sigma-Aldrich (St. Louis, Missouri, USA)
$CaCl_2$	BDH, VWR (Leicestershire, UK)

Calf Thymus Histone	Roche (West Sussex, UK)
Chymotrypsin	Promega (Madison, WI USA)
CNBr-activated Sepharose 4B media	GE Healthcare (Buckinghamshire, UK)
Creatine Monohydrate	Sigma-Aldrich (St. Louis, Missouri, USA)
DC™ Protein Assay	Bio-Rad (Hercules, USA)
Dimethyl Sulfoxide (DMSO)	Sigma-Aldrich (St. Louis, Missouri, USA)
EDTA	Sigma-Aldrich (St. Louis, Missouri, USA)
EGTA	Sigma-Aldrich (St. Louis, Missouri, USA)
Ethanol	Thermo Fischer Scientific (Loughborough, UK)
Ethanolamine	Sigma-Aldrich (St. Louis, Missouri, USA)
Extravidin-Peroxidase Staining Kit	Sigma-Aldrich (St. Louis, Missouri, USA)
EZ-Link™ Plus Activated Peroxidase	Thermo Fisher Scientific (Waltham, USA)
Fetal bovine serum	Sigma-Aldrich (St. Louis, Missouri, USA)
Fibronectin	Sigma-Aldrich (St. Louis, Missouri, USA)
Gelatin	Sigma-Aldrich (St. Louis, Missouri, USA)
Gelatine from Bovine Skin	Sigma-Aldrich (St. Louis, Missouri, USA)
Gibco™ L-Glutamine 200 mM	Invitrogen (Thermo Fisher Scientific, Waltham, USA)
Gibco™ Penicillin-Streptomycin liquid from Invitrogen	Invitrogen (Thermo Fisher Scientific, Waltham, USA)
Glu-C	Promega (Madison, WI USA)
Glucose	Sigma-Aldrich (St. Louis, Missouri, USA)
Glycerol	Sigma-Aldrich (St. Louis, Missouri, USA)

Glycine	Sigma-Aldrich (St. Louis, Missouri, USA)
HCl (Hydrochloric acid)	BDH, VWR (Leicestershire, UK)
HEPES	Sigma-Aldrich (St. Louis, Missouri, USA)
HEPES	Sigma-Aldrich (St. Louis, Missouri, USA)
HiSpeed Plasmid Midi Kit (25)	QIAGEN (Venlo, Netherlands)
Histone $H1^0$ Human, Recombinant	New England Biolabs (Massachusetts, USA)
Histone H2A Human, Recombinant	New England Biolabs (Massachusetts, USA)
Histone H2B Human, Recombinant	New England Biolabs (Massachusetts, USA)
Histone H3.1 Human, Recombinant	New England Biolabs (Massachusetts, USA)
Histone H4 Human, Recombinant	New England Biolabs (Massachusetts, USA)
Hydrogen peroxide (H_2O_2)	Sigma-Aldrich (St. Louis, Missouri, USA)
IGEPAL® CA-630	Sigma-Aldrich (St. Louis, Missouri, USA)
Imidazole	Sigma-Aldrich (St. Louis, Missouri, USA)
Immobilon Western Chemiluminescent HRP Substrate	Millipore (Watford, UK)
Immobilon®-P PVDF Membrane (0.45 µm)	Millipore (Billerica, USA)
Immobilon™ Western Chemiluminescent HRP Substrate	Millipore (Billerica, USA)
Instant Dried Skimmed Milk	Tesco (Liverpool, UK)
IPTG (Isopropyl-β-D-thiogalactopyranoside)	MELFORD (Suffolk, UK)
KCl	BDH, VWR (Leicestershire, UK)
L-Ascorbic Acid	Sigma-Aldrich (St. Louis, Missouri, USA)
L-Glutamine	Sigma-Aldrich (St. Louis, Missouri, USA)
L-Glutathione oxidized	Sigma-Aldrich (St. Louis, Missouri, USA)

L-Glutathione reduced	Sigma-Aldrich (St. Louis, Missouri, USA)
Lys-C	Promega (Madison, WI USA)
Methanol	Thermo Fisher Scientific (Waltham, USA)
$MgCl_2$	BDH, VWR (Leicestershire, UK)
N,N,N′,N′-Tetramethylethylenediamine (TEMED)	Sigma-Aldrich (St. Louis, Missouri, USA)
N-Acetylheparin sodium salt	Sigma-Aldrich (St. Louis, Missouri, USA)
NaCl	Sigma-Aldrich (St. Louis, Missouri, USA)
NaH_2PO_4	BDH, VWR (Leicestershire, UK)
NdeI	New England Biolabs (Massachusetts, USA)
Ni-NTA	QIAGEN (Venlo, Netherlands)
Penicillin/Streptomycin	Sigma-Aldrich (St. Louis, Missouri, USA)
pET-16b	Novagen (Darmastadt, Germany)
Phorbol 12-myristate 13-acetate (PMA)	Sigma-Aldrich (St. Louis, Missouri, USA)
Phosphate Buffered Saline (PBS), 10 × Solution	Thermo Fisher Scientific (Waltham, USA)
Pierce® Chromatography Cartridges Protein A/G	Thermo Fisher Scientific (Waltham, USA)
Propidium iodide solution	Sigma-Aldrich (St. Louis, Missouri, USA)
Prostaglandin E1	Sigma-Aldrich (St. Louis, Missouri, USA)
Protease inhibitor cocktail	Calbiochem, Merck (Nottingham, UK)
Protease type XIV	Sigma-Aldrich (St. Louis, Missouri, USA)
QIAprep Spin Miniprep Kit (250)	QIAGEN (Venlo, Netherlands)
QIAquick Gel Extraction Kit	QIAGEN (Venlo, Netherlands)

Quick Start™ Bovine Serum Albumin (BSA) standard set	Bio-Rad (Hercules, USA)
Rubidium Chloride	Sigma-Aldrich (St. Louis, Missouri, USA)
Sensor Chip SA	GE Healthcare (Buckinghamshire, UK)
Sodium bicarbonate	Sigma-Aldrich (St. Louis, Missouri, USA)
Sodium carbonate	Sigma-Aldrich (St. Louis, Missouri, USA)
Sodium cyanoborohydride solution	Sigma-Aldrich (St. Louis, Missouri, USA)
Sodium Dodecyl Sulphate (SDS)	Sigma-Aldrich (St. Louis, Missouri, USA)
Sodium orthovanadate	Sigma-Aldrich (St. Louis, Missouri, USA)
T4 DNA Ligase	New England Biolabs (Massachusetts, USA)
Taurine	Sigma-Aldrich (St. Louis, Missouri, USA)
Thrombin-α (IIα)	Haematologic Technologies Inc. (Cambridge, UK)
TMB Substrate Reagent Set	BD (Franklin Lakes, USA)
Tris base	Thermo Fisher Scientific (Waltham, USA)
Triton X-100	BDH, VWR (Leicestershire, UK)
Trypisn	Promega (Madison, WI USA)
Trypsin-EDTA	Sigma-Aldrich (St. Louis, Missouri, USA)
TWEEN® 20	Sigma-Aldrich (St. Louis, Missouri, USA)
Versene Solution	Life techonologies (Waltham, USA)
WST-8 cell proliferation assay kit	Enzo life sciences (Exeter, UK)
β-cyclodetrin	Sigma-Aldrich (St. Louis, Missouri, USA)

Appendix 2 Buffers

Buffer	Components
1 × PBS	137 mM NaCl, 2.7 mM KCl, 11.9 mM Phosphate Buffer
1 × TBS-Tween buffer saline	For 1 litre: 100 ml of TBS 10X + 900 ml distilled water + 1ml Tween-20
10 × TBS buffer for western blotting	1.5M NaCl, 0.2M Tris-HCl, ddH_2O, pH 7.4
4 × Laemmli buffer	62.5 mM Tris-HCl, pH6.8, 10% (v/v) Glycerol, 5% (v/v) β-mecaptoethanol, 3% (w/v) SDS, 0.008% (w/v) bromophenol blue
Biosensor suspension buffer 1	100 NaCl, 20 Tris-HCl, pH 7.4
Biosensor suspension buffer 2	100 NaCl, 20 Tris-HCl, pH 7.4, 2 mM EGTA
Biosensor suspension buffer 3	100 NaCl, 20 Tris-HCl, pH 7.4, 2mM $CaCl_2$
Brilliant Blue Staining Buffer	For 1 Litre: 2.5 g Brilliant Blue R, 448 ml Methanol, 100 ml Acetic Acid, 452 ml H_2O
Clear lysis buffer (CLB) for cellular lysis	1% SDS, 10% Glycerol, 120mM Tris-HCL, 25mM EDTA, H_2O, protease inhibitor cocktail 1:500 dilution, sodium Orthovanadate 2nM, pH 6.8
Coomasie blue de-staining buffer	10% Acetic acid, 30% Methanol, 60% H_2O.
CRP elution buffer	100 mM Tris-HCl, 100 mM NaCl, 2 mM EDTA, pH 8.0
ELISA coating buffer	50 mM Na_2CO_3, 50 mM $NaHCO_3$, pH9.6

Gel overlay buffer	100 mM NaCl, 50 mM Tris-HCl, 2 mM $CaCl_2$, 2 mM DTT, 0.5 % (w/v) BSA, 0.25% (w/v) gelatin, 0.5% (v/v) IGEPAL® CA-630
Gel overlay washing buffer	100 mM NaCl, 50 mM Tris-HCl, 2 mM DTT, 0.5% (v/v) IGEPAL® CA-630
Harsh western blotting stripping buffer	For 20 ml: 13.5 ml ddH_2O, 4ml (10%) SDS, 2.5 ml Tris-HCl pH 6.8 (0.5M)
HEP buffer	140 mM NaCl, 2.7 mM KCl, 3.8 mM HEPES, 5 mM EGTA, pH7.4
HEPES-Taurine buffer for rat cardiomyocytes isolation	130mM NaCl, 5.4mM KCl, 1.4mM $MgCl_2.6H_2O$, 0.4mM NaH_2PO_4, 10mM creatine monohydrate, 20mM taurine, 10mM Glucose, 10mM HEPES and 0.75mM $CaCl_2$, pH 7.3
Histone binding protein elution buffer	100 mM Glycine, pH 3.0
Histone binding protein washing buffer	PBS, 0.5% (v/v) Tween 20
HL-1 cardiomyocytes freezing medium	95% FBS, 5% DMSO
HL-1 cardiomyocytes growth medium	10 % FBS, 87% Claycomb medium, Penicillin/Streptomycin 100U/ml:100 μg/ml, 0.1 mM Norepinephrine (in 30mM ascorbic acid), 2mM L-Glutamine
Homogenization buffer for sub-cellular fractionation	1% SDS, 10% Glycerol, 120mM Tris-HCL, 25mM EDTA, H_20, protease inhibitor cocktail 1:500 dilution, sodium orthovanadate 2nM, pH 6.8

HPT digestion buffer	20 mM HEPES, 150 mM NaCl, 5 mM CaCl2, 0.1% (v/v) PEG-8000, pH7.4
MahscFv denaturation buffer	8 M urea, 50 mM Tris-HCl, pH7.4, 500 mM NaCl
MahscFv denaturation elution buffer	8 M urea, 50 mM Tris-HCl, pH7.4, 500 mM NaCl, 250 mM Imidazole
MahscFv denaturation washing buffer	8 M urea, 50 mM Tris-HCl, pH7.4, 500 mM NaCl, 50 mM Imidazole
MahscFv lysis buffer	50 mM Tris-HCl, pH7.4, 500 mM NaCl
MahscFv native purification elution buffer	50 mM Tris-HCl, pH7.4, 500 mM NaCl, 250 mM Imidazole
MahscFv native purification washing buffer	50 mM Tris-HCl, pH7.4, 500 mM NaCl, 50 mM Imidazole
MahscFv refolding dialysis buffer 1	8 M urea
MahscFv refolding dialysis buffer 2	4 M urea
MahscFv refolding dialysis buffer 3	2 M urea
MahscFv refolding dialysis buffer 4	1 M urea
MahscFv refolding dialysis buffer 5	0.5 M urea
MahscFv refolding dialysis buffer 6	50 mM Tris-HCl, pH7.4, 500 mM NaCl
MahscFv refolding dialysis buffer 7	PBS
On-column refolding buffer 1 (wash buffer)	20 mM Tris-HCl, pH 8.0, 4 M Urea, 50 mM Imidazole
On-column refolding buffer 2	20 mM Tris-HCl, pH 8.0, 4 M Urea, 10 mM 2-macaptoethanol

On-column refolding buffer 3	20 mM Tris-HCl, pH7.4, 500 mM NaCl
On-column refolding buffer 4	20 mM Tris-HCl, pH7.4, 100 mM NaCl, 5 mM β-cyclodetrin
On-column refolding buffer 5	20 mM Tris-HCl, pH7.4, 100 mM NaCl
On-column refolding buffer 6 (Elution buffer)	20 mM Tris-HCl, pH7.4, 100 mM NaCl, 300 mM Imidazole
On-column refolding denaturation buffer	40 mM Tris-HCl, pH 8.0, 8 M Urea
PBS-T	1 × PBS, 0.1% Tween-20
Permeabilization buffer for cardiomyocytes "skinning"	Triton X-100 (1%) in PBS
Platelet wash buffer	10 mM sodium citrate, 150 mM NaCl, 1 mM EDTA, 1% (w/v) dextrose, pH7.4
Primary and secondary antibody buffer for Western blotting	5% milk (in 1X TBS-Tween) or 2% BSA (in 1X TBS-Tween)
Refolding dialysis buffer 1	50 mM Tris-HCl, pH8.0, 1 M urea
Refolding dialysis buffer 2	50 mM Tris-HCl, pH8.0, 1 M urea, 150 mM NaCl
Refolding dialysis buffer 3	50 mM Tris-HCl, pH8.0, 1 M urea, 3 mM GSH, 1 mM GSSG
Refolding dialysis buffer 4	50 mM Tris-HCl, pH8.0, 1 M urea, 150 mM NaCl, 3 mM GSH, 1 mM GSSG
Resolving SDS-PAGE gel buffer	1.5 M Tris-HCl, 0.4% SDS, pH 8.8
RF1	100 mM RbCl, 50 mM $MnCl_2$, 30 mM KAc, 10 mM $CaCl_2$, 15% (v/v) Glycerol, pH5.8

RF2	10 mM MOPS, 10 mM RbCl,75 mM CaCl2, 15% (v/v) Glycerol, pH6.8
SDS-PAGE electrophoresis buffer	0.025M Tris, 0.192M Glycine, 0.1% SDS
SDS-PAGE transfer buffer	0.025M Tris, 0.192M Glycine
Sensor Chip SA Regeneration buffer	20 mM HCl
Stacking SDS-PAGE gel buffer	0.5 M Tris-HCl, 0.4% SDS, pH 6.8
Tyrode buffer for rat cardiomyocytes preservation and experimentation	140mM NaCl, 5.4mM KCl, 10mM Glucose, 10mM HEPES, 1mM $CaCl_2$, 1mM $MgCl_2$, pH 7.35
Tyrode's buffer	134 mM NaCl, 12 mM $NaHCO_3$, 2.9 mM KCl, 0.34 mM Na_2HPO4, 1 mM $MgCl_2$, 10 mM HEPES, pH7.4
Western blot block reagent	5% 5% Instant dried skimmed milk (Tesco, UK) and 2% (BSA)

Appendix 3 Equipment and software

Equipment/Software	Use
1.4F pressure-volume catheter (SPR-839) and a pressure volume system (Millar Instruments) and software Miller PVAN 2.9 software (Millar Instruments).	*In vivo* haemodynamic assessment of mice ventricular function
ACUSON Sequoia C256 Echocardiography System	Transthoracic echocardiography assessment on mice
Analog-Digital converter interface (Digidata 120B; Molecular Devices, US)	Ca^{2+} fluorescence signals processing and digitisation
BD FACSCalibur	Cell death sorting
Beckman Coulter Optima-Max ultracentrifuge and rotor TLA 120.2	Ultracentrifugation of sub-cellular fractions
Biacore™ X100	Insight of protein and protein interaction in order to calculate the kinetics, affinity and specificity
BioMAT Class II Microbiological Safety Cabinets	Tissue culture
Cell homogenizer (Ultra-Turrax T8, IKA Labortechnik, Staufen, Germany)	Homogenization of mice heart
Confocal microscope (Carl Zeiss, LSM 710) and Software (Zen 2011)	Ca^{2+} flux measurement in HL-1 cardiomyocytes
Eppendorf centrifuge 5418	Centrifugation of various samples

G box (Syngene) and software GeneSnap (Syngene)	Gel imaging for fluorescence and chemiluminescence
Gallenkamp Magnetic Stirrer	Stirring various buffers
IonOptix, MyoCam-S video edge-recognition system(Dublin, Ireland) and software IonWizard 6.0	Recording of rat and HL-1 cardiomyocyte contractility
Langendorff Apparatus	Rat cardiomyocytes isolation
Microplate reader (Multiskan Spectrum, Thermo electron corporation) and software SkanIt RE for MSS 2.2	Microplate reader
Microprocessor pH meter (HI 221) – Hannah instrument	pH measurement of various buffers
Microsoft excel (2010)	Data arrangement and organization
Microsoft power point (2010)	Figures preparation
Microsoft word (2010)	Thesis preparation
Mini-PROTEAN® Tetra Cell - Bio-Rad	Western blotting electrophoresis system
MODULAR ANALYTICS EVO analyser (Roche)	Measurement of cTnT levels in human serum and plasma
Nanodrop ND-1000 Spectrophotometer	Measure DNA and protein concentration
NanoDrop ND-1000 Spectrophotometer	Operation of Nanodrop ND-1000
Oertling NA164	Sensitive balance
Optoscan monochromator fluorescence	Measurement of $[Ca^{2+}]_i$ in rat cardiomyocytes

photometry system (Cairn Research, Faversham, Kent, UK).	
PL3504 PowerLab 4/35 (ADInstruments)	ECG recording on mice
Platelet aggregation profiler PAP-8E	Exam platelet aggregation with histones treatment, and test the protection with Abs against histones
Platform shaker STR6 (Stuart scientific)	Platform shaker
Sartorius TE214S digital gram scale	Digital balance
SciQuip Ltd centrifuge (1-15K)	Centrifugation of various samples
SciQuip Ltd centrifuge (3-16 PK)	Centrifugation of various samples
SnapGene®	Visualise and document DNA cloning, especially study plasmid.
SPSS (PASW) 18	Statistical analysis (Including ANOVA test)
Ultrasonic cell disruptor (Misonix Inc., US)	Cell disruption and protein lysates preparation
VXR basic Vibrax® - Ika	General shaker
Water bath (Grant GR150)	Temperature preservation/preparation of various buffer